Impact of Diesel Exhaust Inhalation on the Heart and Blood Vessels

by

Ni Bai

A THESIS SUBMITTED IN PARTIAL FULFILLMENT OF THE REQUIREMENT FOR THE DEGREE OF DOCTOR OF PHILOSOPHY

in

The Faculty of Graduate Studies
(Pharmacology and Therapeutics)

THE UNIVERSITY OF BRITISH COLUMBIA
(Vancouver)

June, 2011

Abstract

Numerous epidemiological studies have shown that exposure to ambient particulate matter (PM) is implicated in increased cardiovascular morbidity and mortality; however, the biological mechanisms are not fully understood. Diesel exhaust (DE) is the single biggest contributor to the urban ambient PM, and accounts for up to 90% of the total mass of fine particulate mass in ambient air of many major cities, such as London.

In this dissertation, I evaluated the effects of DE inhalation at an environmentally relevant level in a mouse model of atherosclerosis, the apolipoprotein E deficient (apoE knockout) mouse. *I hypothesized that exposure to DE causes progression of atherosclerosis and vascular dysfunction, which leads to cardiovascular morbidity and mortality*. I used a morphometric analysis to determine the compositional changes in atherosclerotic plaques, and showed that DE inhalation increased lipid accumulation, foam cell formation and smooth muscle cell recruitment in plaques, whereby suggesting a progression of atherogenesis. The magnitude of DE deposition in the lung correlates with foam cell formation suggesting a strong link between DE inhalation and atherogenesis. Oxidative stress markers, including CD36 and nitrotyrosine, were all increased after exposure to DE, suggesting that reactive oxygen species played an important role in this vascular effect. In addition, I showed that exposure to DE up-regulated iNOS and COX2 expression at both protein and mRNA levels in blood vessel and heart tissue. A functional study of blood vessels showed no impairment of acetylcholine (ACh) relaxation, but the sodium nitroprusside-stimulated endothelium-independent relaxation was enhanced following DE exposure. This could be partly explained by an increase in soluble guanylate cyclase expression in blood vessels. However, there was attenuated phenylephrine (PE)-stimulated vasoconstriction induced by DE exposure. An increased iNOS-derived NO production and up-regulation of COX2 could contribute to this attenuated constriction.

In conclusion, I demonstrate that DE inhalation alters the composition of atherosclerotic plaque resulting in unstable plaques that are vulnerable to rupture. Oxidative stress and iNOS up-regulation contribute to these DE exposure-induced vascular effects. We postulate that compensatory effects are activated to minimize the deleterious impact of DE exposure on vascular function.

Preface

This dissertation is based on 4 manuscripts, resulting from collaboration between multiple researchers.

A version of Chapter 3 has been published by *Atherosclerosis*. This paper is co-authored with Ni Bai, Takashi Kido, Hisashi Suzuki, Grace Yang, Terrance J. Kavanagh, Joel D. Kaufman, Michael E. Rosenfeld, Cornelis van Breemen, Stephan F van Eeden. Ni Bai and Stephan van Eeden developed the experimental design and protocols. Ni Bai performed all animal experiments, part of the data analysis (except the immunostaining), and wrote the manuscript. Takashi Kido and Hisashi Suzuki helped with harvesting the tissues. Grace Yang helped with data analysis for immunostaining. Part of the work (DE exposure, sample collection and processing) was conducted in the labs of Drs. Terrance J. Kavanagh, Joel D. Kaufman, and Michael E. Rosenfeld.

A version of Chapter 4 has been accepted for publication by *Toxicology and Applied Pharmacology*. This paper is co-authored with Ni Bai, Takashi Kido, Hisashi Suzuki, Terrance J. Kavanagh, Joel D. Kaufman, Michael E. Rosenfeld, Cornelis van Breemen, Stephan F. van Eeden. Ni Bai and Stephan van Eeden developed the experimental design and protocols. Ni Bai performed all animal experiments, data analysis, and wrote the manuscript. Takashi Kido and Hisashi Suzuki helped with harvesting the tissues. Part of the work (DE exposure and vascular functional study) was conducted in the labs of Drs. Terrance J. Kavanagh, Joel D. Kaufman, and Michael E. Rosenfeld.

A version of Chapter 5 has been submitted to a peer-reviewed journal for publication. The paper is co-authored with Ni Bai, Erin M. Tranfield, Terrance J. Kavanagh, Joel D.

Kaufman, Michael E. Rosenfeld, Stephan F. van Eeden. Ni Bai and Stephan van Eeden developed the experimental design and protocols. Ni Bai performed all animal experiments, data analysis, and wrote the manuscript. Erin M. Tranfield helped with harvesting the tissues. Part of the work (DE exposure and vascular functional study) was conducted in the labs of Drs. Terrance J. Kavanagh, Joel D. Kaufman, and Michael E. Rosenfeld.

A version of Chapter 6 will be submitted to a peer-reviewed journal for publication. This paper is co-authored with Ni Bai, Hisashi Suzuki, Terrance J Kavanagh, Joel D Kaufman, Michael E. Rosenfeld, Stephan F. van Eeden. Ni Bai and Stephan van Eeden developed the experimental design and protocols. Ni Bai performed all animal experiments, data analysis, and wrote the manuscript. Hisashi Suzuki helped with harvest the tissues. Part of the work (DE exposure and vascular functional study) was conducted in the labs of Drs. Terrance J. Kavanagh, Joel D. Kaufman, and Michael E. Rosenfeld.

In addition to general research directions, Dr. Stephan van Eeden, as my supervisor, helped with his numerous suggestions in the course of enhancing the experimental design, data analysis, as well as editing all the manuscripts.

Animal procedures were approved by the Animal Care and Use Committee of the University of Washington (Protocol number: 2132-04).

Table of Contents

List of Tables

List of Figures

List of Abbreviations and Acronyms

ACh	acetylcholine
ANOVA	analysis of variance
BH4	terahydrobiopterin
Ca^{2+}	calcium ion
$[Ca^{2+}]_i$	intracellular Ca^{2+} concentration
$CaCl_2$	calcium chloride
cGMP	cyclic guanosine 3',5'-monophosphate
COX	cyclooxygenase
DE	diesel exhaust
ELISA	enzyme-linked immunosorbent assay
EC_{50}	effective dose eliciting 50 % response
ECE	endothelin-converting enzymes
EDRF	endothelium-dependent relaxing factor
EDTA	ethylenediaminetetraacetic acid
et al	*et alii* (Latin, 'and others')
ET-1	endothelin-1
ET_A	endothelin type A receptor
ET_B	endothelin type B receptor
FA	filtered air
GM-CSF	granulocyte-macrophage colony-stimulating factor
GTP	guanosine 5'-triphosphate
HPRT1	hypoxanthine phosphoribosyltransferase-1
ICAM-1	intercellular adhesion molecule 1
IHC	immunohistochemistry
iNOS	inducible nitric oxide synthase
IL-1	interleukin-1
IP_3	inositol-1,4,5-trisphosphate
K^+	potassium ion
KCl	potassium chloride
kDa	kilodalton
L	litre(s)
L-NAME	*N*G-nitro-L-arginine-methyl ester
M	$mole \cdot l^{-1}$
$MgCl_2$	magnesium chloride
MI	myocardial infarction
MIP	macrophage inflammatory protein
NaCl	sodium chloride
NF-κB	nuclear factor-kappa B
NO	nitric oxide
NOS	nitric oxide synthase
NSAIDs	nonsteroidal anti-inflammatory drugs
NT	nitrotyrosine
OxLDL	oxidized low-density-lipoprotein
PE	phenylephrine
PGH_2	prostaglandin H_2
PKC	protein kinase C

PGI_2	prostagcyclin I_2
PM_{10}	particulate matter air pollution with diameter less than 10μm
PMN	polymorphonuclear leukocyte
PSS	physiological salt solution
ROS	reactive oxidative species
RT-PCR	real-time reverse transcription polymerase chain reaction
SEM	standard error of the mean
sGC	soluble guanylate cyclase
SNP	sodium nitroprusside
SOD	superoxide dismutases
TNF	tumour necrosis factor
TXA2	thromboxane A2
VCAM-1	vascular adhesion molecule-1
VSMC	vascular smooth muscle cell

Acknowledgements

I would like to thank my thesis advisors, Drs. Stephan van Eeden and Cornelis van Breemen, for the experience I have gained working with them, their knowledge, guidance, and profound insight have sharpened my critical thinking during the course of my research. I would also like to thank the members of my committee: Drs. Aly Karsan, Darryl Knight, David Granville for reading my thesis and offering advice.

I would like to send my deepest thanks to my family: my parents, my brother and my husband who always stand by me and without whom none of this would have been possible. Their unconditional love and support are the most invaluable thing I have had in my life.

I would like to acknowledge the financial support from Natural Sciences and Engineering Research Council of Canada, Michael Smith Foundation for Health Research, and Heart and Stroke Foundation of Canada.

Dedication

To my parents, Baosheng Bai and Jinli Wu, my husband, Jie Cai, and my daughter, Annie Yueye Cai

Chapter 1

Introduction

1.1 Background

An association between ambient particulate matter (PM) and mortality was first revealed in December 1930 in the Meuse Valley air pollution episode, in which 60 people died within 3 days in Engis, a town of 3,500 inhabitants in Belgium (1). Studies following the "London Fog Disaster" in December 1952 provided the first solid epidemiological data showing that exposure to PM increases mortality with an excess of 4,000 deaths over 2 weeks (2). Since then, numerous studies have supported the notion that chronic exposure to PM is an independent risk factor for respiratory as well as cardiovascular morbidity and mortality (3-10). In addition, evidence has shown that cardiovascular events can occur within hours to days after exposure to PM. The levels of ambient PM are positively correlated with mortality and morbidity rates from respiratory and cardiovascular diseases. Moreover, respiratory morbidity and mortality are related to admissions for pneumonia, asthma, pulmonary emboli, and chronic obstructive pulmonary disease (COPD) (11-14), while cardiovascular morbidity and mortality are attributable to acute coronary syndrome, arrhythmia, heart failure, and stroke (3; 7; 8-10).

Major improvements in air quality have occurred over the last 50 years, yet the association between ambient PM and cardiovascular mortality is still evident, even when pollution levels are below current national and international targets for air quality. No apparent threshold exists below which the association no longer applies (11). Although the

risk to a given individual at any single time point seems small, given the prodigious number of people being continuously exposed, particulate matter air pollution imparts a tremendous burden to the global public health, and is ranked as the 13th leading cause of mortality. World Health Organization (WHO) estimates that ambient PM is responsible for three million deaths each year (World Health Organization (2002) World Health Report. Geneva [http:www.who.int/whr/2002/en]).

1.1.1 Particulate Matter Air Pollution (PM_{10})

Air pollutants are a heterogeneous mixture of gases and particulate matter. The major gaseous components of air pollution are NO_2, CO, SO_2, and ozone. Particulate matter air pollution consists of solid and liquid particles derived from vehicle emissions, forest fires, and industrial, domestic and agricultural pollutants. Particulate matter air pollution with diameter less than 10 µm is collectively known as PM_{10}. Based on the size, PM_{10} is subdivided into coarse particles ($PM_{2.5}$-PM_{10}, diameter 2.5-10µm), fine particles ($PM_{0.1}$-$PM_{2.5}$, diameter 0.1-2.5µm) and ultrafine particles (diameter <0.1µm) (Fig 1.1).

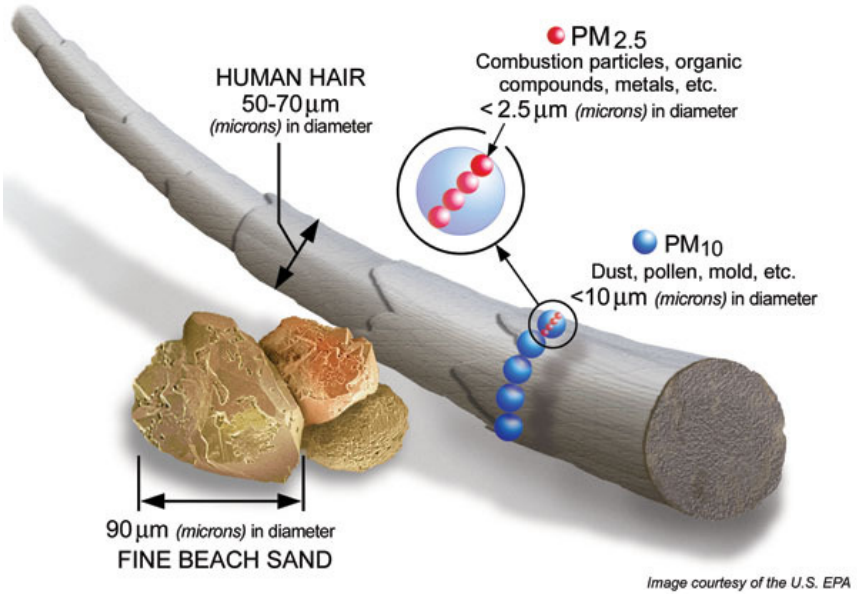

Figure 1.1 The size of different fractions of PM_{10}

Inhaled particles are cleared from the lungs via phagocytosis by alveolar macrophages or via translocation to the tracheobronchial lymph nodes. Chronic inhalation of poorly soluble ambient particles can cause progressive accumulation of aggregated, particle-laden macrophages and lead to lung overload, after the particle deposition rate exceeds that of the clearance by alveolar macrophages (12).

Particulate matter air pollution larger than 10 μm is generally filtered by the defense system in the nose and throat, with particles less than 10 μm being inhaled deep into the bronchi and lungs. Particles with larger diameters tend to settle more quickly, whereas fine and ultrafine particles (UFPs) remain suspended in the air for a longer period, resulting in greater alveolar deposition efficiency. Compared with coarse particles, fine particles and UFPs deposit in greater numbers and into deeper regions of the lungs due to the larger surface area (Fig 1.2). A collection of all particles of these three different particle diameters (Table 1.1) would always give the same airborne mass concentration of 10 $\mu g/m^3$. Nevertheless, the physical characteristics of the cloud are very different for the particle number and surface area, and both of these are properties that are believed to have an important impact on the lung (13) .

Table 1.1 Relationships of the particle surface area, numbers, and size.
(Adapted with permission from Donaldson et al, Occup Environ Med., 2001) (15).

Airborne mass concentration ($\mu g/m^3$)	Particle diameter (μm)	Particles/ml of air	Particle surface area (μ^3/ml air)
10	2	1.2	24
10	0.5	153	120
10	0.02	2400000	3016

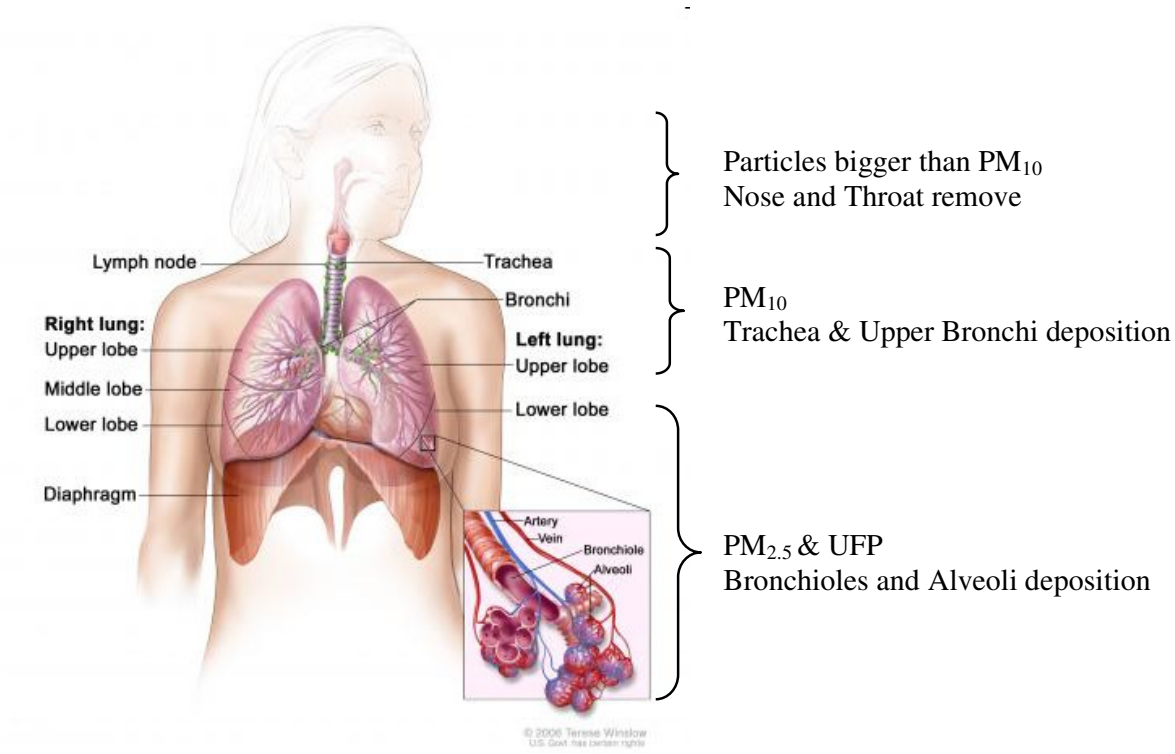

Figure 1.2 Where does PM_{10} go in the respiratory system.
(Adapted from the websites of the National Cancer Institute).

Fine particles and UFPs are mainly generated from the combustion of fossil fuels used in transportation, manufacturing, and power generation. Although diesel engines generate up to 25% less CO_2 (a green house gas implicated in global warming), they emit up to 100-150 times more particles than do gasoline engines (14). Diesel exhaust (DE) is a major contributor to fine particles, accounting for up to 90% of the fine particulate mass in ambient air of many major cities, such as London (15; 16). In North America cities, the contribution of DE to ambient particulate matter is less than that in European cities (Fig 1.3).

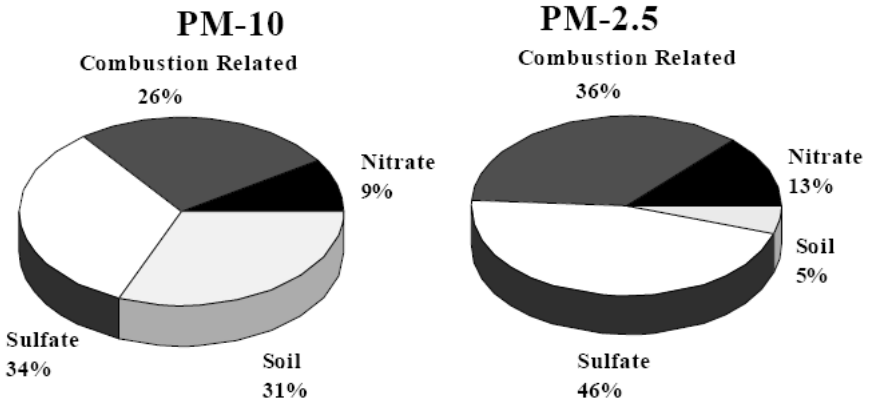

Figure 1.3 Comparison of PM_{10} and $PM_{2.5}$ Sources in Washington, DC. (The pie chart is based on analysis of actual ambient air samples taken during 1992-95 in Washington, DC.) (Adapted from IMPROVE, Cooperative Center for Research in the Atmosphere CSU, Ft. Collins, CO, July 1996).

Many of these individual components of atmospheric PM_{10} are not especially toxic at ambient levels and some major constituents, such as sodium chloride, are harmless. In contrast, DE consists of a central carbon core nucleus onto which an estimated 18,000 combustion products are absorbed, including organic chemicals like polycyclic aromatic hydrocarbons, and oxidized transition metals (17; 18). Toxicological studies have shown that exposure to fine and UFPs causes greater inflammatory effects than large ones of the same material. Although the mechanism remains unclear, evidence indicates that the large surface area of these fine particles and the oxidative stress associated with the transition metals carried by UFPs play essential roles in the strong association between exposure to PM_{10} and health effects (19; 20). In addition, UFPs can evade from being cleared-up or phagocytosed by alveolar macrophages, resulting in more opportunities for UFPs to interact with lung cells, and lead to secondary effect in the lung (Fig 1.4).

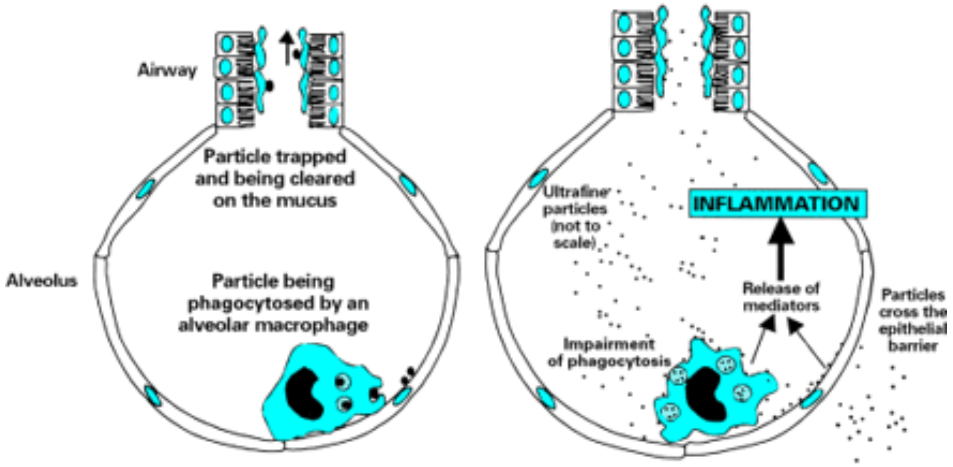

Figure 1.4 Diagrammatic representations of the hypothetical events after exposure to ultrafine particles (right) compared with fine particles (left). The essential elements of the ultrafine response are many particles outside and inside macrophages. Release of mediators from the macrophages and epithelial cells due to activation of signaling pathways mediated by oxidative stress, may then lead to inflammation. The enhanced interaction of particles with the epithelium leads to their transfer to the interstitium. (Adapted with permission from Donaldson K et al. *Occup Environ Med.* 2001) (20).

The typical background concentrations of PM_{10} in North America or Western Europe are 20-50 $\mu g/m^3$, and these concentrations increase to 100-250 $\mu g/m^3$ in industrialized areas and in the developing world. The most recent National Ambient Air Quality Standards issued by the U.S EPA in 2006 for PM_{10} are the annual standard of 55 $\mu g/m^3$, and the 24-hour standard of 150 $\mu g/m^3$. The standards for $PM_{2.5}$ levels have been strengthened to 15 $\mu g/m^3$ (annual) and 35 $\mu g/m^3$ (24-hour) based on vast evidence showing a strong association between fine particles and cardiovascular diseases.

1.1.2 Epidemiological Evidence for Adverse Cardiovascular Effects Associated with Exposure to Particulate Matter Air Pollution (PM_{10})

Evidence from numerous epidemiological studies conducted in different countries across the continents indicates a strong association between increases in PM_{10} and greater acute (Table 1.2) and chronic cardiovascular morbidity and mortality (Table 1.3).

1.1.2.1 Acute Cardiovascular Effects Induced by PM_{10} Exposure

Burnett and colleagues monitored PM_{10} levels for 300,000 elderly residents in 21 US cities between 1985-1999, and found that a 10 $\mu g/m^3$ increase in PM_{10} was associated with a significantly increased risk of hospitalization for myocardial infarction (MI), which occurred within a few hours after exposure (21). Studies examining daily PM_{10}-related mortality effects were also conducted in multiple cities in Europe and Asia, and the results consistently showed that exposure to PM_{10} was significantly associated with daily mortality accounts for all-causes and cardiovascular mortality (Table 1.2). The overall evidence from a time-series analysis conducted worldwide confirms the existence of a small, yet consistent association between increased cardiovascular mortality and short-term (1 to 5-day) elevation of PM_{10} and $PM_{2.5}$ prior to the cardiovascular events.

Table 1.2 Summary of recent multi-city analyses and studies. These studies have been published since 2004 of the comparison of pooled estimated of percent increase (and 95% CI or Posterior Interval or *t* Value) in RR of mortality estimated across meta-analyses and multicity studies of daily changes in exposure (Modified from Brook RD et al. Circulation. 2010) (22).

Studies		Percent Increases in Mortality (95% CI)	
	Exposure Increment ($\mu g/m^3$)	All-Cause	Cardiovascular
Meta-estimate with and without adjustment for publication bias (23)	20 PM10	1.0 (0.8–1.2) 1.2 (1.0–1.4)	
Meta-estimates from COMEAP report to the UK Department of Health on CVD and air pollution (24)	20 PM10		1.8 (1.4–2.4)
	10 PM10		1.4 (0.7–2.2)
NMMAPS, 20 to 100 US cities (25)	20 PM10	0.4 (0.2–0.8)	0.6 (0.3–1.0)[1]
APHEA-2, 15 to 29 European cities (26)	20 PM10	1.2 (0.8–1.4)	1.5 (0.9–2.1)
US, 6 cities (27)	10 PM2.5	1.2 (0.8–1.6)	1.3 (0.3–2.4)[2]
US, 27 cities (28)	10 PM2.5	1.2 (0.3–2.1)	0.9 (–.1, 2.0)
California, 9 cities (29)	10 PM2.5	0.6 (0.2–1.0)	0.6 (0.0, 1.1)
France 9 cities (30)	20 BS	1.2 (0.5–1.8)[3]	1.2 (0.2–2.2)[3]
Japan, 13 cities, age >65 yr (31)	20 SPM	1.0 (0.8–1.3)	1.1 (0.7–1.5)
Asia, 4 cities (32)	10 PM10	0.55 (0.26–0.85)	0.59 (0.22–0.93)
US, 112 cities (33)	10 PM2.5	0.98 (0.75–1.22)	0.85 (0.46–1.24)
	10 PM10-2.5	0.46 (0.21–0.71)	0.32 (0.00–0.64)

CI indicates confidence interval or posterior interval.

1. Cardiovascular and respiratory deaths combined. 2. Ischemic heart disease deaths. 3. Chronic obstructive pulmonary disease deaths. 4. Includes general additive model–based analyses with potentially inadequate convergence. 5. Results for PM10–2.5 are from 47 cities.

1.1.2.2 Chronic Cardiovascular Effects Induced by PM_{10} Exposure

Although short-term changes in PM_{10} concentrations have deleterious health effects, longer-term exposure may have a more pertinent clinical health effect on cardiovascular morbidity and mortality given that individuals are typically exposed to higher air pollution levels over extended periods of time. A 16-year prospective study (Harvard Six City Study), involving 8,000 people living in 6 American cities with different levels of ambient PM (10-fold difference between the most and the least polluted cities), showed a strong association between increases in cardiovascular mortality and high PM_{10} levels after adjusting for cigarette smoking and other major cardiovascular risk factors (34). Another landmark cohort-based mortality study, that enrolled approximately 1.2 million American adults in 1982, found that an elevation of 10 $\mu g/m^3$ $PM_{2.5}$ was associated with ~6% increase in cardiovascular mortality (35). These cohort studies (summarized Table 1.3) demonstrate larger overall mortality effects, compared to those of acute exposures (Table 1.2). In addition, exposure to elevated PM levels over the long-term can reduce life expectancy. A recent large study found that a decrease of 10 $\mu g/m^3$ in the long-term $PM_{2.5}$ concentration was related to an increase in mean life expectancy around one year (36).

That exposure to PM induces cumulative changes causatively linked with mortality is further supported by studies showing that reduction in ambient PM leads to short-term (weeks to months) and long-term (years) decreases in mortality. For instance, a 15 $\mu g/m^3$ decrease in PM_{10} concentration in Utah valley (during a 13-month strike at a local steel mill) was associated with a 3.2% decrease in total mortality (6). Similarly, a 35 $\mu g/m^3$ decrease in mean black smoke concentration attributable to a ban on coal sale in the city of Dublin was accompanied by a 5.7% decrease in non-trauma deaths in 72 months after the ban, compared with the same period before the ban (37). A current update of the Harvard Six City Study extended the mortality follow-up for an additional 8 years showed that a 1 $\mu g/m^3$ reduction

in $PM_{2.5}$ was associated with a 3% decrease in overall mortality (35; 38). These studies strongly support a causal relationship of exposure to PM and cardiovascular morbidity and mortality.

Table 1.3 Summary of recent multi-city analyses and studies for the effects of chronic PM exposure and cardiovascular effects (Modified from Brook RD et al. Circulation. 2010) (22).

				Percent Increases in Mortality (95% CI)	
Studies	Size of Cohort (000s)	Follow-Up Period	Covariates Controlled for	All-Cause	Cardiovascular
Harvard Six Cities, original (3)	~8	1974–1991	Individual (smoking+others)	13 (4.2–23)	
Harvard Six-Cities, extended (38)	~8	1974–1998	Individual (smoking+others)	16 (7–26)	28 (13–44)
Six-Cities Medicare cohort (39)	~340	2000–2002	Individual (age, sex)	21 (15–27)	
ACS, Original (7)	~500	1982–1989	Individual (smoking+others)	6.6 (3.5–9.8)	
ACS, HEI extended (40)	~500	1982–1998	Individual (smoking+others) +ecological	6.2 (1.6–11)	12 (8–15)
US Medicare cohort (41)	~132000	2000–2005	Individual (age, sex) +ecological +COPD	6.8 (4.9–8.7) [1]	
Women's Health Initiative (42)	~66	1994–2002			76 (25–147), 24 (9–41)[2]
French PAARC (43)	~14	1974–2000	Individual (smoking+others)	7 (3–10)[2]	
German women (44)	~5	1980s, 1990s–2003	Individual smoking and socioeconomic status	12 (–8 to 38)	
Oslo, Norway (45)	~144	1992–1998	Individual age, occupational class, education		10 (5–16),[3] 14 (6–21), 5 (1–8), 3 (0–5)
Dutch cohort (46)	~121	1987–1996	Individual (smoking+others) +ecological	6 (–3 to 16)	4 (–10 to 21)
Great Britain (47)	~660	1966–1998	Socioeconomic status	1.3 (1.0–1.6)[4]	1.2 (0.7–1.7)[4]

HEI indicates Health Effects Institute; VA, Veterans Affairs; COPD, chronic obstructive pulmonary disease. 1. Three estimates are for the East, Central, and West regions of the United States, respectively. 2. Any cardiovascular event. 3. Four estimates are for men 51–70 y old, women 51–70 y old, men 71–90 y old, and women 71–90 y old, respectively. 4. Associated with 10 $\mu g/m^3$ British Smoke (BS) or PM_{10}

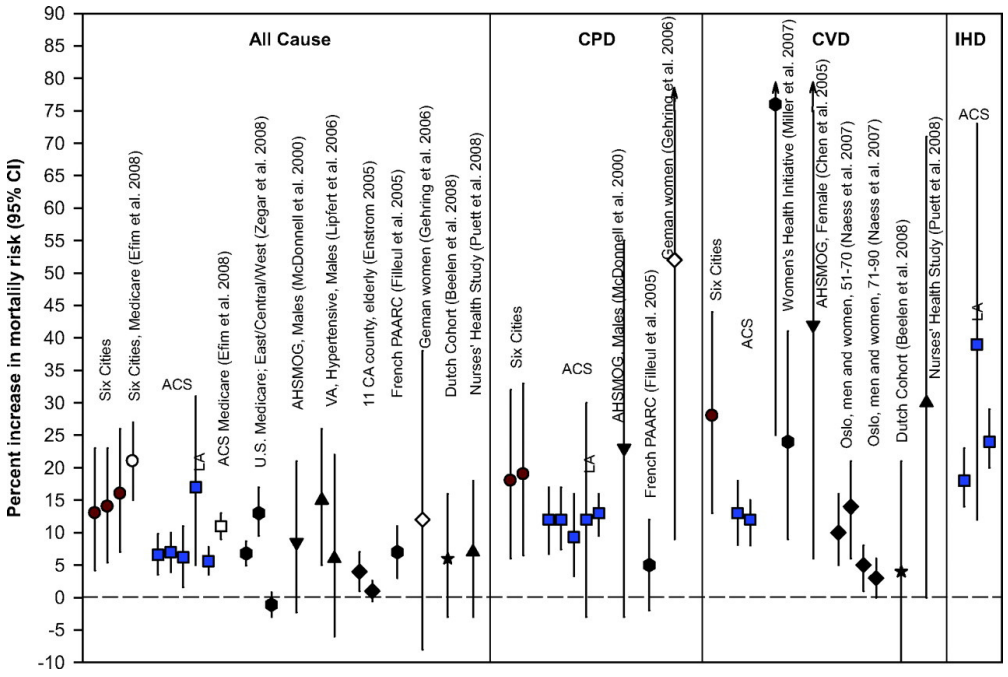

Figure 1.5 Risk estimates provided by several cohort studies per increment of 10 µg/m^3 in $PM_{2.5}$ or PM_{10}. CPD, cardiopulmonary; CVD, cardiovascular disease; IHD, ischemic heart disease. (Adapted with permission from Brook RD et al. Circulation. 2010) (22).

Collectively, the evidence from studies conducted independently in different countries at different periods of time indicates that an elevation of PM_{10} levels is strongly associated with increases in cardiovascular mortality, attributable to atherosclerosis, dysrhythmias, congestive heart failure, ischemic heart disease, and stroke (9; 48-56) (Fig.1.5). Of all common air pollutants, fine ambient particles have the strongest association with mortality (3; 57-59). In addition, having pre-existing cardiovascular risk factors such as coronary heart diseases, heart failure, diabetes mellitus and ageing increases the probability of cardiovascular mortality following PM_{10} exposure (60; 61).

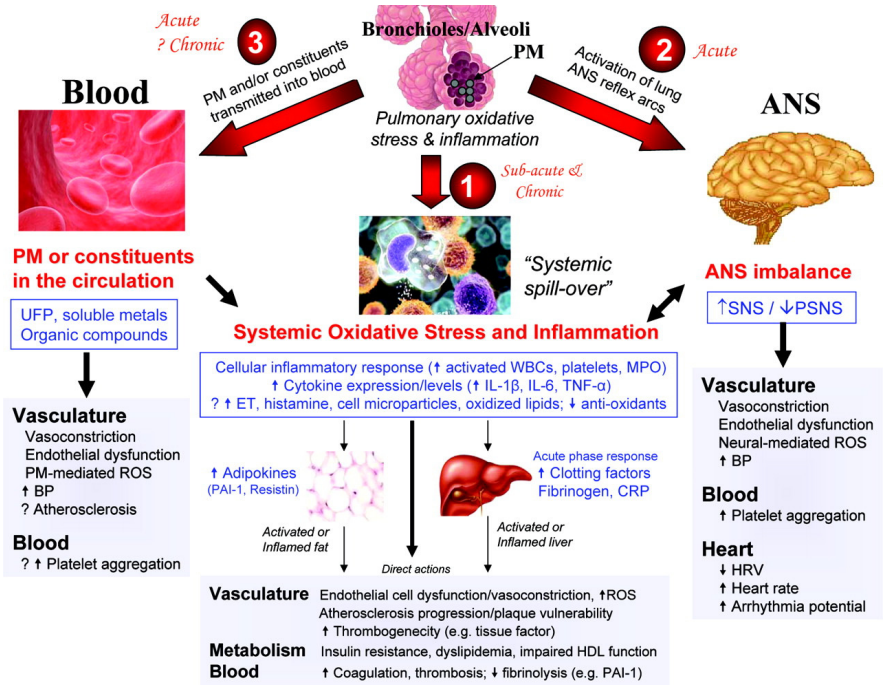

Figure 1.6 Biological pathways linking PM exposure with cardiovascular diseases. The 3 generalized intermediary pathways and the subsequent specific biological responses that could be capable of instigating cardiovascular events are shown. MPO indicates myeloperoxidase; PAI, plasminogen activator inhibitor; PSNS, parasympathetic nervous system; SNS, sympathetic nervous system; and WBCs, white blood cells. A question mark (?) indicates a pathway/mechanism with weak or mixed evidence or a mechanism of likely yet primarily theoretical existence based on the literature. (Adapted with permission from Brook RD et al. Circulation. 2010) (22).

1.1.3 Proposed Pathways for PM_{10}–induced Cardiovascular Effects

The biological pathways by which exposure to PM_{10} exerts cardiovascular effects have been a major focus of research over the past decade. Although the precise pathways are still not fully understood, two hypotheses have been proposed based on population and animal studies. Seaton and colleagues (1995) proposed that the deposition of ambient PM in the lung provoks a low-grade alveolar inflammation with a secondary systemic inflammatory response resulting in downstream cardiovascular death, especially in susceptible individuals

(62). Since then, numerous authors have supported this hypothesis and further expanded it, reporting that exposure to PM_{10} causes changes in plasma viscosity (63), and an increase in the procoagulant state, including elevated levels of fibrinogen (64; 65), platelet activation (66), a pro-inflammatory state of blood (67) that includes bone marrow stimulation with an increase in circulating white cells (68), polymorphonuclear neutrophils (PMNs), and monocytes (69; 70).

In addition, to explain the relative short interval between increases in PM_{10} exposure and cardiovascular events, Godleski et al. suggested that fine particles or UFPs could enter the blood and adversely affect the heart by initiating arrhythmias and sudden death in susceptible subjects (71). Since then, several studies have demonstrated that UFPs have the ability to translocate into the circulation both in animal models and in humans (71-74). These studies suggest that a direct effect of translocated UFPs on the vasculature could result in observed increases in heart rate variability, increases in heart rate, changes in blood pressure (75), and enhanced susceptibility to arrhythmias and modified autonomic or other neurological reflexive effects (76) associated with exposure to PM_{10}. These two hypotheses are not mutually exclusive, and evidence from both human and animal studies indicates that the biological response to inhaled ambient particles is very complex; hence both mechanisms may contribute to the adverse cardiovascular effects of PM_{10} exposure (Fig.1.6).

1.1.3.1 PM_{10}-Induced Pulmonary and Systemic Inflammation

Substantial evidence indicates that inhaled particles provoke an inflammatory response in the lungs with a consequent release of prothrombotic and inflammatory cytokines into the circulation that leads to exacerbations in cardiovascular disease (22; 77).

1.1.3.1.1 Lung Inflammatory Response Induced by PM_{10}

Alveolar macrophages and epithelial cells of the bronchial wall, and alveolar spaces are exposed to inhaled particles, and are the principle cell types that process inhaled ambient particles in the lung. In processing these particles, the cells produce pro-inflammatory mediators that are capable of eliciting both local and systemic inflammatory responses (78; 79).

1.1.3.1.1.1 Alveolar Macrophage Response to PM_{10} Exposure

As a function of self and immune-defense, upon deposition of particles in the lung, alveolar macrophages produce increasing amounts of pro-inflammatory mediators; in particular, interleukin (IL)-1β, IL-6, IL-8, macrophage inflammatory protein (MIP)-1α, and granulocyte-macrophage colony-stimulating factor (GM-CSF) (79-82). IL-1β is one of the "acute response" cytokines released by alveolar macrophages and epithelial cells. IL-1β has a broad stimulating effect on B cells and T cells, and helps to propagate the extension of a local or systemic inflammatory process. IL-6 contributes to the initiation and extension of the inflammatory process, promoting monocyte differentiation toward macrophages (83), activation of B and T lymphocytes, and stimulates hepatocytes to produce acute phase proteins (84). In addition, IL-6 increases granulocyte release into the circulation from the bone marrow, and promotes granulocyte sequestration in microvascular beds (85). IL-6 also increases the production of reactive oxygen species (ROS), and regulating cell adhesion properties by the activation of peripheral blood mononuclear cells to secrete monocyte chemoattractant protein (MCP)-1 (86). IL-8 is a critically important chemoattractant and activator facilitating the recruitment of both polymorphonuclear leukocytes (PMN) and monocytes into the airspace. MIP can activate granulocytes, and can lead to acute neutrophilic inflammation. MIP also induces the synthesis and release of other pro-

inflammatory cytokines, including IL-1 and IL-6. GM-CSF is not only a hematopoietic growth factor but also has an important granulocyte degranulation factor that enhances tissue damage induced by granulocytes (87). IL-10, a cytokine known to inhibit the production of pro-inflammatory factors such as TNF-α, IL-1β, IL-6, and IL-8, is not stimulated by particle exposure (79), suggesting that PM_{10} does not directly induce a significant anti-inflammatory cytokine response. Collectively, the evidence suggests that in response to the exposure of ambient particles, alveolar macrophages release a collection of inflammatory mediators that can elicit a local inflammatory response in the lung, and promote leukocyte recruitment into lung tissues and air space, leading to lung inflammation.

Exposure to ambient particles also modulates the responses of alveolar macrophages to infectious agents. Exposure of human alveolar macrophages to diesel exhaust particles (DEP) significantly suppresses the alveolar macrophage responsiveness to gram-negative (lipopolysaccharide, LPS) and positive (lipoteichoic acid) bacterial products. The impaired alveolar macrophage responsiveness may also contribute to compromised pulmonary defense mechanisms, further explaning the frequently reported association of increased lung infections with exposure to episodes of increased air pollution (88). The suppressed alveolar macrophage responsiveness can be attenuated by scavengers of free radicals, indicating that this is a free radical-mediated process (89). In addition, the compromised alveolar macrophage action is specific in response to DEP exposure and has not been observed with other ambient particles such as carbon black or EHC93 (79; 91), suggesting that the composition of particles plays an important role in the reaction of lung cells (e.g, alveolar macrophages) to inhaled particles. In summary, alveolar macrophages are crucially important in initiating and promoting the lung inflammatory response after exposure to ambient PM.

1.1.3.1.1.2 Lung Epithelial Cell Response to PM_{10} Exposure

The surface area of the lungs is equivalent to the size of a tennis court, and is covered with epithelial cells. Because of its large surface area, lung epithelial cells bear the burden of exposure to inhaled particles and are essential in processing ambient particles. Several studies have shown that exposure of different cell lines of lung epithelial cells to PM_{10} can produce various pro-inflammatory mediators (91-94). Studies using primary cultures of human bronchial epithelial cells (HBEC) revealed that these cells produced IL-1β, IL-8, GM-CSF, and leukemia inhibitory factor (LIF) in a dose-dependent manner in both mRNA and protein levels (91). The cytokine production in the human epithelial cells was attenuated by chelating transitional metals from urban particles, suggesting that metal cations augment the cellular responses of ambient particles (95; 96). In comparison with bronchial epithelial cells, production of cytokines, such as IL-1β, IL-6, GM-CSF, and LIF by particle exposure to HBEC, is absent in A549 cells, a cell line representing alveolar epithelial cells. The A549 cells tend to produce IL-8 and macrophage chemoattractant protein (MCP)-1, which are not only important chemoattractants of PMN and monocytes, but are also able to up-regulate the expression of intercellular adhesion molecule-1 (ICAM-1) on their surface, thus contributing to leukocyte recruitment into the airspace. These studies suggest that bronchial and alveolar epithelial cells respond differently to ambient particles.

1.1.3.1.1.3 Alveolar Macrophage and Lung Epithelial Cell Interaction

The close proximity of alveolar macrophages and epithelial cells in the lung increases the likelihood of the two cell types interacting and amplifying their responses to PM_{10} exposure. Mediators such as IL-1β and TNFα released from alveolar macrophages upon exposure to PM_{10} can, in turn, activate epithelial cells, causing them to enhance their mediator production and release. Supernatants of alveolar macrophages exposed to PM_{10}

increase the expression of IL-1β, LIF, and IL-8 mRNA in HBEC to a greater extent than when do supernatants from alveolar macrophages exposed to control medium (81). Co-cultures of human alveolar macrophages and bronchial epithelial cells synergistically produced GM-CSF and IL-6, both of which are involved in the systemic inflammatory response to inhaled PM (92). The interaction of alveolar macrophages with lung epithelial cells promotes the production of mediators responsible for the release of monocytes from the bone marrow, an important effector cell involved in lung inflammation and the progression of atherosclerosis associated with chronic exposure to PM (97). Recent findings suggest that epithelial cells can also signal other lung cell types. For example, mediators from HBEC exposed to DEP induce maturation of dendritic cells, possibly via the up-regulation of GM-CSF (98). Therefore, PM_{10}-induced interactions of lung cells could be signaled via direct adhesion contact between these cells or via mediators functioning in a paracrine fashion.

Collectively, these studies demonstrate that lung cells phagocytose inhaled ambient particles and produce mediators that induce and further amplify the local inflammatory responses in the lung. Several of the mediators produced in the lung are implicated in the systemic inflammatory response associated with exposure to PM. In addition, chronic exposure to ambient PM could establish a dynamic biological association between particles and chemokine production, providing a source for sustained inflammatory responses, which can constantly recruit inflammatory cells, such as monocytes and neutrophils into the circulation and to interact with the blood vessel wall (99-101). It is worthy noting that the concentrations of PM used in some of the studies(100; 102) were very high and not environmently relavent, therefore, the mechanisms involved may be not the same as what lower-level ambient inhalation exposures(101).

1.1.3.1.2 Systemic Inflammatory Response Induced by PM_{10} Exposure

The systemic inflammatory response induced by exposure to ambient particles occurs in three phases: 1) release of inflammatory mediators into the circulation; 2) activation of the acute phase response; and 3) stimulation of bone marrow with mobilization and activation of inflammatory cells.

1.1.3.1.2.1 Circulating Mediator Release Induced by PM_{10} Exposure

An increase in circulating cytokines and/ or proinflammatory mediators, activated by immune cells, could serve as a mechanism to instigate adverse effects on the heart and vasculature. Numerous experiments have demonstrated increased cellular and inflammatory cytokine content, for example, IL-6, IL-1β, TNFα, interferon-γ, and IL-8, of bronchial fluid, and sometimes, in circulating blood after acute exposure to a variety of pollutants (79; 81; 102-106).

Exposure of healthy young volunteers to an acute elevation of PM_{10} induced increases of blood cytokine levels that promptly declined when the pollutants were cleared (68; 79) albeit that other cuases, including stress, increased physical activity, weather and temperature changes, might not be fully excluded. The positive correlation between reduced circulating cytokine levels and decreased PM_{10} levels supports a strong link between exposure to PM and the systemic inflammatory response. The cytokines (GM-CSF, IL-6, and IL-1β) that increased in the circulation were similar to those produced by alveolar macrophages exposed to urban particles ex vivo, suggesting a link between lung inflammation and the systemic response elicited by air pollution. In support of this finding, Tamagawa and colleagues found that in vivo exposure of rabbits to ambient particles (ECH93) led to increases in circulating levels of IL-6, which was positively correlated with the number of activated alveolar macrophages and the total alveolar macrophages that

phagocytosed particles (104). This suggests an important role of alveolar macrophages in instigating the systemic inflammatory response. We recently demonstrated that IL-6 produced in the lung after PM_{10} exposure translocated to the circulation and was responsible for inducing systemic inflammation and vascular endothelial dysfunction (107).

1.1.3.1.2.2 Acute Phase Response Induced by PM_{10} Exposure

Part of the systemic response to exposure to air pollution is the activation of the acute phase response as indicated by an increase in circulating acute phase proteins (108-110). Exposure to ambient PM up-regulates the production of circulating levels of acute phase proteins such as C reactive protein (CRP), fibrinogen, complement, transferrin, haptoglobin, α_1-antitrypsin, and ceruloplasmin, which is positively correlated with cytokine production, particularly IL-1β, IL-6, and TNFα (108; 110-111). Whether these acute phase proteins are just markers of vascular disease or they actually play a direct role in the pathogenesis of vascular disease associated with air pollution is unresolved and needs further investigation.

1.1.3.1.2.3 Bone Marrow Stimulation Induced by PM_{10} Exposure

An integral component of the systemic inflammatory response is the stimulation of the hematopoietic system, specifically in the bone marrow, which results in an increase in circulating leukocytes. We observed leukocytosis, an independent predictor of MI (112), in both human (9) and animal (69; 103; 113) studies, in response to PM_{10} exposure. This leukocytosis was accompanied by stimulation of the bone marrow, as indicated by the increased release of both PMNs and monocytes. Cytokines, released upon PM_{10} deposition in the lung, also stimulate the bone marrow, leading to a decreased transit time of both monocytes and PMNs through the bone marrow, and accelerated release of these cells into the circulation (69; 92; 97; 113-117). Additional studies showed that monocytes were

released from bone marrow at baseline, earlier and more rapidly than were neutrophils (118). The release of monocytes from the marrow was accelerated further by inflammation in the lung induced by atmospheric particles (69). Newly released, bone marrow-derived PMN expresses higher levels of adhesion molecules (119) and contains more damaging granular enzymes that can amplify tissue inflammation. Evidence has shown that leukocytosis is associated with acute coronary syndrome (112).

The cytokines that increase in circulation following PM_{10} exposure are important for inducing the systemic inflammatory response. Both TNF-α and IL-1β are "acute response" cytokines that can induce secondary cytokine production; act as co-stimulating factors in hematopoiesis; activate the vascular endothelium; and induce the acute phase response (84). IL-6 can induce endothelial dysfunction (104; 107), stimulate the liver to produce acute phase proteins (such as CRP and fibrinogen), and enhance the production of platelets (83; 84). In addition, IL-6 contributes to atherosclerosis and MI by activation of macrophages to secrete MCP-1 (120), which is pivotal for monocyte recruitment into tissues and a central mediator of inflammatory events in atherosclerosis (121; 122). The acute phase protein CRP is thought to be directly involved in the inflammatory response and is associated with a significant risk of acute coronary events (123). CRP is able to increase monocyte infiltration into the arterial wall, amplify inflammatory and pro-coagulant responses, and lead to atherogenesis (124-128). In addition, CRP can cause plaque destabilization and rupture by up-regulation of adhesion molecules, such as VCAM-1, ICAM-1, and E-selectin (126; 129; 130). Fibrinogen contributes to thrombus formation during acute coronary syndromes and is also recognized as a long-term risk for MI (131). GM-CSF, a hematopoietic growth factor not only stimulates granulocyte differentiation and release from the bone marrow, but also activates circulating leukocytes and prolongs their survival in the circulation and at inflammatory sites (83). These cytokines up-regulate the secretion of MCP-1 and promote

the accumulation of monocytes and T lymphocytes in atherosclerotic lesions, resulting in the progression of atherosclerosis (79; 132; 133).

Collectively, pro-inflammatory cytokines (TNF-α, IL-1β, IL-6, and GM-CSF) are key molecules that initiate and promote local and systemic inflammatory response, and contribute to the cardiovascular effects induced by PM_{10} exposure.

1.1.3.2 Extra-Pulmonary Translocation of PM_{10}

The possibility of extra-pulmonary translocation of ambient particles first received direct support from the observation that radioactively labeled UFPs were detected in the blood stream as soon as one minute after exposure and importantly, remained at peak levels for periods of up to 60 minutes (72). In a study, by Nemmar and colleagues, 99mTechnetium-labeled carbon particles were detected in blood after one minute inhalation, suggesting that UFPs may be able to translocate from the lungs directly into the circulation, thus influencing cardiovascular endpoints (73). This notion was supported by several independent studies proposing a number of intriguing putative passages by which inhaled ambient particles travel from the lung into the circulation and gain access to other organs. The proposed loci for this pulmonary extravasation include the fenestrae of sinusoidal endothelial cells (134), the lung-blood barrier (135; 136), and the alveolar-capillary barrier (137). Circulating UFPs can mediate increased synthesis and/or release of fibrinogen via direct contact with hepatocytes (134). UFP translocation provides a plausible explanation for the relatively short interval between exposure to ambient particles and acute coronary events. In addition, UFP translocation could also explain the observation that ambient particles cause adverse effects in critical organs independent of a systemic inflammatory reaction (108; 134; 138). On the other hand, Mills et al reported inhaled Technegas carbon nanoparticles pass directly from the lungs into the systemic circulation in human (139). The discrepancy

may be due to the techniques of labelling these particles, and different physical properties of particles. However, whether translocated ambient particulate matter can cause cardiovascular effects are still controversy.

1.1.4 PM_{10} and Atherosclerosis

Blood vessel inflammation plays an important role in the development of atherosclerosis (140), which is the underlying cause of approximately 80% of cardiovascular diseases. Studies have shown that exposure to PM_{10} causes development and progression of atherosclerosis. Using Watanabe Hereditarily Hyperlipidemic (WHHL) rabbits, an animal model of naturally developing atherosclerosis, Suwa and colleagues demonstrated that a four-week exposure to urban ambient particles (EHC93) caused progression of atherosclerosis in both the aorta and coronary arteries, which was correlated with the number of alveolar macrophages that contained ambient particulate matter, thus foreshadowing a link between ambient particles and atherogenesis (141). This finding is supported by other animal (142; 143), and human studies showing that an elevation of 10 $\mu g/m^3$ or 20 $\mu g/m^3$ in $PM_{2.5}$ was associated with 5.9% and 12.1% increases in the development of atherosclerosis, respectively (143; 144). A cohort study of 4,494 individuals demonstrated that living in close proximity to a major urban road associate with a 7% higher of coronary artery calcium score, a marker of coronary atherosclerosis (145).

1.1.4.1 Atherosclerosis

1.1.4.1.1 Pathogenesis of Atherosclerosis

Atherosclerosis has been recognized as a chronic inflammatory and multisystemic disorder involving the vascular, metabolic, and immune systems (141). The development of atherosclerosis starts at young age and its prevalence increases with age. Fatty streak

formation has been observed in human fetal aorta and is greatly enhanced by hypercholesterolemia. Intimal accumulation of low-density lipoprotein (LDL) and oxidized LDL (oxLDL) causes endothelial dysfunction, resulting in impairment in vasorelaxation, increases in oxidative stress, and up-regulation of adhesion molecules. These adhesion molecules, including intercellular adhesion molecule (ICAM)-1, vascular adhesion molecule-1 (VCAM-1), and selectins promote leukocytes to interact, adhere to the endothelium, and transmigrate into the tunica intima to become macrophages. Macrophages phagocytose lipid deposited in the intima through several receptors, such as the scavenger receptor CD36. Macrophages take up modified LDL through CD36 and become foam cells. The formation of foam cells is the hallmark of atherosclerosis. Repeated cycles of inflammation promote the accumulation of macrophages/foam cells that leads to the formation of fatty streak and produces proinflammatory cytokines as well as a variety of mediators. The cytokines and mediators, including growth factors, can activate neighboring smooth muscle cells to replicate and migrate, contributing to lesion growth and the synthesis of components of the extracellular matrix, leading to plaque progression towards advanced lesions (146) (Fig 1.7). The advanced lesions are mainly composed of lipids, inflammatory cells, (such as macrophages), smooth muscle cells, and less extracellular matrix (collagen and proteoglycans) (147). In addition, the macrophages and smooth muscle cells release metalloproteinases, which are proteolytic enzymes that can break down collagen in a fibrous cap and leave the plaque prone to rupture, which results in thrombosis. Recent evidence indicates that plaque composition, rather than plaque size, is the real determinant of the plaque's evolution toward rupture (148). Not surprisingly, a vulnerable plaque has been associated with a high incidence of cardiovascular events, such as MI and stroke (149; 150).

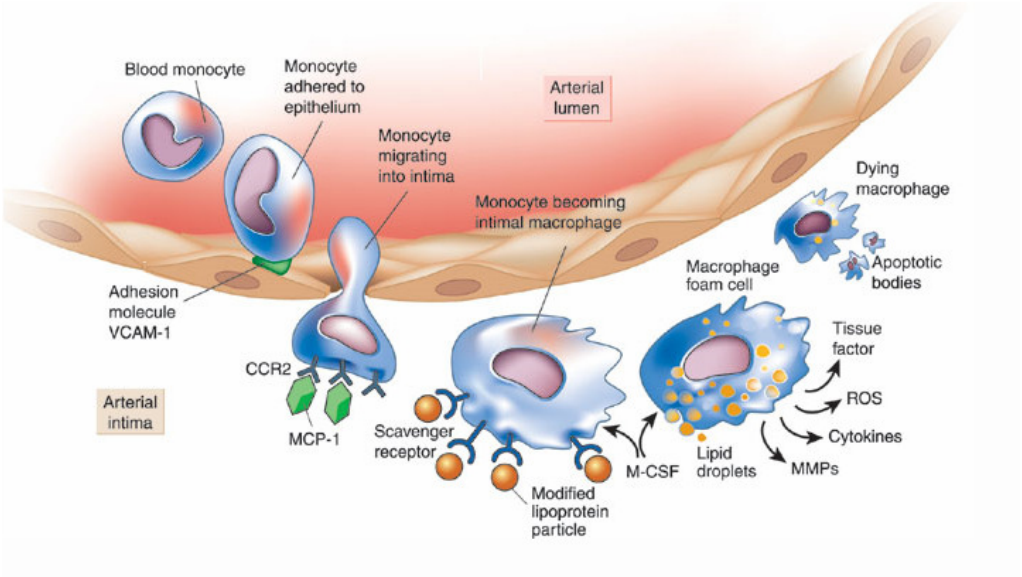

Figure 1.7 Steps in the recruitment of mononuclear phagocytes to the nascent atherosclerotic plaque. The steps are depicted in an approximate time sequence proceeding from left to right. The normal arterial endothelium resists prolonged contact with leukocytes including the blood monocyte. When endothelial cells undergo inflammatory activation, they increase their expression of various leukocyte adhesion molecules. Eventually the macrophages congregate in a central core in the typical atherosclerotic plaque. Macrophages can die in this location, some by apoptosis, hence producing the so-called 'necrotic core' of the atherosclerotic lesion. VCAM-1: Vascular cell adhesion molecule-1; MCP-1: monocyte chemoattractant protein-1; CCR2: MCP-1 receptor; MMPs: matrix metalloproteinases. (Adapted with permission from Libby P, Nature, 2002.) (204).

1.1.4.1.2 Apolipoprotein E Knockout Mouse-a Mouse Model for Atherosclerosis

Apolipoprotein E (ApoE) is 1 of 10 apolipoproteins that coat the surface of lipoprotein and mediate the metabolism of lipoprotein particles. ApoE is synthesized primarily in the liver, and plays a crucial role in receptor-mediated removal of lipoproteins from plasma (152). Via the LDL receptor and LDL receptor-related protein, apoE mediates the clearance of very low-density lipoproteins, chylomicrons and their remnants (153). Subjects with apoE

deficiency may develop type III hyperlipidemia. In addition to its role in lipoprotein metabolism, apoE has other functions, including antioxidant (154), anti-platelet aggregation (155), anti-proliferation (156), and prevention of the onset of Alzheimer's disease (157).

The apoE gene was the first lipoprotein transport gene to be deleted in mice, and in 1992, the ApoE knockout mice were developed (158). Of the genetically engineered models, the apoE -deficient model is the only one that develops extensive atherosclerotic lesions on a normal chow diet. It is also the model in which the lesions have been characterized most thoroughly. Numerous studies have demonstrated an accelerated atherogenesis in ApoE knockout mice (159). ApoE knockout mice have spontaneous elevations of total plasma cholesterol and triglycerides and reduced HDL. ApoE mice fed with regular chow develop arterial lesions in a time-dependent manner. Lesional distribution is centered in the aortic sinus in young mice, and the lesions are widely distributed throughout the arterial tree by the age of 8-9 months. In young mice (3-4 months), subendothelial foam cell deposits are present in the aortic sinus adjacent to valve attachment sites. By 5 months of age, foam cell deposits, free cholesterol, and mixed smooth muscle cells are present in developing atherosclerotic lesions. After 8-9 months of age, the arterial lesions show increased complexity with the presence of foam cells, smooth muscle cells, and a fibrous cap (160).

Atherosclerotic lesions and their development in ApoE knockout mice bear a striking similarity to the process of atherogenesis in humans (161), and hyperlipidemic rabbits (including fat-fed rabbits and Watanabe heritable hyperlipidemic rabbits) (162). Inflammation induces up-regulation of adhesion molecules, the interactions between leukocytes, and the endothelium, migration of leukocytes into the subendothelial space, and conversion of monocytes into macrophages and, ultimately, to foamy macrophages or foam cells (163; 164). The similarities with human lesion formation suggest that this particular mouse model could provide a fertile source for further investigations of atherogenesis.

Interestingly while the lesions of ApoE mice develop into fibrous plaques; no evidence suggest that plaque rupture occurs in this mouse model.

Another well-established mouse model for atherosclerosis is the LDL receptor-deficient model, which has elevated LDL levels and develops advanced lesions on the Western-type diet. Nevertheless, LDL receptor-deficient mice have no lesions, or have only very small lesions, if they are fed a chow diet.

1.1.5 Mediators that Contribute to the Development of Atherosclerosis Induced by Exposure to PM_{10}

1.1.5.1 Endothelium and Nitric Oxide Regulation, and Cardiovascular Dysfunction

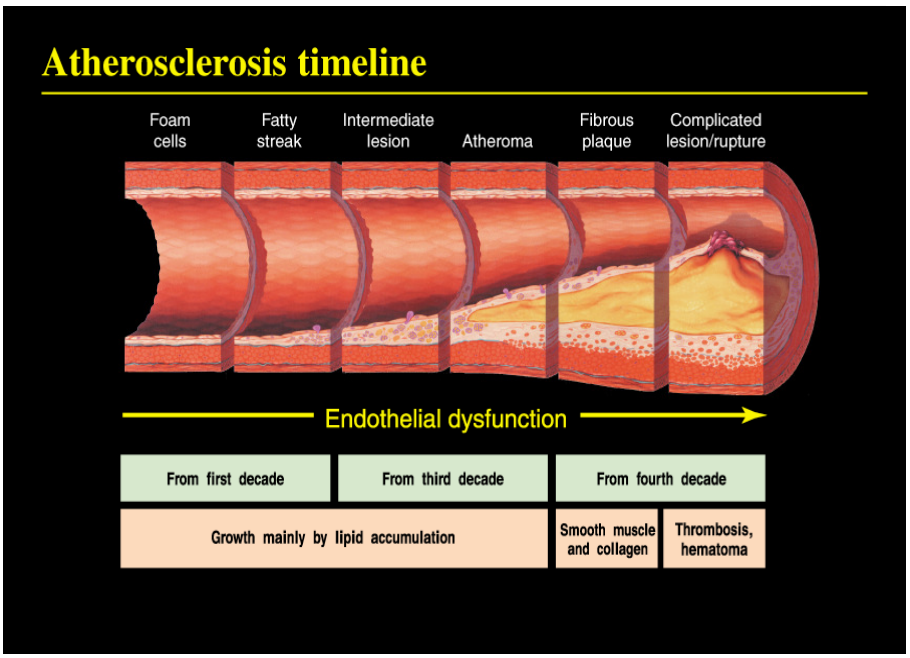

Figure 1.8 The timeline for endothelial dysfunction and the development of Atheroslcerosis (Adapted with permission from Stary HC, et al.*Circulation,*1995 (165).

The vascular endothelium is a single layer of cells representing the interface that separates the circulating blood from the rest of the vascular wall. The endothelium is a dynamic structure of cells that secrete multiple mediators (such as nitric oxide, NO) to control vascular tone, maintain vascular integrity, modulate platelet activity, influence thrombogenicity, and prevent cell migration and proliferation. The most studied aspect of endothelial function is the regulation of vascular tone. Endothelial cells contribute to the regulation of vascular tone by releasing several vasoactive factors, including potent vasodilators (such as NO, endothelium-derived hyperpolarizing factor, and prostacyclin), and vasoconstrictors (such as endothelin (ET)-1, thromboxane A2 (TXA2), prostaglandin H_2,), radical superoxide anion (O_2^-), and components of the renin-angiotensin systems).

NO was discovered by Furchgott and Zawadzki as a "endothelium-derived relaxing factor" (EDRF) in 1980 (166). NO is synthesized by a family of enzymes called NO synthase (NOS). The human genes for the NOS isoforms are officially categorized in the order of their isolation and characterization; thus, human genes encoding neuronal NOS (nNOS), inducible NOS (iNOS), and endothelial NOS (eNOS) are also termed NOS1, NOS2, and NOS3, respectively. eNOS is constitutively expressed by endothelial cells and regulated by transient increases of intracellular Ca^{2+} concentrations ($[Ca^{2+}]_i$) (167).

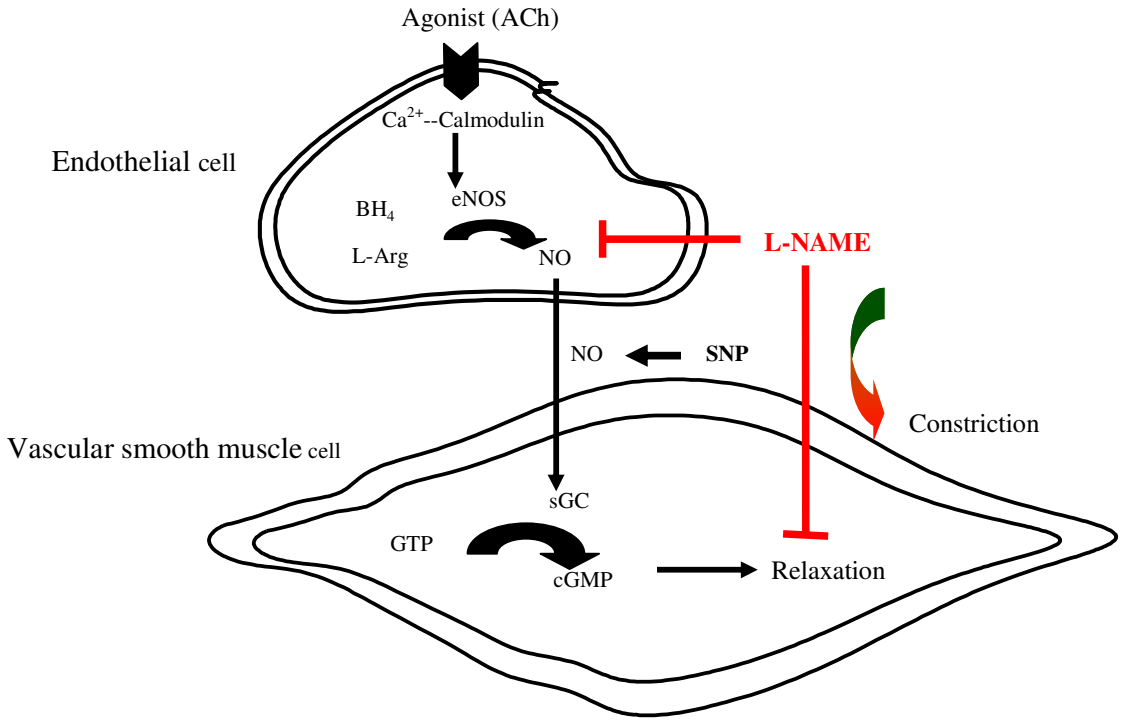

Figure 1.9 NO-mediated vasorelaxation

In a healthy vessel, the endothelium serves as the main source of NO production through eNOS activity. NO relaxes vascular tissue by stimulating soluble guanylate cyclase (sGC) to increase cyclic guanosine 3',5'-monophosphate (cGMP) levels in smooth muscle cells (221) (Fig 1.9).

sGC consists of a larger α (sGCα) and a smaller β (sGCβ) subunit. So far, four sGC genes have been indentified, encoding the sGC subunits α_1, α_2, β_1 and β_2. In many tissues; however, only α_1 and β_1 (sGCα) subunits appear to be present (169). The N-terminal domains of both the α_1 and β_1 subunits are essential for the stimulation of the enzyme by NO (170). NO is believed to freely pass through the lipid bilayer into the cytosol, bind to the smaller β_1 subunit, and, in turn, activate sGC.

In addition to modulating vascular tone, NO influences vascular homeostasis in many ways, including inhibition of smooth muscle cell proliferation, platelet aggregation, platelet and monocyte adhesion to the endothelium, LDL oxidation, expression of adhesion molecules, and endothelin production. NO can also stimulate endothelial cell proliferation and protect endothelial cells from apoptosis.

"Endothelial dysfunction" is now synonymous with decreased NO bioavailability, which can result from insufficient supply of co-factor (tetrahydrobiopterin, BH4) and/or substrate (L-arginine) (171), with increased oxidative stress and suppressed antioxidant enzyme activity. BH4 is a key cofactor for all NOS enzymes. In the absence of BH4, NOS produces superoxide, instead of NO (172). Inflammatory cytokines, such as IL-1β or TNF-α, can cause endothelial dysfunction or activation. Activated endothelial cells produce MCP-1, monocyte colony-stimulating factor (M-CSF), and IL-6, which further amplify the inflammatory cascade (173). The activation of the endothelium also attenuates eNOS activity and reduces in NO bioavailability. Reduced NO bioavailability up-regulates VCAM-1 and MCP-1 expression and promotes interactions of endothelial cells with monocytes, causing increased adhesion of monocyte and platelets, and a predisposition of the vessel to develop atherosclerosis (173;174). eNOS knockout mice have been found to be prone to atherosclerosis (175). Endothelial dysfunction can occur prior to the appearance of symptoms of cardiovascular diseases (140), and people with endothelial dysfunction have an increased risk for cardiovascular events, including atherosclerosis, coronary artery disease, diabetes, hypertension, and stroke.

PM_{10}-induced endothelial dysfunction has been observed in animal studies showing that an exposure to ambient particles impairs both stimulated and endogenous NO production (176-178). DEP significantly retarded the growth of human pulmonary artery endothelial cells (179). Inflammatory cytokines and increased levels of CRP following

exposure to ambient particles can also cause endothelial dysfunction by attenuating NO reactivity and up-regulating the expression of ICAM-1, VCAM-1 and E-selectin (181). Excessive ROS production following exposure to PM_{10} can rapidly scavenge NO and result in reduced NO bioavailability and endothelial dysfunction (182; 183). As a consequence of increased ROS production following exposure to PM_{10}, lipid oxidation and increased oxLDL can decrease eNOS expression (184). Peroxynitrite, produced by the reaction of superoxide anion with NO can also be a culprit for endothelial dysfunction and induce endothelial cell apoptosis (185-189). In addition, peroxynitrite can be rapidly decomposed to hydroxyl radical and nitrogen dioxide which may lead to cause endothelial injury (190).

ET-1 is a potent vasoconstrictor synthesized by the vascular endothelium (191). ET-1-mediated vasoconstriction occurs primarily through the ET_A receptor located on vascular smooth muscle cells. The ET_B receptor located on the vascular endothelium stimulates the production of NO and prostacyclin, and causes vasorelaxation, thus opposing the ET_A-mediated effects. Elevated plasma levels of ET-1 is another footprint of endothelial dysfunction. A variety of factors can directly stimulate endothelial cells to express ET-1 mRNA and release ET-1. These factors include cytokines, growth factors, and vasoactive substances, such as angiotensin II and vasopressin. ET-1 not only elicits significant vasoconstriction, but also activates monocytes and influences the inflammatory response by stimulating the production of monocyte chemoattractant proteins and modulating leukocyte-endothelial cell interactions, which promote the recruitment of leukocytes to the vessel wall (192). Under normal conditions, NO can balance and regulate ET-1 production (193). Nevertheless, plasma ET-1 concentrations are increased in patients with atherosclerosis and coronary artery disease, and are correlated with the severity of many cardiovascular diseases (194; 195). Animals that are exposed to urban PM have up to a 100% elevated levels of endothelin at 2 hours after exposure, and the effect lasts as long as two days (196). This time

course of elevated endothelin correlates well with the increase in acute coronary events associated with elevations in atmospheric PM (197). Short-term exposure to concentrated ambient particles caused significantly increased vasoconstriction of human brachial arteries and rat pulmonary resistance arteries due to increases in ET-1 (198; 199). Extended investigation found that particle inhalation potentiated the mRNA expression of preproET-1 and endothelin-converting enzyme (200). Up-regulation of inflammatory cells and cytokines in response to PM_{10} may stimulate ET-1 synthesis in vascular tissue by down-regulation of angiotensin-converting enzyme in endothelial cells (201; 202).

It has been well established that the status of endothelial cell function represents an integrated index of both the overall cardiovascular risk burden and the sum of all vasculature protective factors (203). Interestingly, endothelial dysfunction can be demonstrated in patients with risk factors for atherosclerosis in the absence of atherosclerosis itself (204; 205). These observations lend credence to the concept that endothelial dysfunction is integral to the development and progression of disease. Endothelial dysfunction could significantly contribute to the development of atherosclerosis, acute coronary syndromes, and MI associated with exposure to ambient particles.

1.1.5.2 iNOS and Cardiovascular Dysfunction

iNOS is not detectable in most cells under normal physiological conditions, but is rapidly up-regulated in response to cytokines and/or microbial products. Unlike Ca^{2+}-dependent activation of eNOS, the regulation of iNOS is independent of $[Ca^{2+}]_i$ (206). The induction of iNOS can be initiated by inflammatory cytokines, such as IFN-γ, TNF-α, or IL-1 (207), to trigger a chain of protein phosphorylation and eventually lead to the activation of transcription factor NF-κB, which is responsible for iNOS up-regulation.

NF-κB is persistently activated in advanced atherosclerotic lesions and its activation is linked to a wide variety of processes, including inflammation, proliferation, differentiation, and apoptosis (208). Evidence from the analysis of human, mouse, and rat iNOS promoters reveals that NF-κB activation plays a key role in regulating iNOS activity and expression. A classical signaling pathway for NF-κB activation is mediated via phosphorylation of two NF-κB inhibitory proteins, IκBα and IκBβ (209). These proteins bind NF-κB in the cytosol under basal conditions, but are degraded upon phosphorylation; hence releasing active NF-κB dimers, which translocate from the cytosol to the nucleus to activate transcription of iNOS and other genes (210). The inhibitory proteins are under complex temporal regulation, allowing for a transient phase of NF-κB activation that is mediated by the quick degradation and subsequent recovery of IκBα, which is followed by a persistent phase of activation mediated by the slower, long-term degradation of IκBβ (211). A large body of literature has demonstrated that ROS play an essential role in the activation of NF-κB (212).

Unlike the function of eNOS-derived NO, iNOS-derived NO is predominately produced by immunologically or chemically activated macrophages, as a function of an immune reaction to kill microorganisms and nitrosylates macromolecules. iNOS generates 100-1000-fold more NO than does eNOS (213). The local release of large amounts of "inflammatory NO" is often concomitantly generated with large amounts of superoxide anion from the same cell or adjacent cells, thus resulting in peroxynitrite ($ONOO^-$) production, which mediates the cytotoxic effects in the vasculature, such as DNA damage, lipid and protein oxidation, which contribute to the pathogenesis of atherosclerosis, MI and heart failure. The presence of iNOS mRNA and protein expression has been detected in macrophages, endothelial cells and smooth muscle cells of atherosclerotic human plaques (214). iNOS expression has been found not only in advanced stages of plaques, but also in the fatty streak stage, suggesting that iNOS plays an important role in both initiating and

promoting atherogenesis (215; 216). iNOS expression colocalizes with oxidized lipid and nitrotyrosine (a marker for peroxynitrite production) in advanced atherosclerosis, and the colocalization suggests that a vicious pathogenic environment is promoted by the enhancing of oxidative and nitrosative stress (217). A genetic deficiency of iNOS was shown to produce decreased atherogenesis, supporting the role of iNOS in atherogenesis (218).

1.1.5.3 CD36 and Cardiovascular Dysfunction

CD36 is a member of the class B scavenger receptor family, and functions as a scavenger receptor for oxLDL (219). CD36 can be expressed in a wide variety of cells and tissues, including macrophages, adipocytes, and striated muscle cells (220). CD36 is regulated by proatherogenic cytokines and lipids, and its levels also increase after exposure of cells to LDL and oxLDL (221). The positive feedback of CD36 expression from oxLDL results in the potential for continued lipid accumulation and foam cell formation, which is a characteristic component of atherosclerotic lesions and a major pathogenic event in the development of atherosclerosis. oxLDL has high affinity for CD36 (222) and evidence shows that 65-90% of the binding and uptake of oxLDL is CD36-dependent (222; 223). A high level of CD36 expression was found in macrophages/foam cells in human atherosclerotic lesions (223; 224). Macrophages, derived from mice lacking the CD36 scavenger receptor, demonstrate reduced uptake of modified LDL (225) and reduced atherosclerosis when crossed with the ApoE mouse (222). CD36 and ApoE double knockout mice show a profound (80%) decrease in atherosclerotic lesions compared to those seen in ApoE knockout mice (222), supporting the critical role of scavenger receptors in atherogenesis.

1.1.5.4 Peroxynitrite and Cardiovascular Dysfunction

Peroxynitrite is produced by the reaction of superoxide anion with NO. Generally, superoxide dismutase (SOD) is the major scavenger for removing superoxide. At normal physiological conditions, concentrations of NO that cause vasorelaxation are in the order of 5-10 nM, and do not effectively compete with SOD for superoxide to make peroxynitrite. Under pathophysiological conditions; however, when iNOS is up-regulated, iNOS can produce substantially higher concentrations of NO, which rise to micromolar concentrations and can effectively compete with SOD, since the reaction between superoxide and NO is 7,000-times faster than the reaction of SOD reaction with superoxide.

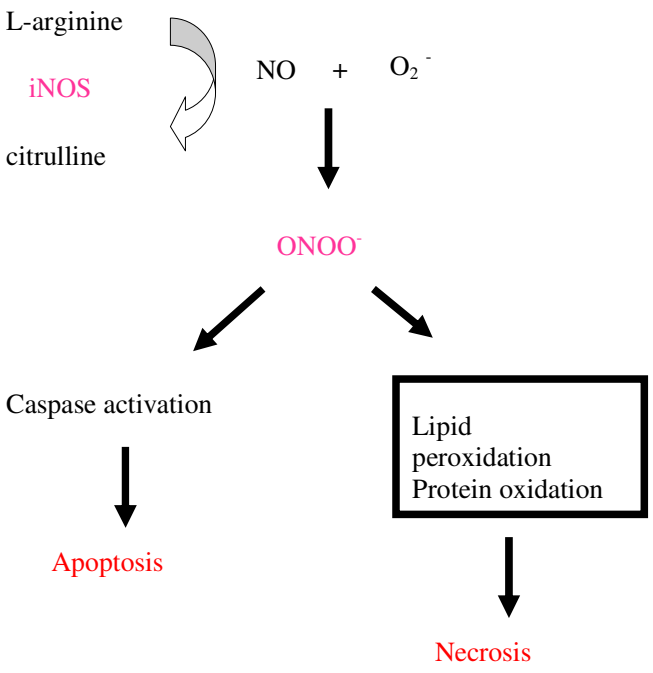

Figure 1.10 Peroxynitrite ($ONOO^-$) induced apoptotic and necrotic cell death

Peroxynitrite is a well-known culprit causing endothelial injury and many other cardiovascular dysfunctions. The major mechanisms of endothelial injury associated with peroxynitrite include suppression of the production of NO and induction of endothelial cell apoptosis (186-189). Peroxynitrite and its secondary radicals can lead to various oxidative damage to proteins, lipids and DNA, resulting in inactivated metabolic enzymes, ionic pumps, and structural proteins, disrupted cell membranes, and damaged nucleic acids, ultimately leading to the dysfunction of multiple cellular processes and the induction of cell death through both apoptosis and necrosis (228) (Fig 1.10).

1.1.5.5 PM_{10} Exposure and Oxidative Stress

Oxidative stress refers to a condition in which levels of free radicals or reactive oxygen/nitrogen species (e.g., O_2^-, H_2O_2, $ONOO^-$) are higher than normal. ROS are capable of exerting many adverse biological effects, such as lipid/protein/DNA oxidation, and initiation of proinflammatory cascades. Oxidative stress is often induced by, and elicits inflammatory processes, and the two processes are biologically linked.

iNOS, CD36, and peroxynitrite are important mediators of the ROS-regulated pathways. Leukocytes are major producers of ROS, secreted at sites of inflammation, when they phagocytose ambient particles. In addition, transition metals attached on the surface of ambient particles also contribute to ROS production (229-231). The relative importance of these two potential pathogenic factors has not been elucidated. It is believed that the induction of ROS rises first at the particle surface, and is then augmented by oxidants generated by recruited inflammatory leukocytes. The mechanisms underlying the generation of oxidative stress after exposure to PM have also not been clarified. Using an oxidant indicator dye, dichlorofluorescein, Donaldson and colleagues showed that ultrafine carbon black particles had much more surface free radical activity, compared to non-ultrafine

carbon black particles, suggesting a direct generation of oxidative stress at the particle surface (232).

Moreover, PM_{10}-modulated alteration of intracellular Ca^{2+} concentration ($[Ca^{2+}]_i$) has been suggested to be an additional mechanistic pathway mediating ROS generation (300; 301). PM_{10} and ultrafine carbon black induced rapid increases in $[Ca^{2+}]_i$ irrespective of the presence of metal chelators. Moreover, the inhibition of Ca^{2+} entry was associated with reduced levels of IL-6, IL-8, and TNFα transcription (230; 303). Support for a Ca^{2+}-modulated mechanism for ROS production was further strengthened by studies in both rat alveolar macrophages and human blood monocytes showing that UFPs stimulated the opening of voltage-gated Ca^{2+} channels, which consequently led to modifications in various oxidants via Ca^{2+}-mediated transcription factor activation (304; 305).

Ca^{2+} is a ubiquitous cellular second messenger that mediates a vast array of cellular processes. Elevation of intracellular Ca^{2+} activates signaling cascades that are able to target the nucleus, where they modify gene transcription via the activation of transcription factors such as NF-κB and the nuclear factor of activated T cells (306). Recent studies demonstrated that noncytotoxic doses of ultrafine carbon black particles and ultrafine latex particles induce alterations in Ca^{2+} signaling in both human monocytic cell lines and rat bronchoalveolar lavage cells (> 85% macrophages) (232). The data suggest that, in the presence of a second stimulus: for example, a proinflammatory mediator, UFPs can have a substantial effect on intracellular Ca^{2+} signaling pathways and, potentially, on the expression of proinflammatory genes. Moreover, susceptible individuals, including those with pre-existing inflammation, may be more responsive to ambient particle exposure because they are already primed for Ca^{2+} stimulation by the cytokines in the inflammatory milieu (238). Therefore, a Ca^{2+}-modulated signaling cascade could amplify and/or propagate the deleterious effects associated with ambient particles via ROS-dependent pathways.

Owing to their biological activity, ROS have the propensity to exacerbate cardiovascular endpoint interactions with lipids, proteins, and DNA. For instance, ROS stimulates lipid peroxidation to produce oxLDL, which is a stimulus for monocyte migration into the subendothelial space, an early step of atherogenesis (140; 239). Human CRP is able to acquire the ability to augment platelet reactivity when treated with a transition metal-ascorbate system that generates reactive oxygen intermediates (240). Moreover, a link has been found between oxidative stress and the potentiation of inflammation via activation of oxidative stress-responsive transcription factors such as NF-κB and activator protein 1, which control proinflammatory genes via redox changes (241). Furthermore, the generation of oxidative stress, especially via depletion of reduced glutathione, can increase the permeability of the lung epithelium (242), allowing for the passage of particles and particle-loaded macrophages into the interstitium and possibly to the circulation. Subsequently, particles could gain access to endothelial cells, the blood, and possibly be transported to other organs, though little evidence supports this hypothesis at the present.

1.1.5.6 Cyclooxygenase (COX) and Cardiovascular Dysfunction

Despite the wide use of non-steroidal anti-inflammatory drugs (NSAIDs) over the last century, the mechanism of NSAID action was not fully appreciated until 1971, when Vane published his seminal observations proposing that the ability of NSAIDs to suppress inflammation is primarily attributable to their ability to inhibit the cyclooxygenase (COX) enzyme (243).

COX (PGH synthase) is the key enzyme required for the conversion of arachidonic acid to prostaglandin G2 (PHG2) and PGH2, which are subsequently converted to a variety of eicosanoids, including PGE2, PGD2, PGF2a, PGI_2, and thromboxane A2 (TXA2). The array of PGs produced varies depending on the downstream enzymatic machinery present in

a particular cell type. For example, endothelial cells primarily produce PGI_2, whereas platelets mainly produce TXA2. Eicosanoids are critical regulators of several pathophysiological responses, including inflammation, blood clotting, wound healing, blood vessel tone, and immune responses.

Two COX isoforms have been identified, referred to as COX-1 and COX-2. In general, the COX-1 enzyme is produced constitutively by nearly all normal tissues (244), whereas COX-2 is inducible (e.g., at sites of inflammation), and the expression of COX-1 is low or undetectable under physiological conditions, except in the brain and kidney, where COX-2 is constitutively expressed.

COX-1 is a constitutive enzyme with its expression regulated developmentally. COX-1 produces prostaglandins in the endoplasmic reticulum, and these prostaglandins mediate many physiological responses via G protein-linked receptors (245). Prostaglandins, produced by COX-1, are responsible for the regulation of renal and sodium reabsorption, gastroprotection in the stomach, and vascular homeostasis. One important site of COX-1 function is at the platelet, where the enzyme is responsible for providing precursors for thromboxane synthesis, which are responsible for platelet aggregation and thrombogenesis (246). In endothelial cells, prostaglandins play a different role. The release of eicosanoids by activated platelets provides both a substrate and stimulus for the generation of prostacyclin (PGI_2) by the endothelium. PGI_2 stimulates vasodilatation, counteracting the vasoconstrictor, thromboxane.

In contrast to COX-1, COX-2 is an inducible enzyme, similar to iNOS, which is normally absent from tissues, but is expressed in response to a wide range of extracellular and intracellular stimuli, such as growth factors, tumour promoters, or cytokines (IL-1β and TNF-α) (245). COX-2 is expressed by cells that are involved in inflammation (e.g., macrophages and monocytes); thus it has emerged as the isoform primarily responsible for

the synthesis of the prostanoids involved in pathological processes, such as acute and chronic inflammatory states. The promoter of the COX-2 gene contains binding sites for several transcription factors, including NF-κB, the nuclear factor for IL-6 expression (NF-IL-6), and the cyclic-AMP response element binding protein (247).

Although COX-1 is mainly responsible for the biosynthesis of prostaglandins involved in homeostatic regulation, and COX-2 is primarily involved in producing prostaglandins in response to a wide spectrum of environmental insults and internal stimuli, the expression of both COX-1 and COX-2 have been detected in human atherosclerotic lesions (248). In symptomatic patients, the expression of COX-2 in atherosclerotic plaque is higher than that in asymptomatic patients (249). In addition, COX-2 knockout mice showed a 51% reduction in atherosclerotic lesions (250), and COX-2 inhibition had beneficial effects in patients with coronary artery disease by improving endothelium-dependent vasodilation and reducing low-grade chronic inflammation and oxidative stress (251).

1.2 Objective, Hypothesis, and Specific Aims

1.2.1 PM_{10} and Cardiovascular Diseases

Abundant epidemiological and experimental studies have consistently identified PM_{10} as a new and independent risk factor (in addition to smoking, hypertension, hyperlipidemia and diabetes) for developing and exacerbating of cardiovascular diseases. The risk of death from cardiac causes is much higher than from all other causes and significantly greater than from lung disease, which has been traditionally considered as the major adverse outcome of ambient pollutant exposure (77; 252; 253). Reductions in PM_{10} levels are linked with improvements in health outcomes (6; 27; 38; 254-255), and these findings not only indicate a causative effect of exposure to PM_{10} and health consequences, but also imply that PM_{10} effects are partly reversible.

Increased levels of ambient PM, as a consequence of rapid industrialization and urbanization, have become a major concern of public health professionals and the governments around the world. Positive steps have been taken by the governments to prevent and reduce ambient pollution since the London fog disaster in 1952. Nevertheless, a permanent reduction in urban ambient particles needs time. Because of its ubiquitous and involuntary nature, exposure to PM_{10} may continuously enhance the cardiovascular risk among millions of susceptible people worldwide in an often inconspicuous manner. Beyond serving as a simple trigger, exposure to PM_{10} can also elicit numerous adverse biological responses (such as systemic inflammation) that may further augment cardiovascular risk over the long term after months to years of exposure. Therefore, understanding the biological signaling pathways and then initiating medical prevention could be an immediate and effective strategy for alleviating PM_{10}-induced cardiovascular mortality and morbidity. Since the early 1990's, numerous researchers and clinicians have vigorously worked on delineating

the signaling pathways mediating exposure to PM_{10}-augmented cardiovascular morbidity and mortality; yet, the way in which PM_{10} negatively influences cardiovascular function has not been well understood. In any case, two hypotheses have been proposed. The majority of studies suggest that inhaled ambient PM provokes an inflammatory response in the lung, which causes lung inflammation with consequent release of prothrombotic and inflammatory cytokines into the circulation (81; 103; 104). Meanwhile lung inflammation stimulates the release of bone-marrow-derived neutrophils and monocytes that contribute to the secondary cardiovascular effects.

1.2.2 Shortcomings of Published Studies

Population and experimental-based studies have provided some insights into the mechanisms whereby exposure to PM_{10} promotes cardiovascular abnormalities, including endothelial dysfunction and increased blood pressure (22). Nevertheless, epidemiological studies, by their very nature, provide only a partial view of causative mechanisms. In addition, these epidemiological data are limited by imprecise measurements of the ambient particle levels. The evidence from mechanismic investigations is mainly from in vitro models or from a simplified approach (instillation model) injecting PM_{10} collected from filters or surrogate particles into the trachea. Despite several advantages of the instillation model, questions arise about how well instillation exposure can represent the inhalation in the real world. In addition, the recovery of particles on filters is variable, and a question may be asked whether or not all components can be retrieved in quantities that reflect the original particles.

In this dissertation, we conducted a study in a diesel exhaust (DE) exposure facility at the University of Washington, and overcame many shortcomings of the in vitro and instillation experiments. The facility consists of a DE exposure system, which incorporates a

diesel-electric generator for producing diesel exhaust. DE was sampled from the generator exhaust pipe, and then delivered to a dilution/ventilation system, where the concentrations were controlled and monitored. In addition, the temperature and humidity of the DE were conditioned and maintained before being conveyed to the animal exposure chambers.

1.2.3 Diesel Exhaust (DE)

Mounting evidence has consistently shown that traffic-derived pollution is strongly associated with increased cardiovascular diseases (256-258). The analyses of many cohort studies from different countries, including the United States (259), Germany (145), the United Kingdom (15), Canada (260), and the Netherlands (261), indicate that high traffic density and living near major roads are associated with increased cardiovascular mortality. Chronic exposure to traffic-generated PM has been linked with an increased risk of fatal MI in Sweden (262). Recently, an analysis from a cohort in the Netherlands demonstrated that traffic intensity was associated with cardiovascular mortality with the highest relative risk for ischemic heart disease after adjusting for higher levels of traffic noise (263). Another population-based study, with 4,494 subjects from Germany found that residential proximity to major roadways was associated with increased coronary atherosclerosis (145). Of the traffic-related air pollution, DE is the single biggest contributor, accounting for up to 90% of the total particles in some cities.

1.2.4 Objective, Hpothesis, Rationales, and Specific Aims

Recent analysis of the American Cancer Society data from 1.2 million adults residing in 50 states indicates that the largest specific cause of death associated with exposure to ambient PM is ischaemic heart disease, which accounts for 25% of all causes (40). Atherosclerosis plays an important role in the pathogenesis of ischemic heart diseases. The development of atherosclerosis is well known to result from the chronic inflammatory

response (140). Studies from our laboratory have reported that intratracheal instillation of PM_{10} promoted the development of atherosclerosis in Watanabe heritable hyperlipidemic rabbits (141). Nevertheless, no study using an inhalation model has demonstrated whether or not exposure to DE causes atherogenesis. *Thus, the overall objective of this work is to examine the impact of DE inhalation on the progression of atherosclerosis, and to investigate mechanismtic links between DE exposure and atherogenesis.*

1.2.4.1 Rationale for Specific Aim 1

ROS is known to be implicated in the development of atherosclerosis; and some human studies have directly investigated the occurrence of systemic oxidative stress in relation to DE, or traffic-related exposure (264). Bräuner and colleagues recently reported that the exposure to ambient urban particles derived from traffic led to DNA oxidation in healthy young adults (264). Studies of young adults, conducted in Denmark, also showed elevations in biomarkers of protein, lipid, and DNA oxidation induced by traffic-derived ambient particle exposure (265-267). Nevertheless, the morphological modifications of atherosclerostic plaques induced by DE inhalation have not been examined.

Specific Aim 1: Assess the impact of DE inhalation on atherogenesis by quantifying the compositional changes of atherosclerotic plaques, and relate these changes to the level of systemic oxidative stress.

1.2.4.2 Rationale for Specific Aim 2

Inducible nitric oxide synthase (iNOS) is up-regulated in response to inflammatory cytokines as part of the host defense responses (268), and can generate 100–1000-fold more nitric oxide (NO) than can eNOS. The large amount of locally released NO has been linked to the generation of harmful oxidative products, such as peroxynitrite, which is implicated in

the iNOS-mediated development of atherosclerosis (143; 186; 189). Atherosclerotic lesions were diminished in iNOS/ApoE double knockout mice (218; 269), suggesting that iNOS plays an important role in atherogenesis. iNOS over-expression was shown to be responsible for DEP-induced lung inflammation (186; 270), while iNOS knockout mice had a significant reduction of cytokines in the lung after exposure to ambient particles (271). Sun and colleagues recently reported that exposure ApoE knockout mice to concentrated ambient particles for six months increased the iNOS expression in the aortic root (143). The potential role of iNOS in the progression of atherosclerosis induced by exposure to DE; however, is still unknown.

Specific Aim 2: Examine the potential role of iNOS in atherogenesis induced by DE exposure.

1.2.4.3 Rationale for Specific Aim 3

Prostanoids play an imperative role in cardiovascular function, such as in regulating vascular tone, modulating the inflammatory response, control leukocyte-endothelial cell adhesion and in platelet aggregation (272). Cyclooxygenase (COX) is the key regulatory enzyme responsible for the formation of prostanoids. Two COX isozymes, COX-1 and COX-2, have been characterized, and implicated in cardiovascular diseases, such as atherosclerosis (250; 273). In vitro studies showed that exposure of PM_{10} to human airway epithelial cells induced overexpression of COX-2, which led to lung inflammation and injury (274). It was also reported that incubation of DE with human macrophage cells increased COX-2 protein and mRNA expression, which were associated with a subsequent increase in cholesterol accumulation and foam cell formation (275). Nevertheless, whether or not DE inhalation modifies COX-1 and/or COX-2 activity and expression in blood vessels has not been investigated.

Specific Aim 3: Determine the impact of DE inhalation on COX function and expression in blood vessels.

1.2.4.4 Rationales for Specific Aim 4

The endothelium, a monolayer of cells separating blood from the vascular wall, serves as an important regulator to maintain vascular tone and vasculature integrity (276-278). It does so by producing a number of mediators, in particular, nitric oxide (NO) and endothelin (ET). Endothelium-derived NO prevents blood vessels from developing atherosclerosis (279). Many in vitro and ex vivo experiments have demonstrated the capacity of DE attenuated NO-dependent dilation, which was mediated via proinflammatory and ROS-dependent mechanisms (183; 280-282). In contrast to NO, ET is a vasoconstrictor and implicated in the pathogenesis of atherosclerosis (283). Exposure to PM_{10} causes excessive ET-1 production (196), increased vascular sensitivity to ET-1 (284), and up-regulation of ET-1 mRNA expression (200), which results in exaggerated vasoconstriction and could contribute to vascular events such as MI and stroke. In any case, whether or not exposure to DE causes endothelial dysfunction, which could contribute to atherogenesis, is unknown.

Specific Aim 4: Assess the effects of exposure to DE on NO-mediated vascular endothelial function.

Chapter 2

Methodology

2.1 Exposure Protocol and Experimental Animals

2.1.1 DE Exposure System

DE was derived from a 2002 model turbocharged direct-injection 5.9 liter Cummins B-series engine (6BT5.9G6, Cummins, Inc., Columbus, IN) in a 100 kW generator set located just outside the laboratory. This engine is comparable to that used in heavy-duty road applications such as delivery trucks and school buses. Fuel is #2 un-dyed on-highway fuel from a commercial source that was remain stable throughout the experiments. Load is maintained at 75% of rated capacity, using a load-adjusting load bank (Simplex, Springfield, IL), throughout the experiments. All dilution air for the system was passed through HEPA, and carbon filters, permitting a filtered air control exposure option with very low particulate and gaseous organic pollutant levels (Table 2.1). The air entering the exposure room was conditioned to 18°C and 60% relative humidity. During the exposures, DE concentrations were continuously measured. Multistage samples were collected on a micro-orifice uniform deposition impactor (MOUDI; MSP, Shoreview, MN) which indicated a mass median diameter of 0.104 μm. The aerosol number-size distribution between 40nm and 2.5μm aerodynamic diameter were measured with a differential mobility analyzer (DMA), condensation particle counter sensor (CPC, 40 to 600nm) and an aerodynamic particle counter (APS, 500nm to 10μm). The two CPCs (one with 100 nm diffusion screen) provide assurance that the particle size distribution did not change between the intensive

characterization procedures. This measurement of the absolute number concentration as a function of particle size was made with 15-minute time resolution. Several gas phase chemicals (CO, CO_2, NO, NO_2, water vapor and hydrocarbon species) were monitored continuously using Fourier-Transformed Infrared Technology (FTIR).

The maximum 24-hour PM_{10} concentrations reported by US Environmental Protection Agency (EPA) range from 26 to 534 $\mu g/m^3$ (US Environmental Protection Agency: http://www.epa.gov/airtrends/msafactbook-db.pdf.). The exposure level (200$\mu g/m^3$) in this study was determined to reflect the ambient PM level of a heavy traffic condition. The average calculated exposure throughout a 24-hour period in our study was less than 35 $\mu g/m^3$, which is within the range of the National Ambient Air Quality Standard (285) and is environmentally relevant (15).

2.1.2. Animals and Exposure Protocol

Male ApoE knockout mice were housed in a temperature- and humidity-controlled environment with a 12-h light/dark cycle with free access to water, and standard rodent chow diet (Harlan Teklad). At the age of 30 weeks, these mice were moved to a "Biozone" facility adjacent to the exposure chamber where exposure was controlled by opening or closing a valve to animal cages resulting in minimal stress for animals during the exposure period. ApoE knockout mice (24/group) were randomly chosen and exposed for 7 weeks (5days/week, 6hrs/day) to DE at the concentration of 200 $\mu g/m^3$ particulate matter. Mice exposed to filtered air were the control. Animal procedures were approved by the Animal Care and Use Committee of the University of Washington.

2.2 Sample Collection

After exposure, sodium pentobarbital (100mg/kg, Abbott Laboratories, IL) and heparin sulfate (500U/kg) were administered intraperitoneally. Upon the loss of all reflexes,

blood was collected from inferior vena cava and put into EDTA tubes. Plasma was obtained after centrifugation of blood and stored at –80°C until assay. Urine was collected and kept at –80°C until assay. The thoracic aorta, aortic root, and the lung were carefully dissected from their connective tissues and kept in appropriate conditions until assay. The thoracic aorta was harvested and preserved in three ways for different analysis: 1) fresh tissue (~4mm) for vascular function study using wire myograph; 2) part of the thoracic aorta (~5mm) was embedded in OCT (Sakura Finetek)**,** rapidly frozen on dry ice, and kept at –80°C; 3) the rest of the thoracic aorta (~5mm) was fixed with 10% neutral formalin for 24 hours, then embedded in paraffin. Some of the aortic roots were fixed with 10% neutral formalin for 24 hours, then embedded in paraffin, and some of the roots were in OCT and rapidly frozen on dry ice, then kept at –80°C.

Table 2.1 Composition of Diesel Exhaust Particles (DEP) generated at the Northlake exposure facility.

	Filtered Air	DEP
$PM_{2.5}(\mu g/m^3)^*$	12.99	187.71
CO(ppm)	0.28	0.76
NO(ppb)	38.63	1515.80
NO2(ppb)	15.50	25.56
Particle #/cm^3	600	60,000

* Measured in the mouse cages.

2.3 Peripheral Band Cell Count

To examine the systemic inflammatory response, the peripheral band cell count was performed. Blood smears were fixed with methanol and stained with Wright staining (Sigma Chemicals). A hundred PMNs from randomly selected fields were manually counted and the percentage of band cells was determined.

2.4 Tissue Processing and Image Acquisition

Before staining, paraffin-embedded blood vessel sections were cut into 5μm thick section, deparaffinized in xylene and hydrated by passing through a series of graded alcohol, and cryosections (5μm) were air-dry for 1h, fixed with cold (4°C) acetone for 15min. After the sections were stained for specific targets as explained in details in the following sections, images were captured by a spot digital camera (Microspot, Nikon, Tokyo, Japan), coded and examined without knowledge of the experimental groups. The size of an atherosclerotic plaque, and its compositions were determined by quantitative a morphologic analysis explained in detailed in the following sections.

2.5 Morphometric Analysis of the Lung Tissue and the Composition of Atherosclerotic Plaque

2.5.1 Lung Tissue

Lungs were inflated via the trachea with 10% neutral formalin for 24 hours, cut into 4 longitudinal slices, embedded in paraffin blocks, sectioned at 5μm and stained with hematoxylin and eosin (H&E). The images were captured, coded, and analyzed using point counting method. Briefly, a grid of points was superimposed onto the captured images by Image Pro Plus software. The density of the grid, and the number of fields were selected to maintain the coefficient of error of the estimate of the volume below 0.1. The points that had contact with alveolar macrophages were counted. The volume fraction (V/v %) of alveolar macrophages was obtained by normalizing the total points on alveolar macrophages to the total points on the lung alveoli. In addition, 100 alveolar macrophages were randomly selected in these lung sections (4 views/sections total 16 views/mouse), and the number of alveolar macrophages positive for particles was enumerated.

2.5.2 Atheroslcerotic Lesions in Aortic Root

2.5.2.1 Lesion Size, Foam Cells, and Cellularity

Sections that contained three complete valve leaflets were stained with Movat pentachrome to quantify atherosclerotic lesion area, total cell counts, and foam cells. To identify foam cells, we stained the aortic root sections with rat monoclonal anti F4/80 antibody (1:50, AbD Serotec), a specific marker for mature mouse macrophages. Some of the foam cells were not stained with the F4/80 antibody, whereas some of these stained cells did not contain any lipid in their cytoplasm. Therefore, we used a combination of positive staining for F4/80 antibody, and Movat pentachrome staining, where foam cells or macrophages contain lipid in their cytoplasm to identify foam cells. The images were captured, coded, and analyzed using a grid of points superimposed onto the captured images by Image Pro Plus software. The volume fraction (V/v %) of atherosclerotic lesions was obtained by counting the total points falling in the atherosclerotic lesions divided by the total points on the valve leaflets area. Using the same method, total points for foam cells in atherosclerotic lesions were counted and normalized to the total points in the lesion area to obtain the volume fraction of foam cells in plaques. The nuclei of all cells in atherosclerotic lesions were also counted and normalized to the size of atherosclerotic lesion to obtain the volume fraction of cellularity.

2.5.2.2 Lipid Content of Plaque

Frozen aortic roots embedded in OCT (Sakura Finetek) were cut 5μm thick by a microtome. Sections that contained three complete valve leaflets were fixed in 4% paraformaldehyde at room temperature for 30 min, and stained with Oil-Red-O (Sigma Chemicals) to identify lipid in the plaques. The area of positive staining was quantified by

colour segmentation using Image Pro Plus software, and normalized to the area of atherosclerotic lesion to obtain the volume fraction (V/v %) of positive staining which represents the lipid.

2.5.2.2 Collagen Content of Plaque

Aortic root sections that contained three complete valve leaflets were stained in picro-sirius red (Sigma Chemicals) for one hour, washed in two changes of acidified water, dehydrated in three changes of 100% ethanol. Using Image Pro Plus software, the area of red staining was recognized, quantified by colour segmentation, and normalized to the area of the atherosclerotic lesion to obtain the volume fraction (V/v %) of positive staining for picro-sirius red, representing collagen content.

2.6 Vascular Function Study

Thoracic aortae were carefully cleaned off connective tissue without damaging the endothelium, and placed in ice-cold physiological salt solution (PSS). The vessels were cut to 2mm rings and mounted on a wire myograph (Model 610M; Danish Myo Technology, Aarhus, Denmark). Each vessel was bathed in oxygenated PSS at 37°C for an hour during which the resting tension was gradually increased to 6mN with three changes of PSS at 10 minute intervals followed by stabilizing the vessels at resting tension (6mN) for 30min. Thereafter, the vessels were stimulated with 80 mM KCl twice. Smooth muscle contractility was studied by the addition of cumulative concentrations of phenylephrine (PE, 1nM-10μM). To examine the impact of DE on iNOS activity, 1400W, a specific inhibitor for inducible NO synthase (iNOS), was used. To access the effect of DE exposure on cyclooxygenase (COX), indomechacin (1μM) was applied. To examine the specific roles of COX1 and COX2, SC560 (10μM) and NS398 (10μM) were used to inhibit COX1 and COX2,

respectively. To examine the impact of DE exposure on the ET-1 production, the ET receptor antagonist (bosentan, 10μM), the selective inhibitors for ET_A (BQ123, 10μM), and ET_B (BQ788, 10μM) were administered, respectively. PE (1nM-10μM) dose-response curves were conducted before and after incubating with these antagonists, respectively.

Once a sustained constriction was evoked, cumulative concentrations of ACh (1nM-10μM) or SNP (1nM-10μM) were applied to evaluate endothelium-dependent or independent NO-mediated vasodilation, respectively. To examine the effect of DE exposure on the endogenous NO production, the vessels were incubated with *N*G-nitro-L-arginine-methyl ester (L-NAME; 200μM), a NO synthase (NOS) inhibitor.

2.7 Immunohistochemical Analysis of Macrophages (F4/80), iNOS, CD36, Nitrotyrosine, α-actin, COX-1, COX-2, eNOS, and sGC Expression

Paraffin-embedded thoracic aorta and aortic root sections that contained three complete valve leaflets were deparaffinized in xylene and hydrated by passing through a series of graded alcohol. Citrate buffer (Invitrogen) was used for antigen retrieval. Sections were then incubated with 10% goat serum at room temperature for 30min to block non-specific binding proteins. Aortic root sections were respectively incubated with these antibodies: rabbit polyclonal biotinylated antibodies to inducible nitric oxide synthase (iNOS) (1:100, Santa Cruz); CD36 (1:50, Santa Cruz); nitrotyrosine (NT) (1:400, Upstate Biotechnology), α-actin (1:600, Abcam), COX-1 (1:150, Cayman Chemical), COX-2 (1:100, Santa Cruz), and rat monoclonal biotinylated anti F4/80 antibody (1:50, AbD Serotec) at 4°C overnight. Thoracic aorta sections were incubated with rabbit polyclonal antibodies to COX-1 (1:150, Cayman Chemical), COX-2 (1:100, Santa Cruz), sGCα1 (1:200, Abcam) and sGCβ1 (1:200, Abcam) at 4°C overnight. Negative controls were included with non-immune isotype antibody, or omission of the primary antibody. Subsequently, sections were

incubated with biotinylated goat anti rabbit IgG (1:800, Vector Laboratories) at room temperature for 30min, followed by avidin-biotin conjugated alkaline phosphatase, and Vector red (Vector Laboratories) to detect the antigen-antibody complexes.

To detect the eNOS expression in the thoracic aorta, cryosections (5μm) were air-dry for 1h, fixed with cold (4°C) acetone for 15min. M.O.M. kit (Vector Laboratories) was used to block non-specific binding proteins following the manufacture's instruction. Thereafter, sections were incubated with monoclonal anti-eNOS antibody (1:50, BD Transduction Laboratories) at room temperature for 1h, followed by M.O.M biotinylated anti-mouse IgG (Vector Laboratories) at room temperature for 10min, then incubated by avidin-biotin conjugated alkaline phosphatase and Vector red (Vector Laboratories) to detect the antigen-antibody complexes.

The positive red staining was recognized, quantified by colour segmentation analysis using Image Pro Plus software, and normalized to the area of the atherosclerotic lesion in aortic roots, or normalized to the thickness of the vascular wall for the sGC expression, or normalized to the length of the intima for the eNOS expression, to obtain the volume fraction of each specific protein expression.

2.8 Western Immunoblotting Analysis of iNOS Expression

Due to limited quantity of vessel samples, the heart tissues were used to evaluate the iNOS expression by western immunoblotting. The frozen heart tissues were homogenized in 10 volumes of ice-cold RIPA buffer (Sigma Chemicals) supplemented with protease inhibitor cocktail (Roche Diagnostics). Supernatant was obtained following centrifugation of homogenates at 12,000 rpm for 15 min, and the protein concentration was quantified by Bradford method using Bio-Rad DC Protein Assay kit according to the manufacturer's instructions (Biorad). Protein samples (40μg/lane) were separated on 7.5% SDS-PAGE gel,

subsequently electrotransferred to polyvinyldifluoride membranes (Biorad) and blocked with 5% bovine serum albumin (BSA) dissolved in 0.1% TBS-Tween 20 for 60min at room temperature. The membrane was incubated with specific primary antibody for iNOS (1:500, Santa Cruz) at 4°C overnight, followed by 1-hour incubation with horseradish peroxidase–conjugated goat anti-rabbit IgG (Santa Cruz). Immunoreactive bands were visualized by enhanced chemiluminescence kit (Amersham Life Sciences). Densitometry was carried out using Image J (NIH), and the results were expressed in optical intensity per mg protein.

2.9 ELISA of NF-κB (p65) Activity

Nuclear extracts from the frozen heart tissues were obtained using nuclear extract kit (Cayman Chemical). Protein concentrations of the nuclear extract were quantified by Bradford method using Bio-Rad DC Protein Assay kit according to the manufacturer's instructions (Biorad). NF-κB (p65) activity in the nuclear extracts from heart tissues was measured by enzyme-linked immunosorbent assay (ELISA) using the NF-κB (p65) transcription factor kit (Cayman Chemical) according to the manufacturer's instructions. This kit is a non-radioactive, sensitive method for detecting NF-κB (p65) DNA binding activity in nuclear extracts as a replacement for the radioactive electrophoretic mobility shift assay. Results were expressed as absorbance (450nm) per mg protein.

2.10 Assessment of Systemic Oxidative Stress

It has been reported that isoprostanes are stable end products of arachidonic acid peroxidation (391). Of the variety of isoprostanes detected, 15-F_{2t}-isoprostane (15-F_{2t}-IsoP) has been found to be a specific, reliable marker of lipid oxidation. Urine samples were purified using 8-isoprostane affinity sorbent, and the levels of 15-F_{2t}-IsoP in urine were

measured using 8-Isoprostane EIA kit according to the manufacturer's instruction (Cayman Chemical). Urine creatinine levels were measured by creatinine assay kit (Cayman Chemical). The results were expressed in pg of 15-F_{2t}-Iso per mmol creatinine.

8-hydroxy-2-deoxy guanosine (8-OH-dG) is produced by oxidative damage of DNA due to the production of reactive oxygen and nitrogen species, and has been served as an established marker for DNA oxidation. Because of the complexity of plasma samples, urine is more suitable for measuring free 8-OH-dG. 8-OH-dG concentration was measured using 8-OH-dG kit (Cayman Chemical). The urine creatinine levels were measured by creatinine asssy kit (Cayman Chemical). The results were expressed in pg of 8-OH-dG per mmol creatinine.

2.11 Measurement of Urine 2,3-dinor-6-keto prostaglandin F1α

2,3-dinor-6-keto prostaglandin F1α is a major urinary metabolite converted from PGI_2. PGI_2 level was assessed by measuring urine 2,3-dinor-6-keto prostaglandin F1α using an EIA kit according to the manufacturer's instruction (Cayman Chemical). The urine creatinine levels were measured by creatinine asssy kit (Cayman Chemical). The results were normalized to urine creatinine levels and expressed in pg/ml PGI_2 per mg/dl creatinine.

2.12 Measurement of Plasma Nitrite and Urine cGMP

Under physiological conditions, within a few seconds, NO is oxidized to nitrites or nitrates, which are stable metabolites of NO. Plasma NO levels were assessed by measuring nitrite levels using a NO-specific chemiluminescence analyzer (Sievers, Boulder). cGMP was measured in urine using cGMP EIA kit according to the manufacturer's instruction (Cayman Chemical). Creatinine levels were measured by creatinine assay kit (Cayman Chemical).

2.13 Real-Time Reverse Transcription Polymerase Chain Reaction (RT-PCR) of mRNA Expression of iNOS, NT, NFκB, COX1, COX2 and PGI_2 in the Heart, and mRNA Expression of eNOS and sGCα in the Abodominal Aorta

Total RNA was extracted from the heart tissues or the abdominal aortae (for eNOS, and sGC) using RNeasy Fibrous Tissue Mini Kit (Qiagen). RNA concentration was measured using Nanodrop (Thermo Scientific). Reverse transcription was performed using a RT kit (Invitrogen). The same amount of RNA was loaded in triplicates for each assay, and RT-PCR was performed using TaqMan Universal PCR master mix (Applied Biosystems) according to the manufacturer's instructions. The mRNA expression of iNOS, NT, NFκB, COX1, COX2, PGI_2, eNOS, sGC, β-actin, and hypoxanthine phosphoribosyltransferase-1 (HPRT1) was measured by qRT-PCR (TaqMan) using the ABI Prism 7900HT sequence detection system (Applied Biosystems, 40 cycles consisting of 15s at 95°C and 1min. at 60°C). The values of gene expression were calculated based on the comparative threshold cycle (Ct) method, normalized to the expression values of β-actin and HPRT1, and displayed as ratio relative to β-actin.

2.14 Solutions and Chemicals

The PSS consisted of the following (in mM): NaCl 119, KCl 4.7, KH_2PO_4 1.18, $NaHCO_3$ 24, $MgSO_47H_2O$ 1.17, $CaCl_2$ 1.6, glucose 5.5 and EDTA 0.026. All reagents were purchased from Sigma Chemicals unless specifically mentioned.

2.15 Statistical Analysis

Results are reported as mean±SEM. The statistical significance was evaluated using the Student's t test for unpaired values of two groups. The concentration-response curves of

the different groups were compared by ANOVA for repeated measurements followed by Bonferroni's correction. $P<0.05$ was considered to be significant. In all experiments, n equals the number of mice from which samples were obtained.

Chapter 3

Changes in Atherosclerotic Plaques Induced by Inhalation of Diesel Exhaust[1]

3.1 Introduction

Epidemiological studies conducted over the past 20 years showed that exposure to ambient particulate matter air pollution with aerodynamic diameter less than 2.5μm ($PM_{2.5}$) maybe an independent risk factor for increased cardiovascular morbidity and mortality (22; 257), and recent studies suggest that reducing ambient particles resulted in declined cardiovascular morbidity and deaths (37; 38). Evidence from other and our own laboratories suggested that the deposition of particles in the lung causes alveolar inflammation resulting in a systemic inflammatory response that impacts blood vessels (5), which could be responsible for the downstream adverse cardiovascular effects (22). This hypothesis is supported by several animal studies (6-8), and human studies showing that an elevation of 10 $\mu g/m^3$ or 20 $\mu g/m^3$ in $PM_{2.5}$ was associated with 5.9% or 12.1% increases in the development of atherosclerosis, respectively (144).

Inflammation plays a central role in all stages of atherosclerosis development (398). Exposure to ambient PM results in excessive production of reactive oxidative species (ROS) (287). ROS contribute to many cardiovascular complications via exacerbating interactions with lipids, proteins, and DNA. For instance, in vitro study showed that diesel exhaust

---

[1]A modified version (with more detailed Methods) of this chapter has been published. Ni Bai, Takashi Kido, Hisashi Suzuki, Grace Yang, Terrance J. Kavanagh, Joel D. Kaufman, Michael E. Rosenfeld, Cornelis van Breemen, Stephan F. van Eeden (2011). *Atherosclerosis*.

particles (DEP)-induced ROS exerted lipid peroxidation to produce oxidized low-density-lipoprotein (oxLDL), which can serve as a stimulus for monocyte migration into the sub-endothelial space representing an key step in atherosclerosis (140; 181). These monocyte-derived macrophages phagocytose oxLDL, contributing to foam cell formation, and the development of fatty streaks, a hallmark of early atherosclerotic lesion (141). Macrophage CD36 is the major scavenger receptor for oxLDL, hence promoting the progression of atherosclerosis (403). Active unstable atherosclerotic plaques are characterized by increased lipid accumulation, foam cell formation, smooth muscle migration from the sub-endothelial layer, and a thin fibrous cap (289). Plaque disruption and atherothrombosis are the underlying causes of approximately 60-80% of all sudden cardiac deaths (290).

Diesel exhaust (DE) is a major component of urban $PM_{2.5}$, accounting for up to 90% of the fine particulate mass in ambient air of many major cities, such as London (291). DE is a mixture of fine particles and gases, and represents a useful model of traffic-related air pollutants. The particulate from DE consists of a central carbon core nucleus onto which an estimated 18,000 combustion products are adsorbed, including organic chemicals, such as polycyclic aromatic hydrocarbons, and transition metals (19; 292).

Recent studies have shown an association between progression of atherosclerosis and people living near major roads, and traffic-related air pollution exposure and acute coronary events (293). The association between DE exposure and cardiovascular diseases is compelling; however, the impact of DE exposure on atherogenesis is poorly understood. In this study, we exposed ApoE knockout mice to DE via whole-body inhalation for 7 weeks, and measured morphological alterations of atherosclerotic lesions to test the hypothesis that DE inhalation causes changes in atherosclerotic plaque characteristic of unstable plaque or plaque vulnerable to cause acute vascular events. We also explored the impact of the

magnitude of DE exposure, and downstream oxidative stress on changes in plaque morphology.

3.2 Methods and Materials (Please refer to Chapter 2 for details)

3.2.1 Methods

Male ApoE knockout mice fed with regular chow, at the age of 30-week old, were exposed for 7 weeks (5days/week, 6hrs/day) to DE (200 μg/m^3 of particulate matter). Mice exposed to filtered air were the control. After exposure, mice were euthanized, and the plasma, thoracic aorta, aortic root and lung were collected and kept at appropriate conditions until assay.

Blood smears were fixed with methanol and stained with Wright staining. A hundred PMNs from randomly selected fields were manually counted and the percentage of band cells was determined.

Plasma cholesterol and triglyceride levels were measured using commercially available kits.

For morphometric analysis, images were captured by a spot digital camera (Microspot, Nikon, Japan), coded and analyzed using Image Pro Plus software. 10-12 fields per view for each animal were randomly chosen.

Lung were inflated and fixed with 10% neutral formalin for 24 hours, sectioned at 5μm and stained with hematoxylin and eosin (H&E). Random images (16 views/mouse) were captured to represent the whole lung and analyzed using point counting to determine the volume fraction (V/v%) of alveolar macrophages. The V/v% of alveolar macrophages positive for particulate matter was measure of the magnitude of lung exposure.

Aortic root was used to quantify compositional changes in plaque. Aortic root tissues were fixed with 10% neutral formalin for 24 hours, embedded in paraffin, sectioned at 5μm

and stained with Movat pentachrome to determine the V/v% of plaques size, total cell counts (plaque cellularity), and foam cells. The nuclei of cells in each lesion were enumerated and normalized to the plaque size. Picro-sirius red staining was used to identify collagen content in aortic root lesions. Frozen aortic root tissues were embedded in OCT, sectioned at 5μm, stained with Oil-Red-O and the V/v of positive staining was determined.

The expression of iNOS, CD36, nitrotyrosine, and α-actin was quantified after immunohistochemical staining for aortic root tissues. Sections were incubated with antibodies F4/80, a marker for mature macrophages (1:50); inducible nitric oxide synthase (iNOS) (1:100); CD36 (1:50); nitrotyrosine (NT) (1:400), and α-actin (1:600) at 4°C overnight. Subsequently, sections were incubated with biotinylated goat anti rabbit IgG (1:800), followed by avidin- biotin conjugated alkaline phosphatase and Vector red (Vector Laboratories) to detect the antigen-antibody complexes. The area of positive staining was recognized, and the volume fraction (V/v %) of iNOS, CD36, and NT was determined.

Urine samples were purified using 8-isoprostane affinity sorbent, and the concentration of 15-F_{2t}-isoprostane (15-F_{2t}-IsoP), a marker of lipid oxidation, was measured using a 8-Isoprostane EIA kit. As a marker of DNA oxidation, 8-hydroxy-2-deoxy guanosine (8-OH-dG) concentration was measured using a 8-OH-dG kit. Creatinine levels were measured by a creatinine assay kit. Plasma MPO levels were also measured using a myeloperoxidase (MPO) ELISA kit.

3.2.2 Statistical Analysis

Data are shown as mean±SEM. The statistical significance was evaluated using the unpaired Student's t test for simple comparison between two values. Linear regression modeling was used to assess the relationship between exposure markers (alveolar macrophages with particles) and compositional changes in plaques and oxidative stress

markers. In all experiments, n equals the number of mice from which samples were obtained. P<0.05 was considered to be significant.

3.3 Results

3.3.1 Plasma Lipid

To examine whether DE exposure had any effect on the lipid profile, we measured plasma cholesterol and triglyceride. The plasma cholesterol and triglyceride level were similar after exposure to DE, compared with the filtered air control (Table 3.1).

Table 3.1 Plasma cholesterol and triglyceride level (Values are mean±SEM).

	Filtered air	DE	
Cholesterol (M)	26.2 ± 1.0	28.0 ± 1.8	n=12, P=0.4
Triglyceride (mg/dl)	135.8 ± 11.8	140.6 ± 12.9	n=12, P=0.8

3.3.2 Alveolar Macrophages in the Lung Tissue

DE exposure significantly increased the number of alveolar macrophages positive for particles (3.5±1.2% in Filtered air vs.85.7±1.7% in DE; p<0.0001) (Fig.3.1A). The total number of alveolar macrophages was also increased in DE exposure group, compared with filtered air exposure (1.3±0.2% vs.10.2±1.1%; Filtered air vs. DE; p<0.01) (Fig.3.1B).

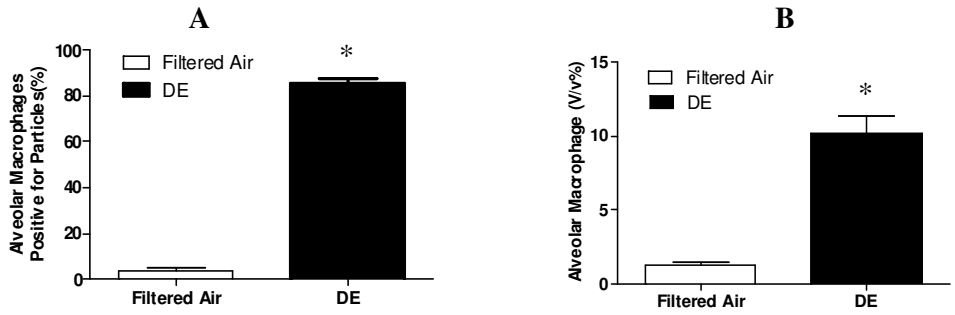

Figure 3.1 Exposure effects. A) Exposure to DE increased the number of alveolar macrophages positive for particles, n=10, *P<0.0001; B) Total alveolar macrophages were also increased after DE exposure, n=9, *P<0.01. Values are mean±SEM.

3.3.3 Increased Circulating Band Cells and Positive Correlation with Lung Inflammation

The blood smear band cell counts were significantly higher after DE exposure than the control (filtered air) (Fig.3.2A). In adition, the elevation of band cell counts was positively correlated with increased alveolar macrophages (Fig.3.2B), suggesting a strong link between lung inflammation, and the systemic response.

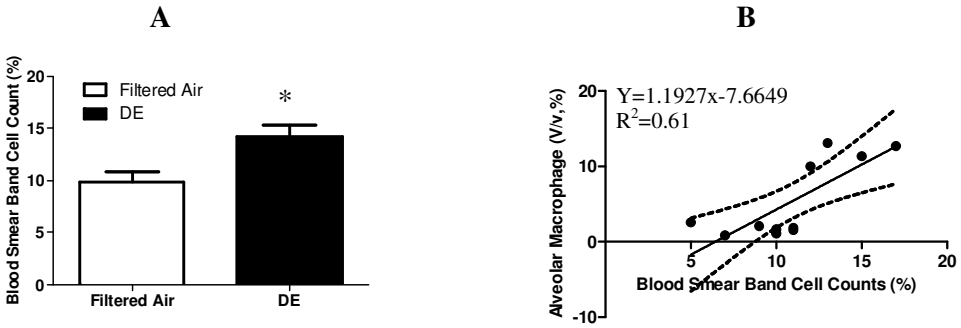

Figure 3.2 Circulating band cell counts and their relationship with alveolar macrophages. A) Increased circulating band cells after DE exposure, compared with the filtered air exposure. n=12, *P<0.01;. B) Positive correlation between circulating band cells and alveolar macrophages, P=0.0045. Values are mean±SEM.

3.3.4 Compositional Changes in Atherosclerotic Plaque

Figure 3.3A, C, and E show different morphological features of plaques on Movat stains. There was no difference in the volume fraction of the size of atherosclerotic lesions between DE and filtered air exposed mice (Fig.3.3B). Histological characterization of plaque morphology reveals that DE exposure increased plaque cellularity (70.0±4.0 vs. 100.0±9.8cells/100μm of lesion area; Filtered air vs. DE; $p<0.02$) (Fig.3.3D), foam cell formation (12.2±1.7% vs. 28.1±7.8%; Filtered air vs DE; $p<0.04$) (Fig.3.3G), increased lipid accumulation (16.1±2.1% vs. 31.9±4.7%; Filtered air vs. DE; $p<0.02$) (Fig.3.4A,B,C), and smooth muscle cell content (7.5±2.0% vs. 25.5±9.1%; Filtered air vs DE; $p<0.05$) (Fig.3.4D,E,F). We observed a trend for decreased collagen content of plaques (90.2±9.6% vs. 69.4±9.1%; Filtered air vs DE; $p>0.05$) (Fig.3.4G,H,I). The proteoglycan content of plaques was similar between DE and filtered air exposure groups (Appendix A).

A

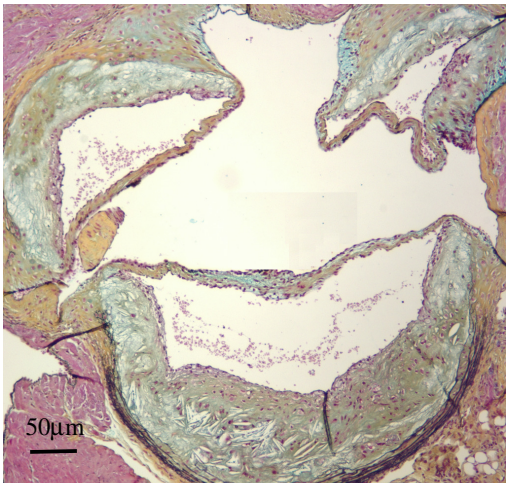
50µm

B

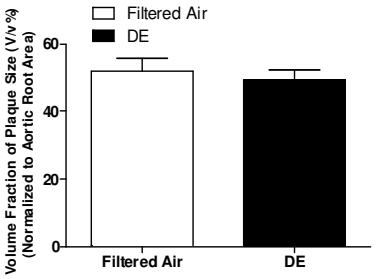
Filtered Air
DE
Volume Fraction of Plaque Size (V/v%)
(Normalized to Aortic Root Area)
60
40
20
0
Filtered Air
DE

C

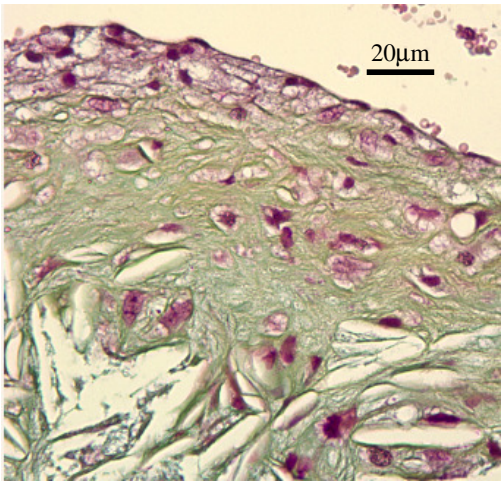
20µm

D

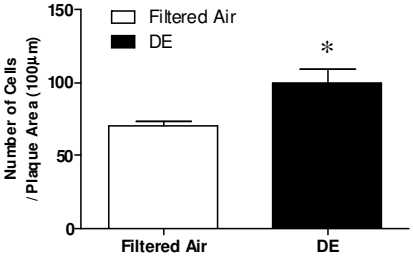
Filtered Air
DE
Number of Cells
/Plaque Area (100µm)
150
100
50
0
*
Filtered Air
DE

E

F

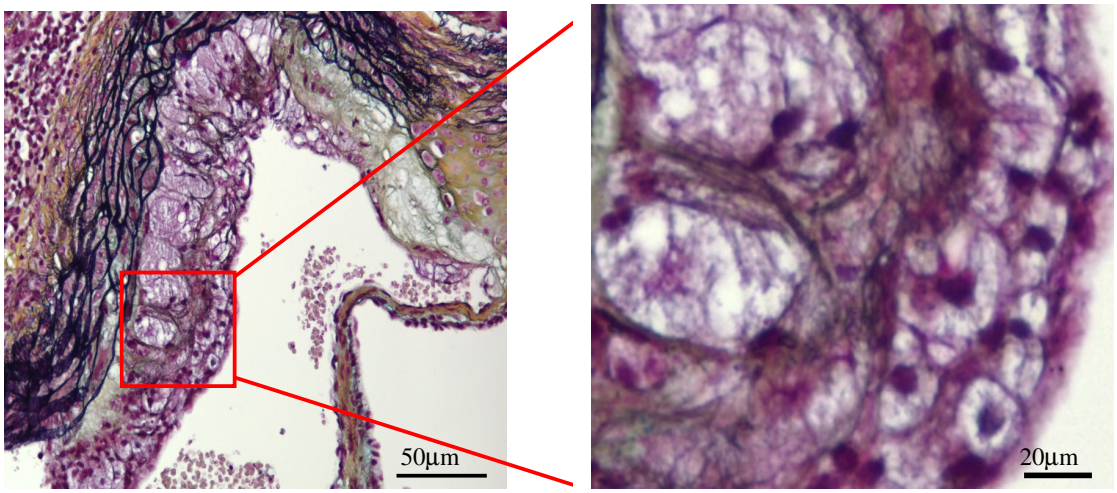

G

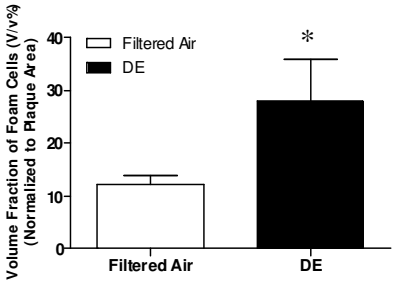

Figure 3.3 Movat staining analysis of atherosclerotic lesion size, cellularity and the number of foam cells in aortic root. A) Representative photomicrographs of Movat staining for plaque size analysis (100X); B) No changes in volume fraction of the size of aortic root lesions were observed, n=10, P>0.05; C) Movat staining for total cell count (400X); D) The cellularity in atherosclerotic lesion was significantly increased after DE exposure, n=9, *P<0.02; Movat staining for foam cells E) (200X); F) (400X) G) DE exposure significantly increased foam cells formation, n=8, *P<0.04. Values are mean±SEM.

Filtered Air

DE

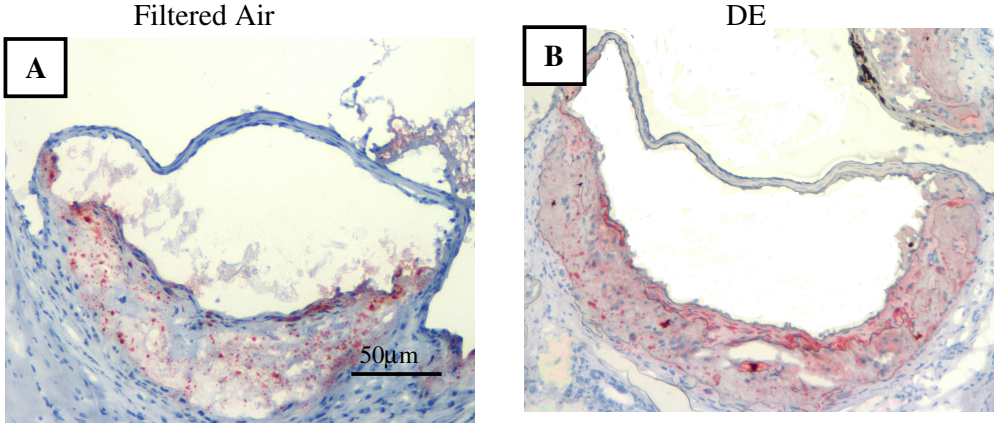

C

Filtered Air

DE

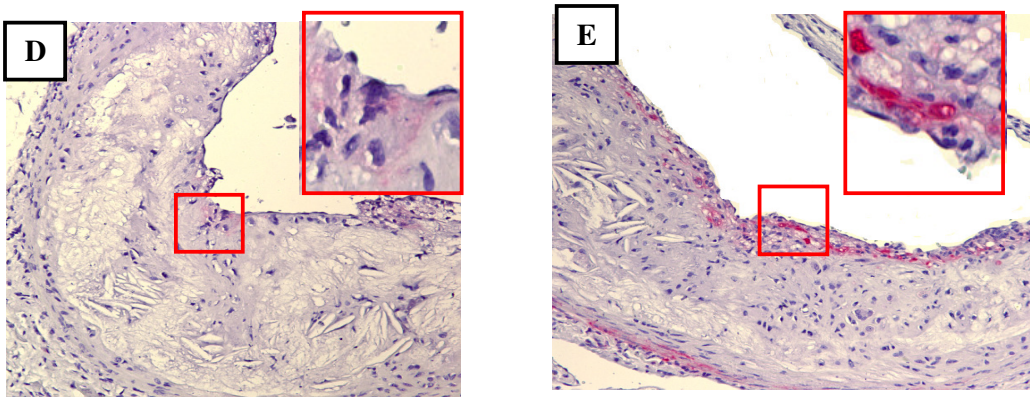

F

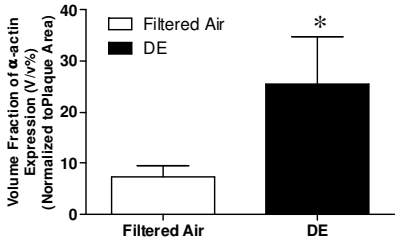

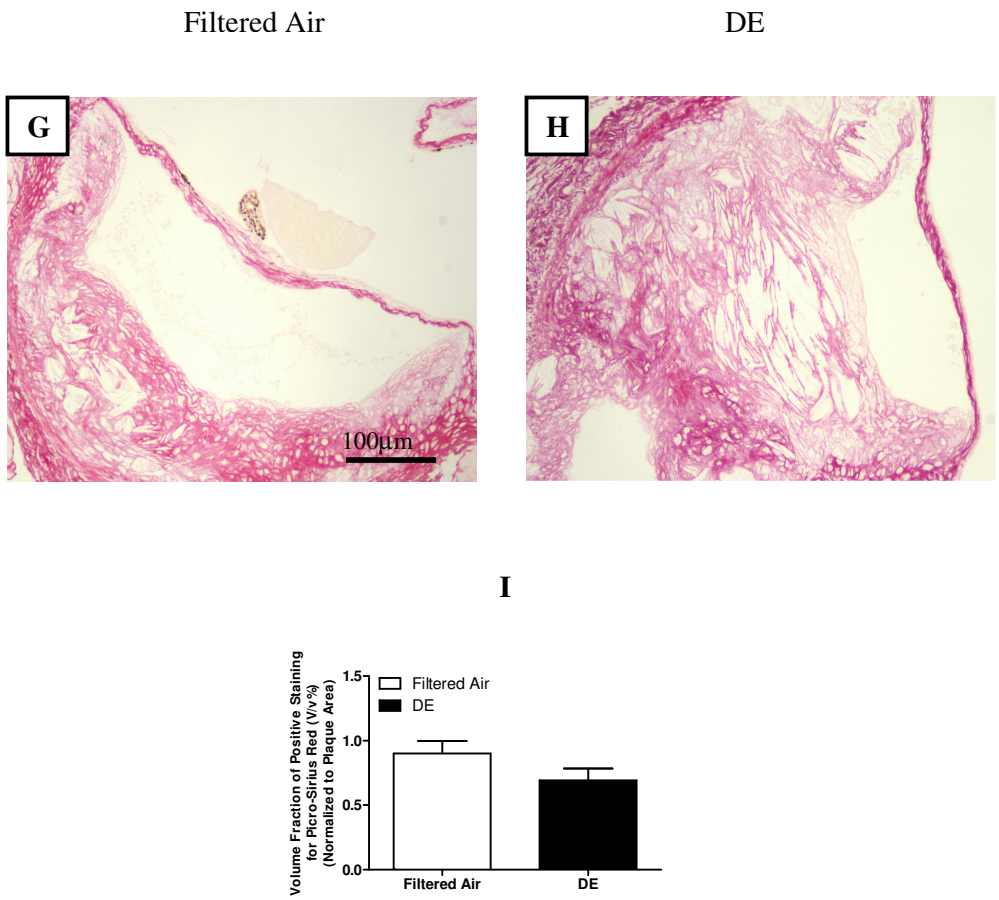

Figure 3.4 Histochemical analysis of the components of atherosclerotic plaque in aortic root. A,B) Representative photomicrographs of Oil red O staining for lipid content (200X); C) Exposure to DE increased lipid content occupied in atherosclerotic lesions, n=6, *P<0.02; D,E) Staining of α-actin for smooth muscle cells (200X), insets are higher magnification (400X) photomicrographs showing smooth muscle cells in the plaque; F) The smooth muscle cell content was significantly increased after DE exposure, n=8, *P<0.05; G,H) Picro-sirius red staining for collagen content (100X); I) DE exposure induced a trend of reduction in collagen content, n=10, P=0.14. Values are mean±SEM.

3.3.5 Increased Oxidative Stress in Atherosclerotic Plaque

The expression of tissue oxidative stress markers (iNOS, CD36, and Nitrotyrosine) in plaques were significantly increased after DE exposure; iNOS (18.7±5.5% vs. 50.8±12.2%; Filtered air vs. DE; $p<0.05$) (Fig.3.5A,B,C), CD36 (36.1±5.6% vs. 64.6±8.9%; Filtered air vs. DE; $p<0.05$) (Fig.3.5D,E,F), and nitrotyrosine (43.4±8.9% vs. 75.6±8.6%; Filtered air vs. DE; $p<0.02$) (Fig.3.5G,H,I). To further examine the relationship between the magnitude of DE exposure and the down stream effects, we examined the association between the number of alveolar macrophages positive for particles and the number of foam cells, the expression of CD36 and iNOS in plaques, respectively. As the number of alveolar macrophages positive for particles in filtered air group is significantly lower than that in DE exposure group (3.5±1.2% in F Filtered air vs.85.7±1.7% in DE), we used data from DE exposed mice. We found that there were positive correlations between alveolar macrophages positive for particles and plaque foam cell formation ($R^2=0.35$, $p=0.027$), the CD36 expression ($R^2=0.49$, $p=0.015$) and the iNOS expression ($R^2=0.72$, $p=0.0081$), respectively (Fig.3.6).

Filtered Air

DE

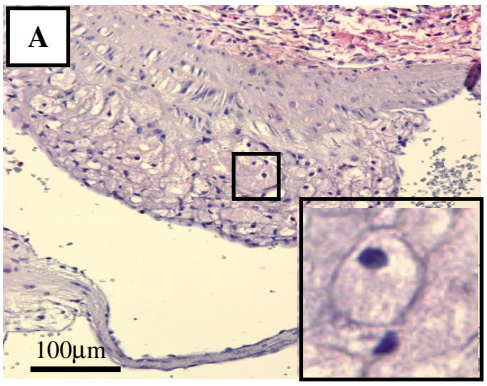

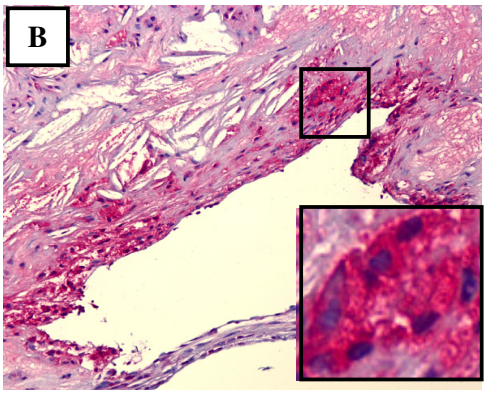

C

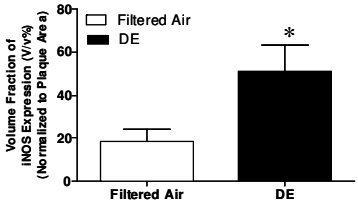

Filtered Air

DE

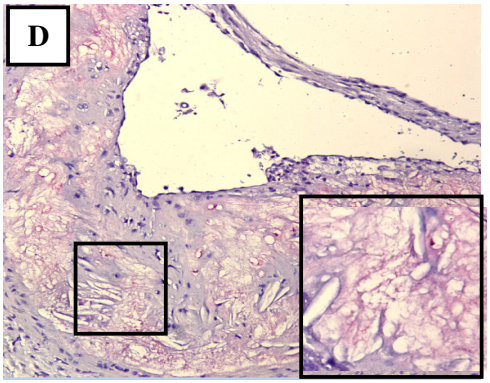

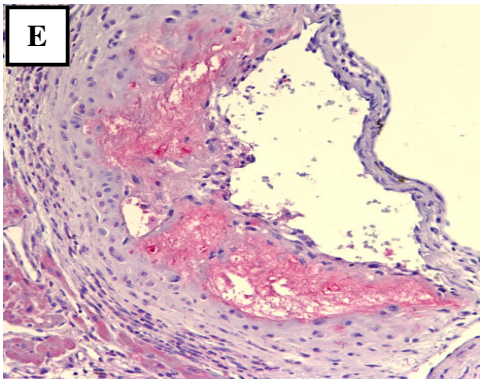

F

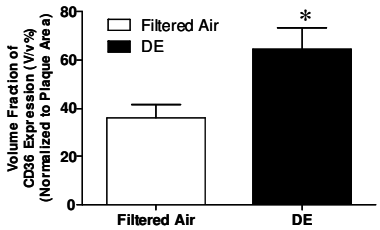

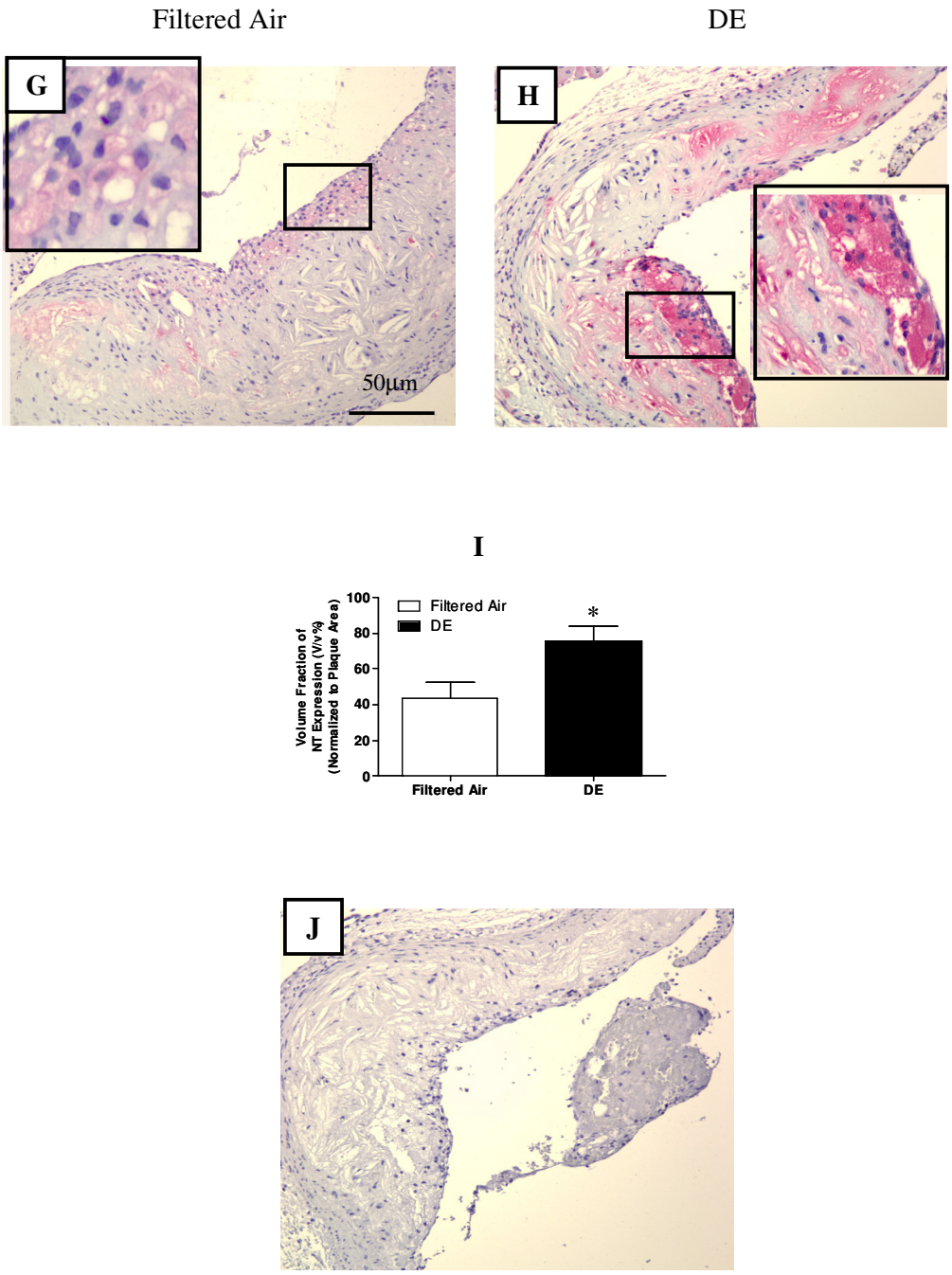

Figure 3.5 Immunohistochemical analysis of the expression of oxidative stress markers in the aortic root lesions. A,B) Representative photomicrographs of immunohistochemical staining for iNOS expression in aortic root (100X); C) Exposure to DE increased iNOS expression, n=8, *P<0.03; D,E) Immunohistochemical staining for CD36 expression (100X); F) CD36 expression was significantly increased after DE exposure, n=9, *P<0.05; G, H) Immunohistochemical staining of nitrotyrosine (NT) expression (200X); I) DE exposure significantly enhanced nitrotyrosine expression, n=9, *P<0.04; J) Negative control for H (200X). Insets are photomicrographs with higher magnification (400X).

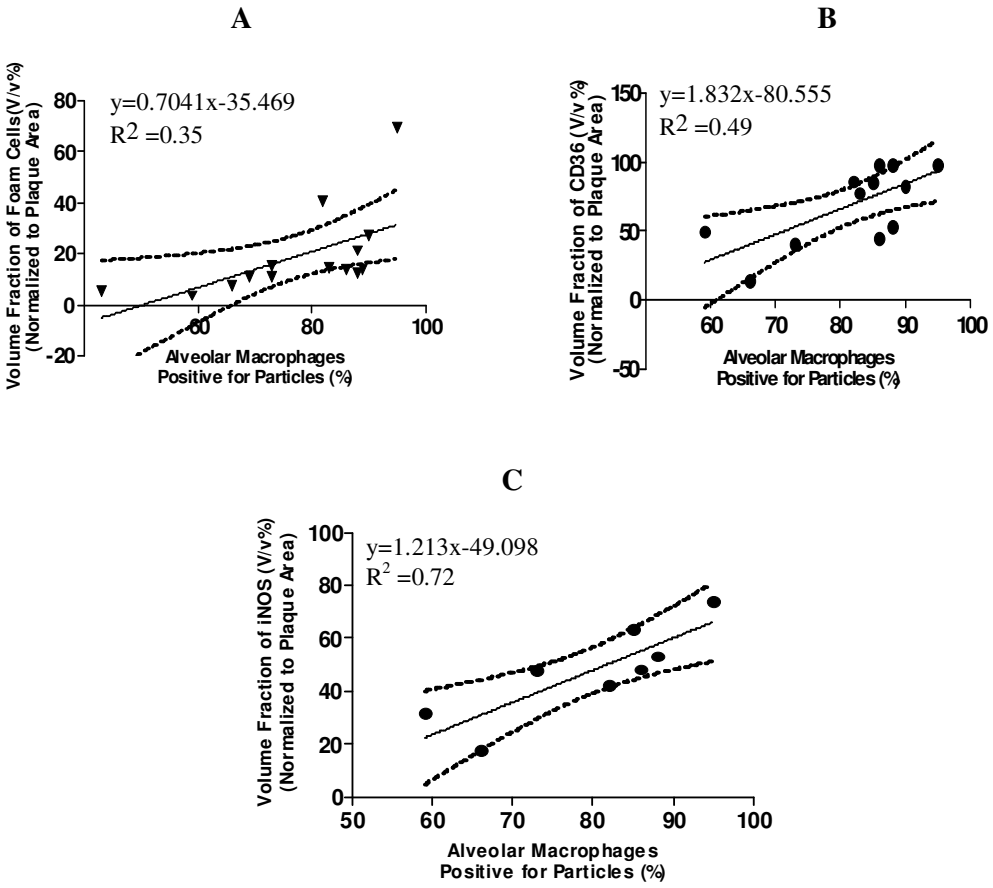

Figure 3.6 Association of DE exposure, plaque foam cell formation and the oxidative stress markers. A) Positive correlation between increased foam cell formation and alveolar macrophages positive for particles, P=0.027; B) Positive correlation between enhanced CD36 expression in aterosclerostic lesion in aortic root and alveolar macrophages positive for particles, P=0.015; C) Positive correlation between iNOS expression in aortic root and alveolar macrophages positive for particles, P=0.0081.

3.3.6 Systemic Oxidative Stress

Urine levels of both 15-F_{2t}-isoprostane (11.7±3.4 vs. 27.7±4.1ng/creatinine (mmol); Filtered air vs. DE; p<0.02), and 8-hydroxy-2-deoxy guanosine (1422±106 vs. 5110±1452 ng/creatinine (mmol); Filtered air vs. DE; p<0.02) were increased after DE exposure (Fig.3.7). The plasma MPO levels were similar between DE and filtered air exposure groups (Fig.3.8).

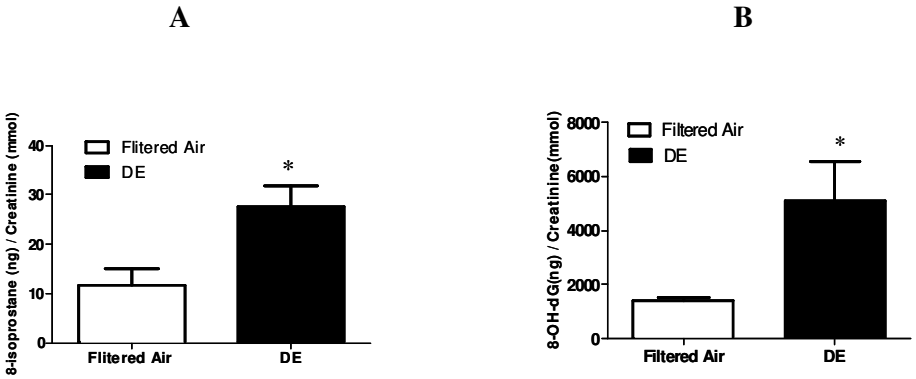

Figure 3.7 Analysis of systemic oxidative stress. A) Increased protein oxidation supported by enhanced urine 8-isoprostane production, n=10, *P<0.02; B) Increased DNA oxidation demonstrated by augmented urine 8-OH-dG production, n=11, *P<0.02. Values are mean±SEM.

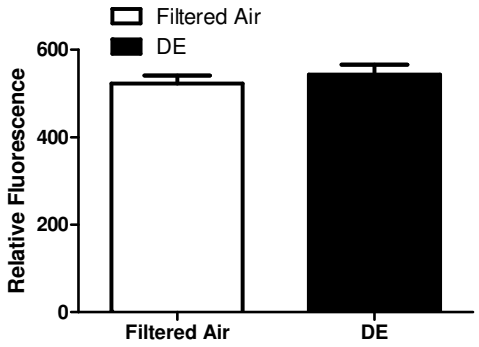

Figure 3.8 Plasma myeloperoxidase (MPO) levels. The MPO levels were not significantly different between filtered air and DE exposed mice (n=10). Values are mean±SEM.

3.4 Discussion

In this study, we demonstrate that DE exposure induced changes in atherosclerostic plaque that are characteristic of unstable plaques associated with vascular events (294). We show that exposure to DE increased plaque lipid content, plaque cellularity, foam cell formation, and smooth muscle cell migration into plaques (Fig.3.5 & Fig.3.7). The positive correlation between increased plaque foam cell formation, and alveolar macrophages positive for particles (Fig. 3.6A), links DE exposure to the compositional changes in atherosclerotic lesions. We also show an increase in oxidative stress markers both in the circulation (e.g., 15-F_{2t}-isoprostane and 8-OH-dG) and in the plaques themselves (e.g., iNOS, CD36, and NT) (Fig. 3.5 & Fig.3.7), and the positive association between particles in the lung and the increased expression of iNOS and CD36 in aortic root (Fig.3.6B,C) suggests that oxidative stress contributes to the DE-induced compositional changes.

With the rapid industrialization in both developed and developing world, DE has become one of the most important components of urban particulate matter (15). This is the first study to quantify the morphological changes in atherosclerotic plaque induced by exposure to DE and linked these changes to oxidative stress.

In this study, we exposed ApoE knockout mice to DE for 7 weeks using a well-controlled inhalation system that mimics real-world exposure near roadways. The average calculated exposure throughout a 24-hour period in our study was less than 35 $\mu g/m^3$, which is within the range of the National Ambient Air Quality Standard for $PM_{2.5}$ (22).

We demonstrate that exposure to DE resulted in an increase in alveolar macrophages that phagocytosed particles, and the total number of alveolar macrophages (Fig.3.1), indicating the lung inflammation. Alveolar macrophages are key cells in processing inhaled particulate matter, and this study confirms previous findings from our laboratory that used a different exposure model (EHC93 instillation) (79; 287). Alveolar macrophages are also

powerful producers of the mediators (such as IL-1β, IL-6, IL-8, and GM-CSF) that fuel the systemic inflammatory response when processing inhaled ambient PM (79). These pro-inflammatory mediators are known to activate the endothelium and up-regulate VCAM-1, ICAM-1, selectins, which are the key steps for monocyte migration into the subendothelium to engorge lipid, hence promoting atherogenesis (140). We have recently shown that mediators produced in the lung translocate to the blood stream following PM_{10} exposure (107), underscoring the importance of the lung inflammatory response induced by PM_{10} exposure to the downstream vascular responses (1;10). These findings support the concept that the systemic inflammatory response is responsible for the downstream adverse vascular effects following exposure to ambient PM. The association between lung alveolar macrophages phagocytosed particles and foam cell formation in plaques (Fig.3.6A) supports the link between the magnitude of exposure to DE and atherogenesis.

3.4.1 Compositional Changes in Atherosclerotic Plaque

Instability and rupture of an atherosclerotic plaque are implicated in the majority of acute ischemic syndromes, including MI and stroke. Histopathological features of these vulnerable plaques in humans include a large necrotic core ($\geq$ 40% of plaque area), increased inflammatory cells (including macrophages/foam cells) with less smooth muscle cells, and a thin fibrous cap (<65 μm) accompanied by reduced collagen and proteoglycans. Although the features of vulnerable plaque in animal models are controversial (295), the features in murine atherosclerotic lesions, including a large lipid core, increased inflammatory cells (e.g., macrophages), can be considered as histological markers for plaque progression and vulnerability (294).

Our study shows that exposure to DE promoted compositional changes in plaques, such as an increase in lipid accumulation, higher cellularity, more foam cell formation, and

smooth muscle cell content (Fig.3.3 & Fig.3.4). Studies from other (7; 8), and our own laboratories (6) suggest that exposure to ambient PM is associated with the development and progression of athereosclerosis. Using Watanabe heritable hyperlipidemic rabbits, and instillation of PM_{10} into the lung, we previously demonstrated that exposure to PM_{10} collected over a major North American city (EHC93) not only caused an increase in the extent of atherosclerosis (6), but also induced compositional changes in plaques (such as increase cellularity and lipid accumulation), similar to what we found in this study using an inhalation model. In subsequent studies using the rabbit model, we showed increased adhesion molecule expression in the endothelium overlying plaques and acceleration of monocyte migration into atherosclerotic lesions (133). Using a high fat diet mouse model, Sun and colleagues demonstrated that 6-month inhalation exposure to concentrated ambient $PM_{2.5}$ particles enlarged plaque area and increased lipid content of atherosclerosis (8). Similar to the method of Sun's study, we also used ApoE knockout mice and inhalation exposure, but we fed these mice with regular chow and our exposure period was shorter (7 weeks vs. 6 months). Albeit the shorter exposure period, we found more extensive compositional modifications of atherosclerotic lesions (Fig.3.3 & Fig.3.4), and enhanced oxidative stress in plaques (Fig.3.5), suggesting that DE may be more active in modifying atherosclerotic plaques (296), and particle composition may play an important role in PM-induced adverse cardiovascular effects (297).

In the study, we did not observe significant differences of body weight, food consumption, and lipid levels (Table 3.1) between two groups. Using aortic root as a representative of large vessel atherosclerosis, we show that the volume fraction of the size of atherosclerotic lesions was not different between DE and filtered air exposed mice (Fig.3.3A,B). This results support findings from a recently published study using an even longer DE exposure model (297). Studies in humans showed that the majority of acute

vascular events originate in active plaques with more lipid accumulation and inflammatory cells (e.g., macrophages) (148), and this phenomena underlines the importance of plaque composition rather than plaque size as a risk for vascular events. We show that DE exposure caused increased foam cell formation, cells originate from circulating monocytes (133) that differentiate into macrophages that specialize in phagocytosis of modified LDLs via their scavenger receptors, such as CD36, thereby transforming into foam cells (140). Lipid uptake by macrophages stimulates the release of various cytokines, which support foam cell formation and smooth muscle cell recruitment from the media into the intima. Pro-inflammatory mediators (e.g., IL-1, IL-6, MIP-1α, and TNFα) promote smooth muscle cell migration, contributing to the evolvement of smooth muscle cells from “contractile" phenotype state to the active "synthetic" state. Synthetic smooth muscle cells synthesize pro-inflammatory cytokines, release matrix metalloproteinases that can digest the components of extracellular matrix, such as collagen and proteoglycan, and lead to weakening the integrity or the stability of plaques (298). Our findings of increased plaque lipid content, increased cellularity with more foam cells and smooth muscle cells support the notion that DE exposure causes a persistent inflammatory milieu in plaques, all hallmarks of unstable vulnerable plaques. As mentioned, human studies have shown that plaque activity reflected by plaque composition rather than plaque size is a stronger indicator for downstream vascular events (27). We postulate that DE-induced compositional changes in atherosclerotic plaque could explain at least part of the epidemiological associations between traffic pollution and cardiovascular events (257: 290) .

3.4.2 Oxidative Stress and Compositional Changes in Atherosclerotic Plaque

Our results suggest that DE exposure induces oxidative stress that contributes to the compositional changes observed in atherosclerotic plaque. This notion is supported by the

increased expression of iNOS, CD36, and nitrotyrosine in atheroslclerotic lesions (Fig.3.5), enhanced systemic lipid and DNA oxidation, and the association between alveolar macrophages that phagocytosed particles (magnitude of exposure) and increased surrogate markers for tissue oxidative stress: iNOS and CD36 (Fig.3.6B,C). ROS generation can arise directly from the surface of ambient particles and soluble compounds (e.g., transition metals and/or organic compounds) (287). In addition, the airway alveolar macrophages are the first cells to come in contact with inhaled particles, and these cells release a large number of pro-inflammatory mediators upon DE stimulation, at the same time, they produce ROS at the sites of inflammation, resulting persistent local and systemic inflammatory response (287). Nitric oxide (NO) is an important biological mediator in living organisms that is synthesized from L-arginine using NADPH and molecular oxygen. The overproduction of NO catalyzed by iNOS is cytotoxic. iNOS is not expressed under physiology conditions, but up-regulated by pro-inflammatory mediators. iNOS not only catalyze NO production, but also generate superoxide in macrophages (299). The concomitant NO production and the accompanied increase in the level of superoxide lead to the generation of a strong NO-derived oxidant, peroxynitrite, which is implicated in the pathogenesis of a number of cardiovascular diseases, including atherosclerosis (217).

Oxidative modification of LDL accelerates lipoprotein-uptake by macrophages promoting the formation of foam cells, which is the landmark of development of atherosclerosis. This oxLDL uptake is mainly mediated by a macrophage scavenger receptor CD36, also known as oxLDL receptor (288). CD36 is regulated by proatherogenic cytokines and lipids. We suspect that the enhanced CD36 expression in plaques promotes the increased foam cell formation, and lipid accumulation as we observed (Fig.3.3G & Fig.3.4C). Collectively, the increases in both systemic and tissue oxidative stress markers support our

hypothesis that exposure to DE induces ROS, which promote the compositional changes we observed in the atherosclerotic lesions.

3.5 Conclusions

In summary, we demonstrate that DE exposure results in specific changes in atherosclerotic plaque that are associated with plaque activity and vulnerability. We also show a strong association between the compositional changes in plaques and the particle uptake in alveolar macrophages. The association between traffic related air pollution exposure and vascular events is well established in epidemiology studies (22), and our study support the notion that changes in atherosclerotic plaques induced by traffic related pollutants, (e.g., DE), contribute to the vascular events.

Chapter 4

Exposure to Diesel Exhaust Up-regulates iNOS Activity in ApoE Knockout Mice[1]

4.1 Introduction

Numerous epidemiological studies have demonstrated an association between exposure to particulate matter air pollution with diameter less than 10μm (or called PM_{10}) and increased cardiovascular morbidity and mortality (42; 56;57). Recent studies also showed that reducing PM_{10} levels resulted in a declined in cardiovascular deaths by 10.3% (37; 38), suggesting a causal effect of PM_{10} and cardiovascular mortality. It has been well established that deposition of ambient particles in the lung provokes low-grade alveolar inflammation with a secondary systemic inflammatory response resulting in downstream cardiovascular dysfunction.

Atherosclerosis has been recognized as a chronic inflammatory disorder of blood vessels involving the vascular, metabolic, and immune systems(140; 285). We have previously shown that exposure to PM_{10} caused progression of atherosclerosis of coronary arteries and aortae in rabbits that naturally developed atherosclerosis (141). This sentinel finding was confirmed in ApoE knockout mice (143) and a human study by showing an association between progression of carotid atherosclerosis and levels of ambient air pollution

---

[1]A modified version (with more detailed Methods) of this chapter has been accepted for publication by *Toxicology and Applied Pharmacology.* Ni Bai, Takashi Kido, Terrance J. Kavanagh, Joel D. Kaufman, Michael E. Rosenfeld, Cornelis van Breemen, Stephan F. van Eeden (2011) .

in Los Angeles (144). The progression of atherosclerosis induced by PM_{10} exposure could contribute to the increased cardiovascular morbidity and mortality. The observations of PM_{10}-induced atherosclerosis progression are very compelling; however, the mechanisms whereby PM_{10} exposure causes progression in atherosclerosis, have not been fully elucidated.

Diesel exhaust (DE) is a mixture of fine particles and gases, and represents a useful model of traffic-related air pollutants, which accounts for up to 90% of the fine particulate mass in ambient air of many major cities, such as London (15). A recent study demonstrated an association between progression of atherosclerosis and living near major roads (300). In addition, 6% of coronary heart disease deaths were linked to traffic-related pollution (15; 293).

Inducible nitric oxide synthase (iNOS) is up-regulated in response to inflammatory cytokines as part of the host defense responses (286), and generates 100-1000-fold more nitric oxide (NO) than does endothelial NOS (eNOS) (micromolar vs. nanomolar levels). NO derived from eNOS plays an important role in protecting vasculature from inflammation and atherosclerosis. However, excessive NO production from iNOS has detrimental effects on cardiovascular function. The large amount of locally released NO has been linked to the generation of harmful oxidative products, such as peroxynitrite, which is implicated in iNOS-mediated development of atherosclerosis (143; 186; 189). iNOS is undetectable under normal physiological conditions, but its expression can be found in macrophages, endothelial cells and smooth muscle cells of human atherosclerotic plaques (214). The notion that iNOS plays a causative role in the progression of atherosclerosis is supported by the observation that atherosclerotic lesions were diminished in iNOS/ApoE double knockout mice, compared with ApoE knockout mice (218). iNOS overexpression was shown to be responsible for DE-induced lung inflammation (143; 186), while iNOS knockout mice had a significant reduction in cytokine levels in the lung after exposure to ambient PM (271). iNOS

expression is up-regulated by NF-κB, which is sensitive to inflammation and oxidative stress stimulation (301). We recently have shown that DE exposure accelerates the progression of atherosclerosis in ApoE mice via oxidative stress pathways. In this study, we test our hypothesis that DE exposure up-regulates iNOS expression in vasculature via a NF-κB-mediated pathway that could ultimately contribute to the progression of atherosclerosis and cardiovascular events linked to exposure to traffic related pollution.

4.2 Methods and Materials (Please refer to Chapter 2 for details)

4.2.1 Methods

30-week old male ApoE knockout mice fed with regular chow were exposed to DE for 7 weeks (5days/week, 6hrs/day) at the concentration of 200 $\mu g/m^3$. Exposing mice to filtered air was the control. Animal procedures were approved by the Animal Care and Use Committee of the University of Washington.

After exposure, mice were euthanized with sodium pentobarbital (100mg/kg) and heparin sulfate (500U/kg) intraperitoneally. Plasma was obtained after the centrifugation of the blood and stored at -80°C until assay. Thoracic aorta, aortic root, and heart were carefully dissected from their connective tissues and kept in appropriate conditions until assay.

To measurement vascular tone and iNOS activity, the thoracic aorta was carefully cleaned off connective tissues without damaging the endothelium, and mounted in a wire myograph. Smooth muscle contractility was studied by the addition of cumulative concentrations of phenylephrine (PE, 1nM-10μM). To examine the effect of DE on iNOS activity, a iNOS specific inhibitor (1400W) was used. iNOS activity was determined by the fractional changes of maximum PE constriction with and without the presence of 1400W.

Immunohistochemistry was performed to quantify the expression of iNOS, macrophages, smooth muscle cells, CD36, and nitrotyrosine in the thoracic aorta and aortic root sections that contained three complete valve leaflets by specific primary antibodies: iNOS (1:100); F4/80 (1:50); α-actin (1:600); CD36 (1:50); and nitrotyrosine (1:400).

Western immunoblotting analysis was conducted to assess iNOS expression in heart tissue. Frozen heart tissues were homogenized and protein samples (40μg/lane) were separated on 7.5% SDS-PAGE gel, subsequently electrotransferred to polyvinyldifluoride membranes and blocked with 5% BSA dissolved in 0.1% TBS-Tween 20 for 60 min at room temperature. The membrane was incubated with specific primary antibody for iNOS (1:500) at 4°C overnight. Densitometry was carried out using Image J (NIH), and the results were expressed in optical intensity per mg protein.

NF-κB (p65) activity was assessed on nuclear extracts from frozen heart tissue by enzyme-linked immunosorbent assay (ELISA) using a NF-κB (p65) transcription factor kit. Results were expressed as absorbance (450nm) per mg protein.

Real-time reverse transcription polymerase chain reaction (RT-PCR) was conducted to quantify mRNA expression for iNOS and NF-κB. Total RNA was extracted from heart tissue and the same amount of RNA was loaded in triplicates for each assay, and qRT-PCR was performed using TaqMan universal PCR master mix and Taqman gene expression assay system (Applied Biosystems). mRNA expression for iNOS, NF-κB, β-actin, and hypoxanthine phosphoribosyltransferase-1 (HPRT1) was determined by qRT-PCR using ABI Prism 7900HT sequence detection system. Gene expression values were calculated and displayed as ratio relative to β-actin.

4.2.2 Solutions and Chemicals

The PSS consisted of the following (in mM): NaCl 119, KCl 4.7, KH_2PO_4 1.18, $NaHCO_3$ 24, $MgSO_47H_2O$ 1.17, $CaCl_2$ 1.6, glucose 5.5 and EDTA 0.026. All reagents were purchased from Sigma (St. Louis, MO).

4.2.3 Statistical Analysis

Data are shown as mean±SEM. The statistical significance was evaluated using the unpaired Student t test for simple comparison between 2 values. Non-parametric analysis (Kruskall-Wallis test) was used to analyze data that were not normally distributed and Bonferroni correction was used for multiple comparisons. Linear regression modeling was used to assess the correlation relationship between parameters. In all experiments, n equals the number of mice from which samples were obtained. $P<0.05$ was considered to be significant.

4.3 Results

4.3.1 iNOS Activity and Expression in the Thoracic Aorta

PE-stimulated vasoconstriction of ApoE mouse thoracic aorta was suppressed by ~23% after DE exposure (9.5±0.6mN vs. 7.4±0.6mN; Filtered air vs. DE; $p<0.02$) (Fig.4.1A,B). In the presence of 1400W, the fractional changes of PE-elicited vasoconstriction were significantly increased in DE exposure group, compared with the control (5.2±3.0% vs. 24.1±7.6% of increased maximum constriction; Filtered air vs. DE; $p<0.04$) (Fig.4.1C,D,E), suggesting an increase in iNOS activity after DE exposure. To verify whether the reduced vasoconstriction was due to morphological abnormalities of blood vessels, we stained the thoracic aorta that was adjacent to the segment used for functional studies, with hematoxylin and eosin, and measured the thickness of the vascular

wall using quantitative morphologic analysis. We found no difference of the thickness and structure of the vessels after DE exposure, compared with the control (Appendix B). Immunohistochemical staining demonstrates that iNOS was predominantly expressed by smooth muscle cells and macrophages in the vessels (Fig.4.2A,B,C). The increased iNOS activity is supported by quantitative immunohistological analysis showing that the iNOS expression in thoracic aorta was significantly elevated (~4 fold) after DE exposure (11.9±3.2% vs. 40.2±6.5%; Filtered air vs. DE; $p<0.002$) (Fig.4.2D).

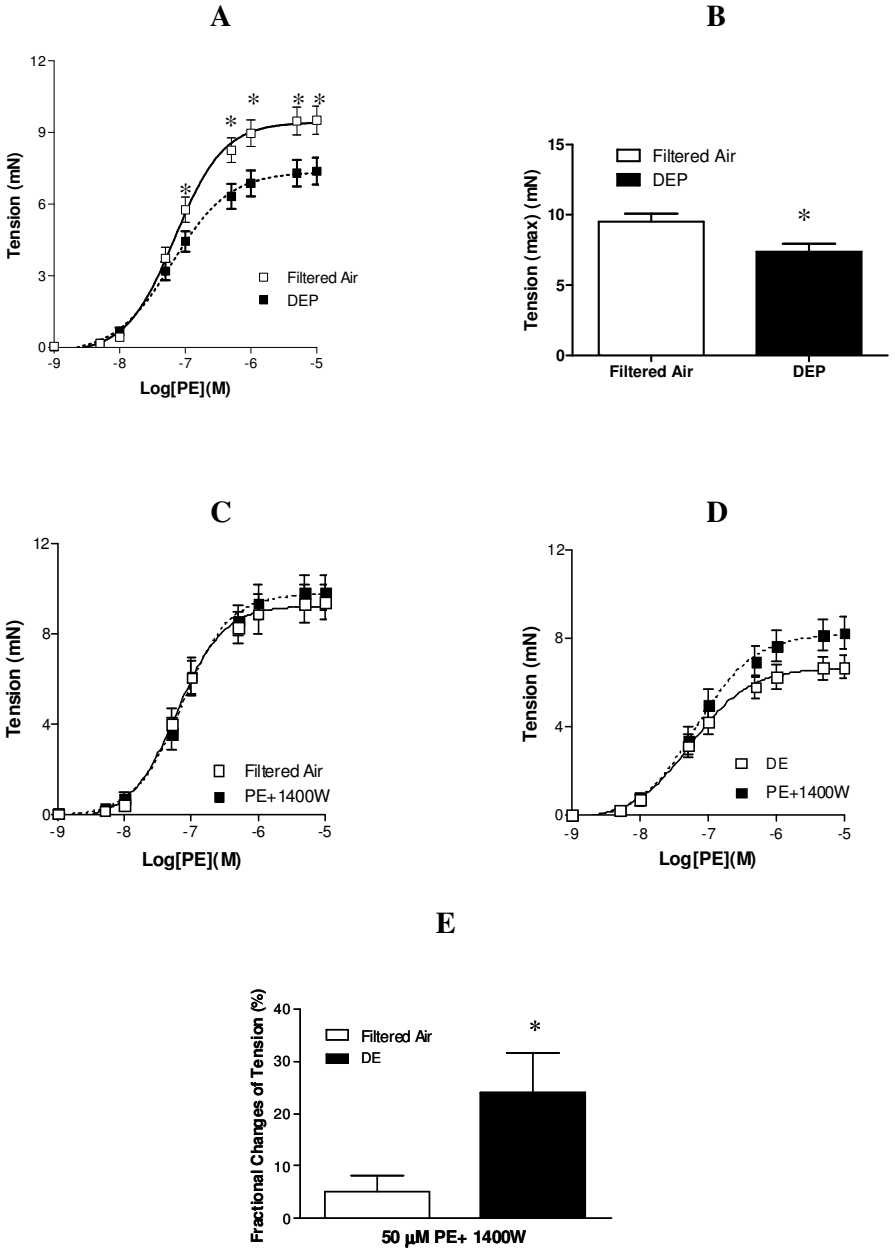

Figure 4.1 Reduced vasoconstriction and increased iNOS activity in the thoracic aorta. A) Dose-response curves of PE-elicited constriction show that exposure to DE attenuated vasoconstriction, n=9, *P<0.02; B) DE exposure caused significant attenuation of maximum vasoconstriction, compared with the control, n=9, *P<0.02; C) In the control group, the presence of iNOS blocker (1400W) had no effect on PE-elicited constriction; D) In DE exposure group, the reduced vasoconstriction was partly restored by 1400W; E) Inhibition of iNOS by 1400W caused a significant elevation of maximum vasoconstriction in DE exposure group, n=9, *P<0.04. Values are mean±SEM.

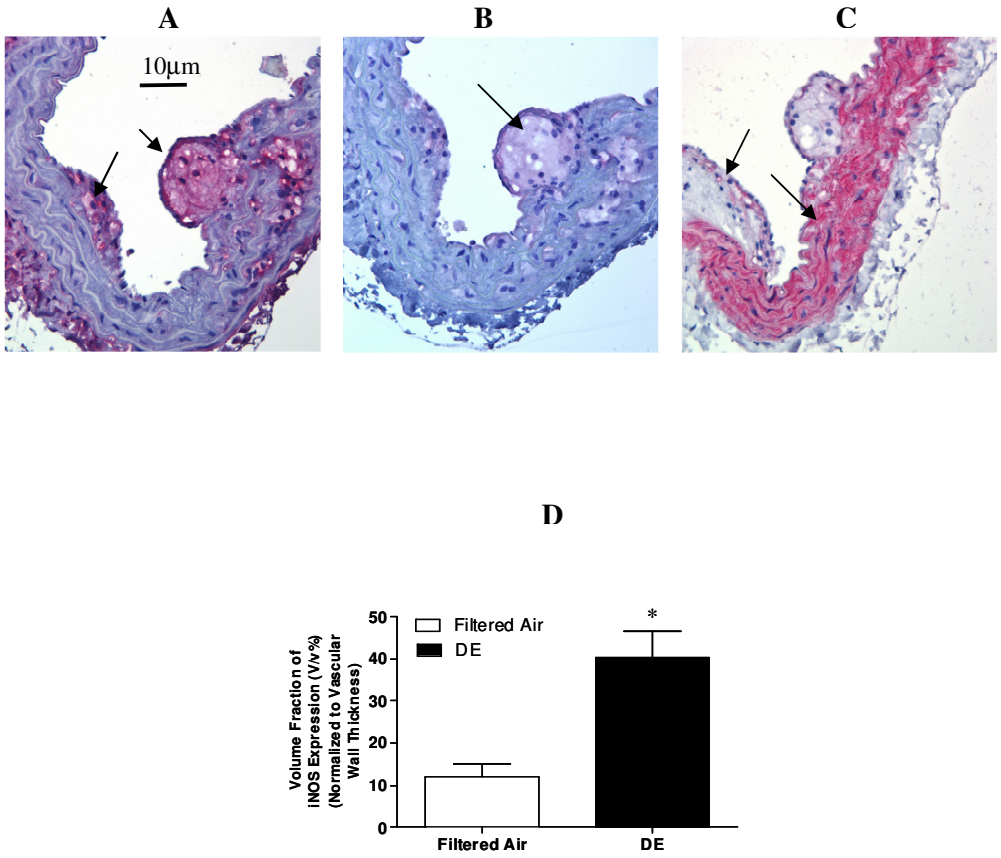

Figure 4.2 Immunohistochemical analysis of iNOS expression in the thoracic aorta. Representative photomicrographs of staining for A) iNOS (arrow); B) Macrophages (F4/80) (arrow); C) Smooth muscle cells (α-actin) (arrow); D) Exposure to DE increased iNOS expression in the thoracic aorta, n=8, *P<0.002. Values are means ± SE; L: lumen. Magnification: orginalX400. Values are mean±SEM.

4.3.2 iNOS Expression in the Heart

Quantitative immunohistochemical staining shows that iNOS expression was increased in the heart tissues after DE expousure (73.5±10.0% vs. 116.9±7.6%; Filtered air vs. DE exposure; $p<0.01$) (Fig.4.3C). Consistently, western immunoblotting shows that DE exposure caused augmented iNOS expression in the heart tissues (0.7±0.1% vs. 1.0±0.1%; Filtered air vs. DE; $p<0.03$) (Fig.4.3D,E).

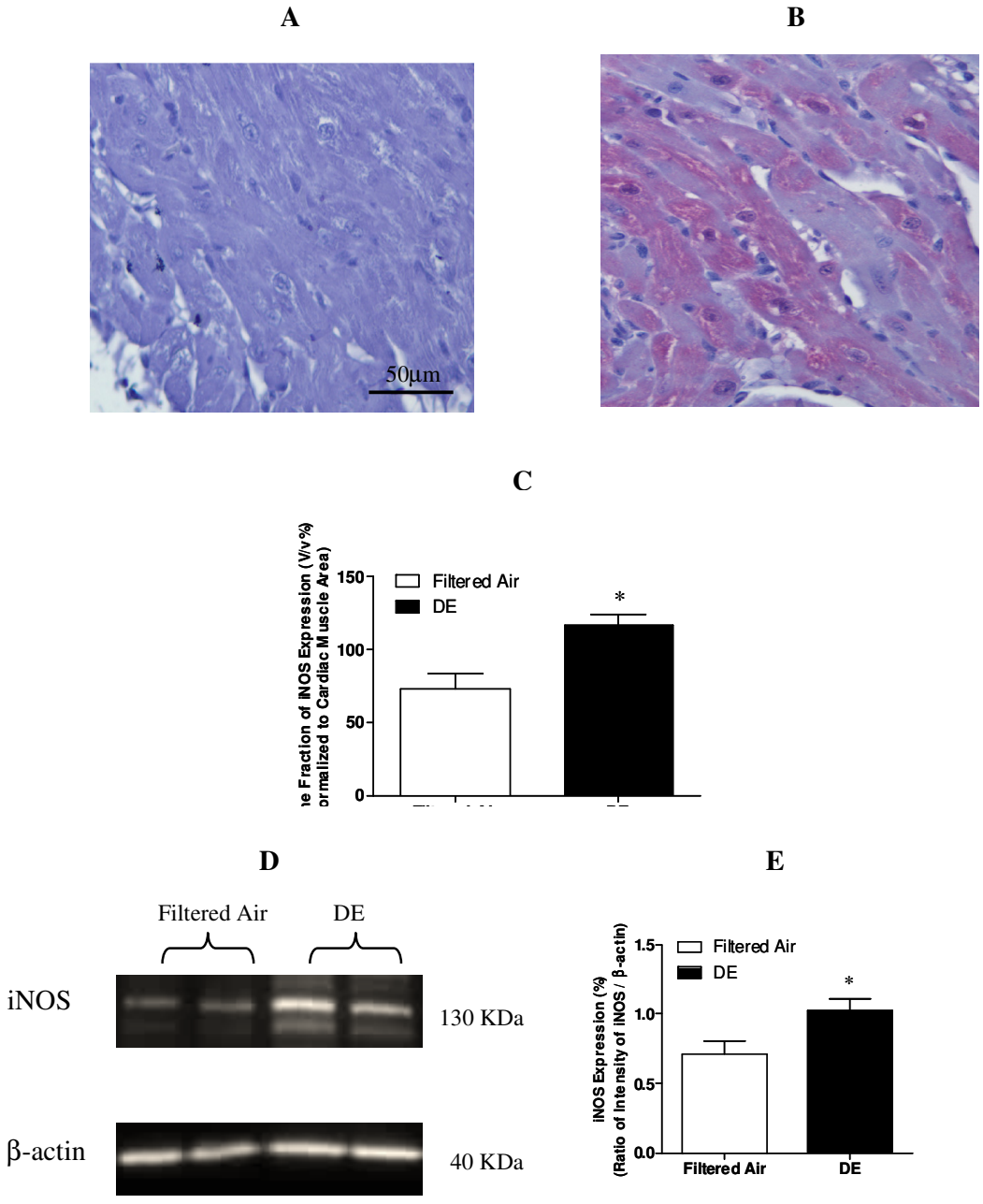

Figure 4.3 Immunohistochemical and Western blotting analysis of iNOS expression in the heart. Representative photomicrograph of staining for A) negative control; and B) iNOS in cardiac muscle cells; C) Quantitative immunostaining analysis shows that exposure to DE increased iNOS expression in the heart, n=9, *P<0.01; D) Representative photomicrograph of western blotting of iNOS expression in the heart; E) Quantitative western blotting analysis demonstrats that iNOS expression was enhanced following DE exposure, n=8, *P<0.03. Magnification: orginal X200. Values are mean±SEM.

4.3.3 Co-localization of iNOS, CD36 and Nitrotyrosine Expression

iNOS was predominantly expressed in macrophages in the aortic root tissues (Fig.4.4B,C). The expressions of iNOS, CD36, and nitrotyrosine were co-localized in macrophages (Fig.4.4D,E,F), In addition, iNOS expression was positively associated with CD36 expression (R^2= 0.458, P=0.01) (Fig.4.4G), and CD36 expression was correlated with nitrotyrosine formation (R^2= 0.4629, P=0.01) (Fig.4.4H).

A

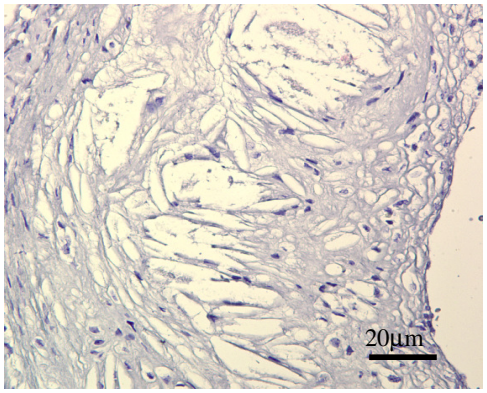

B

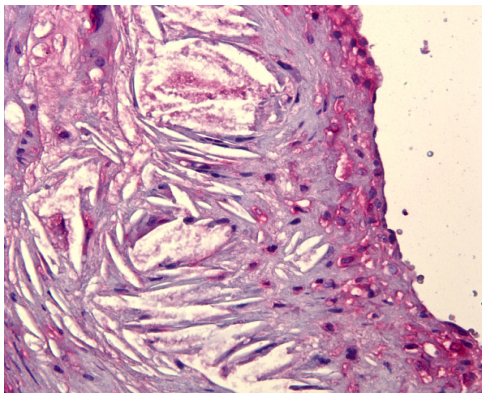

C

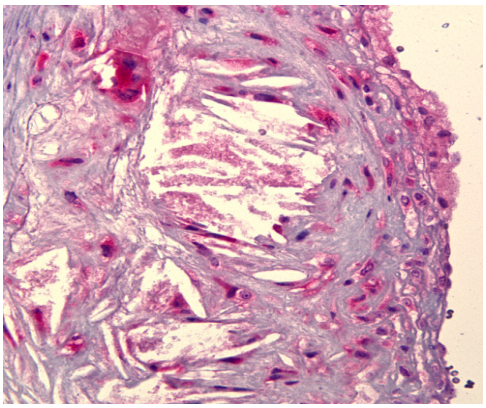

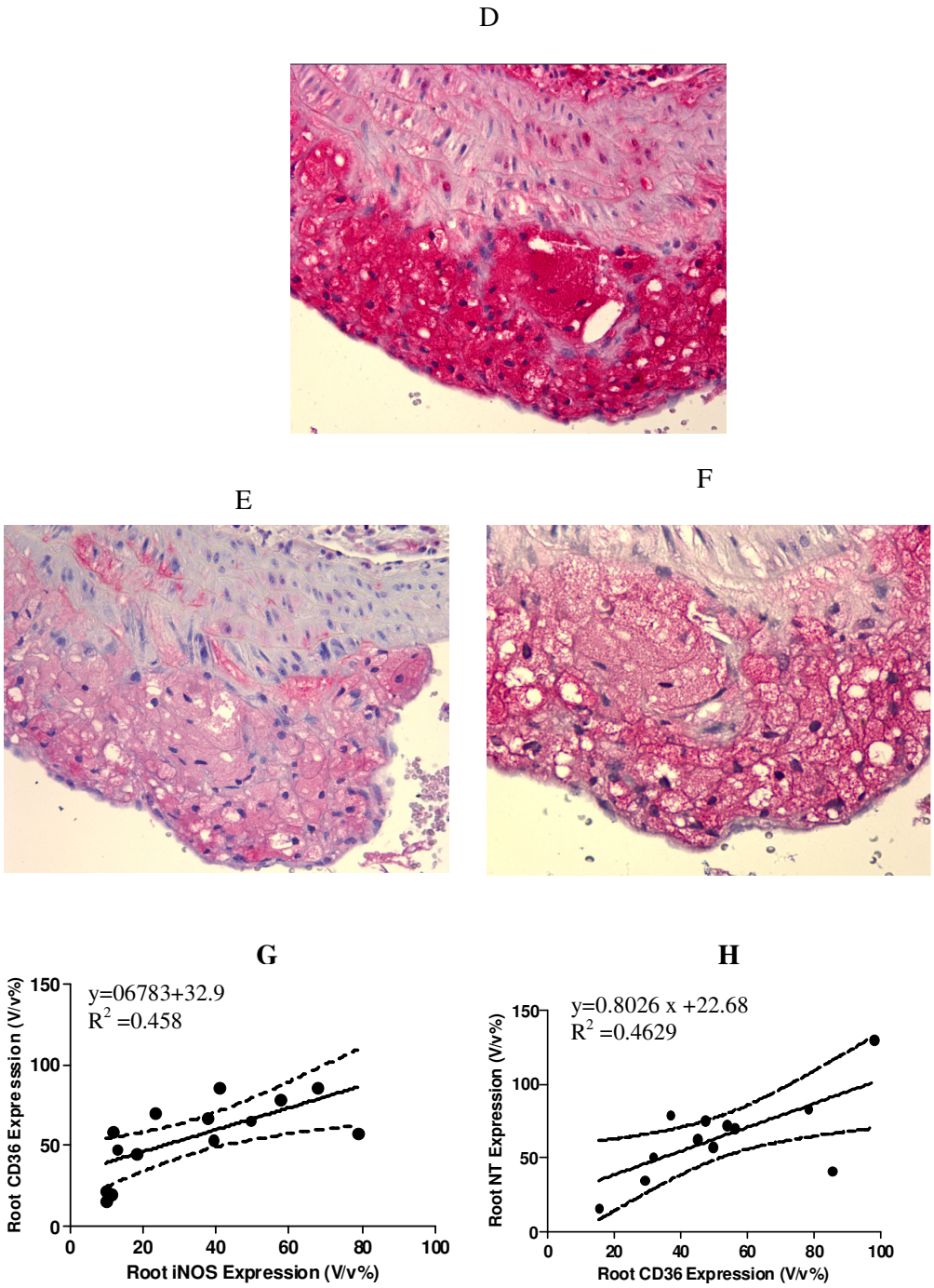

Figure 4.4 iNOS expression in atherosclerotic plaque in aortic root and its relationship with the expression of CD36 and nitrotyrosine. Represetitive photomicrographs of staining for A) Negative control; B) iNOS; and C) Macrophages (F4/80); co-localized expression of D) iNOS; E) CD36; and F) nitrotyrosine in aortic root; G) Positive correlation between iNOS and CD36, P=0.01; H) Positive correlation between CD36 and NT, P=0.01. Magnification: original X400.

4.3.4 NF-κB (p65)-Mediated iNOS Expression

mRNA expression of iNOS (76±3% vs 90± 6%; filtered air vs. DE; p<0.004) (Fig.4.5A) and NF-κB (83±1% vs 88 ± 3%; Filtered air vs. DE; p<0.01) (Fig.4.5B) were significantly higher in the heart tissues of DE exposed mice than the control. To assess whether iNOS was regulated at the transcription level via NF-κB activation, we extracted nuclear protein from the frozen hearts, and NF-κB activity was evaluated by ELISA. DE exposure up-regulated NF-κB (p65) activity (0.014±0.0004 vs. 0.029 ±0.006 absorbance of 450nm/mg protein; Filtered air vs. DE; p<0.01) (Fig.4.6A). iNOS expression was positively correlated with NF-κB activation (R^2= 0.5998, p<0.0005) (Fig.4.6B), suggesting that DE exposure up-regulated iNOS expression at transcriptional level via NF-κB activation (p65).

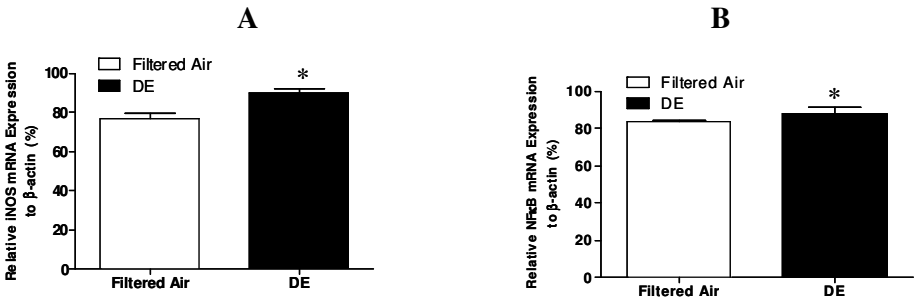

Figure 4.5 Increased mRNA expression of iNOS and NF-κB in the heart. A) Increased mRNA expression for iNOS in the heart after DE exposure, n=7 (filtered air), n=8 (DE) *P<0.004; B) Exposure to DE increased NF-κB mRNA expression, n=7 (filtered air), n=8 (DE), *P<0.01. Values are mean±SEM.

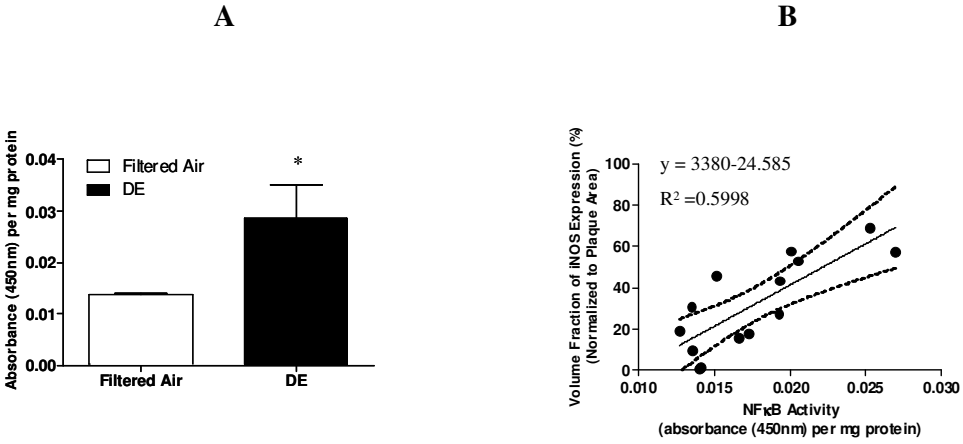

Figure 4.6 Increased NF-κB activity of heart nuclear extract. A) The NF-κB activity in the heart was significantly increased after DE exposure (n=10, *P<0.01). Values are mean±SEM; B) The increased NF-κB activity was positively correlated with iNOS expression.

4.4 Discussion

Studies from our (141) and other (143; 144) laboratories have shown that exposure to PM_{10} is associated with development of athereosclerosis. In this study, we show that exposure to DE, a major contributor to urban particulate matter, increased iNOS expression in the thoracic aorta and heart tissues. iNOS was expressed by smooth muscle cells, macrophages, and cardiac myocytes (Fig.4.2, Fig.4.3B, Fig.4.4B). DE exposure enhanced iNOS activity in blood vessels, which resulted in decreased vascular contractility (Fig.4.1). We have recently reported DE exposure enhanced iNOS expression in plaque tissues of the aortic root (377). In this study, we show that the expression of iNOS, CD36 and nitrotyrosine were all co-localized in the plaque tissues (Fig. 4.4D,E,F). There was a positive association between enhanced NF-κB activity and iNOS expression (Fig.4.6B), suggesting that the activation of NF-κB plays a pivotal role in the enhanced iNOS activity. The augmented iNOS and NF-κB mRNA expression (Fig.4.6) also indicate that iNOS was up-

regulated at both transcription and translation levels. To our knowledge, this is first study demonstrating that DE exposure up-regulates iNOS activity and expression in the vasculature as well as the heart tissues. We speculate that oxidative stress-induced NF-κB activation contributes to the increased iNOS expression and activity.

4.4.1 The Level of DE Exposure

In the study, we exposed ApoE knockout mice to DE for 7 weeks, using a well-controlled inhalation system that mimics real-world exposure. Our average particulate matter concentration throughout a 24-hour period is less than 35 $\mu g/m^3$, which is environmentally relevant and within the National Ambient Air Quality Standard (8).

4.4.2 DE Exposure and Up-regulation of iNOS

Nitric oxide (NO) is an essential biological mediator protecting the vessels from inflammation and atherosclerosis. Nevertheless, overproduction of NO catalyzed by iNOS is cytotoxic. iNOS is not expressed under normal physiological conditions, but can be up-regulated in response to pro-inflammatory mediators, and oxidative stress stimulation. Up-regulation of iNOS is implicated in the pathogenesis of a number of cardiovascular diseases, including atherosclerosis (217). In this study, we showed that DE exposure increased iNOS activity (Fig.4.1) and enhanced iNOS expression in the blood vessels (Fig.4.2) and heart (Fig.4.4) at both protein and mRNA levels (Fig.4.5A). We also found a positive correlation between the iNOS expression with both foam cell formation and the number of smooth muscle cells in atherosclerotic plaque in aortic root (Appendix C). The association suggests that the up-regulation of iNOS contributes to the progression of atherosclerosis induced by DE exposure.

Similar to the finding of Sun and colleagues, in which ApoE knockout mice were exposed to concentrated ambient particles for 6 months (143), we found that iNOS

expression was up-regulated at both protein and mRNA levels after exposure to DE for a shorter exposure period (7 weeks vs. 6 months), suggesting that the constituents of DE may be more active, comparing with concentrated ambient particles (296). Sun and colleagues found that exposure to concentrated ambient particles exaggerated vasoconstriction to phenylephrine, which likely resulted from reduced NO production or endothelial dysfunction. However, exposure to DE for 7 weeks appeared to have a greater effect on smooth muscle cells, and we found suppressed vasoconstriction to phenylephrine, which was likely due to excessive NO production derived from iNOS (Fig 4.1). In addition, no impairment of ACh-stimulated endothelium-dependent relaxation was observed in our study (Fig 6.1A). Sun and colleagues were also observed that mice fed with regular chow did not develop endothelial dysfunction after exposure to concentrated ambient particles (supporting our finding), suggesting that high fat diet-mediated modifications on vasculature are important elements for ambient particle exposure-induced endothelial dysfunction.

iNOS activation is mainly regulated at transcriptional level by NF-κB (302). Oxidative stress-induced NF-κB activation has been observed in epithelial cells exposed to ambient particles (105). NF-κB is known to regulate the transcription of various genes participating in oxidative stress responses. NF-κB dimers (p50/65) are sequestered in the cytoplasm by a family of inhibitors, called inhibitors of κB (IκB). Activation of NF-κB is initiated by degradation of IκB proteins triggered by oxidative stress. NF-κB complex enters into the nucleus in which it can turn on the expression of specific genes by binding to their promoters. In this study we found that NF-κB activity and mRNA expression were increased (Fig.4.5B & Fig.4.6A). The correlation between iNOS and increased NF-κB activity (Fig.4.6B) suggests that NF-κB contributes to the up-regulation of iNOS following DE exposure. The promoter of the murine gene coding for iNOS contains the binding sites for NF-κB, which are sensitive to oxidative stress stimulation (303). DE exposure was found to cause ROS

generation in epithelial cells, alveolar macrophages, blood vessels, endothelial cells, and cardiac myocytes (105;177; 180; 186; 304). We recently demonstrated that DE exposure increased oxidative stress in atherosclerotic lesions in the aortic root, and systemic protein and DNA oxidation (377). In this study, we showed that the enhanced CD36 and nitrotyrosine were concomitantly up-regulated with iNOS (Fig.4.4), suggesting that ROS may play a role in the activation of NF-κB, which mediated the up-regulation of iNOS expression and activation. ROS generation can rise directly from the surface of ambient particles (305), and soluble compounds (e.g., transition metals, or organic compounds (183; 296; 308). In addition, direct interactions between DE and airway epithelial cells and alveolar macrophages could also contribute to ROS generation (287; 309).

4.4.3 iNOS and Atherosclerosis

The notion that overexpression of iNOS results in development of atherosclerosis has previously been established by showing that atherosclerotic lesions were attenuated when iNOS was knocked out in ApoE mice (218; 269). iNOS is capable of generating superoxide, which can rapidly deplete endothelium-derived NO, attenuate eNOS activity and expression, leading to endothelial dysfunction and development of atherosclerosis. It is well known that oxidative modification of low-density lipoprotein (LDL) accelerates lipoprotein-uptake by macrophages and the formation of foam cells (310), which is the characteristic component of atherosclerotic lesions and landmark of development of atherosclerosis. This oxidized LDL (oxLDL) uptake is mainly mediated by a macrophage scavenger receptor CD36, also known as oxLDL receptor (311). We previously reported that DE exposure increased CD36 expression. CD36 is up-regulated by proatherogenic cytokines and oxidized lipid. In this study we showed that the expression of iNOS and CD36 was co-localized in atherosclerotic lesions (Fig.4.4D,E). The positive correlation between iNOS and CD36 (Fig.4.4G) suggests

that iNOS, as a free radical generator, may also play a role in the augmented CD36 expression, which contributes to the foam formation and progression of atherosclerosis. In addition to generating free radicals, iNOS also contributes to the production of peroxynitrite, which is a potent oxidant and implicated in the pathogenesis of several cardiovascular diseases, including atherosclerosis, MI, and heart failure (312).In summary, we show that DE exposure enhanced iNOS activity and caused up-regulation of iNOS at both protein and mRNA levels. We also show that DE induced oxidative stress, and increased NF-kB expression and activity, suggesting a pathway of the up-regulation of iNOS expression and activity. Our study provides novel insights into the mechanisms underlying DE exposure-induced progression of atherosclerosis, and potential future therapeutic targets to decrease the impact of ambient PM on cardiovascular morbidity and mortality.

Chapter 5

Exposure to Diesel Exhaust Causes Up-regulation of COX2 Activity in ApoE Knockout Mice

5.1 Introduction

Epidemiological studies have shown that exposure to ambient particulate matter air pollution with diameter less than 10μm (PM_{10}) is an independent risk factor for cardiovascular morbidity and mortality (3; 22; 287). The mechanisms underlying PM_{10} induced cardiovascular disease have not been fully investigated. Both human and animal studies have indicated that the deposition of particles in the lung provokes a low-grade lung inflammation with a secondary systemic inflammatory response charactierized by increased circulating pro-inflammatroy mediators, such as IL-1, IL-6, and TNFα. The systemic responses are thought to cause the downstream cardiovascular diseases (22; 287).

Prostanoids play an important role in cardiovascular function, such as regulating vascular tone, modulating vascular inflammatory response, controlling leukocyte-endothelial cell adhesion and platelet aggregation (368). Cyclooxygenase (COX) is the key regulatory enzyme responsible for the formation of prostanoids. COX catalyzes the conversion of arachidonic acid to prostaglandin (PG) H_2, which is subsequently converted to a variety of eicosanoids, including PGE_2, PGD_2, $PGF_{2\alpha}$, prostacyclin I_2 (PGI_2), and thromboxane A2 (TXA2) (245). The array of PGs produced varies, depending on the downstream enzymes present in different types of cells. For example, endothelial cells primarily produce PGI_2, whereas platelets mainly produce TXA2. Two COX-isozymes, COX1 and COX2, have been

characterized. COX1 is the enzyme responsible for basal, constitutive prostaglandin synthesis, whereas COX2, like iNOS is implicated in various inflammatory settings (313). PGI_2 (vasodilator) and TXA2 (vasoconstrictor) are important components of prostaglandin metabolism that regulate cardiovascular homeostasis. Under physiological conditions, PGI_2 is released by endothelial cells to mediate several protective effects on the vascular wall, including regulation of vascular tone, and inhibition of platelet aggregation and adhesion (314; 315). TXA2, a potent vasoconstrictor, is the predominant mediator opposite to the effect of PGI_2. Under pathological conditions, such as inflammation or atherosclerosis, PGI_2 production decreases, and the release of TXA2 becomes dominant (316). TXA2 is implicated in endothelial dysfunction, hypertension, and atherothrombosis.

Exposure to PM_{10} causes overexpression of COX2 in human airway epithelial cells, resulting in the lung inflammation and injury (274). In vitro study showed that exposure to diesel exhaust particels increased COX2 protein and mRNA expression that were associated with a subsequent increase in cholesterol accumulation and foam cell formation (275). We previously showed that exposure to PM_{10} caused progression of atherosclerosis in rabbits (141), and recently demonstrated that exposure of ApoE knockout mice to diesel exhaust (DE) for 7 weeks promoted compositional changes of atherosclerotic lesions (e.g., increased foam cell formation, and lipid accumulation) (377). The underlying mechanisms for the changes in plaques are not fully understood. We hypothesize that DE exposure up-regulates COX2 activity and expression that could contribute to the DE exposure-induced compositional changes in atherosclerotic plaque.

5.2 Methods and Materials (Please refer to Chapter 2 for details)

5.2.1 Methods

Male ApoE knockout mice at the age of 30 weeks, were exposed to DE for 7 weeks (5days/week, 6hrs/day) at the concentration of 200 $\mu g/m^3$. Exposing mice to filtered air was the control. Animal procedures were approved by the Animal Care and Use Committee of the University of Washington.

Plasma was obtained after the centrifugation of the blood and stored at –80°C until assay. The thoracic aorta, aortic root, heart, and lung were carefully dissected from their connective tissue and kept in appropriate solution until assay.

The thoracic aorta was cut to 2mm rings and mounted on a wire myograph. Smooth muscle contractility was studied by the addition of cumulative concentrations of phenylephrine (PE, 1nM-10μM). To access the effect of DE exposure on COX, indomechacin (1μM) was applied. To examine the specific roles of COX1 and COX2, SC560 and NS398 were used to inhibit COX1 and COX2, respectively.

Aortic root sections were incubated with specific primary antibodies: rabbit anti mouse antibody for COX1 (1:150), rabbit anti mouse antibody for COX2 (1:100), and rat anti mouse antibody for F4/80 (1:50) at 4°C overnight. The positive red staining was recognized, quantified by colour segmentation (Image Pro Plus), and normalized to the area of the atherosclerotic lesion.

PGI_2 level was assessed by measuring urine 2,3-dinor-6-keto prostaglandin F1α, the major urinary metabolite converted from PGI_2, using an EIA kit. Creatinine levels were measured using a creatinine assay kit.

Due to the limited quantity of vessel samples, total RNA was extracted from the heart tissues using RNeasy Fibrous Tissue Mini Kit (Qiagen). The mRNA expression of COX1, COX2, PGI_2, β-actin, and hypoxanthine phosphoribosyltransferase-1 (HPRT1) was

measured by qRT-PCR (TaqMan) using the ABI Prism 7900HT sequence detection system (Applied Biosystems).

5.2.2 Solutions and Chemicals

The PSS consisted of the following (in mM): NaCl 119, KCl 4.7, KH_2PO_4 1.18, $NaHCO_3$ 24, $MgSO_47H_2O$ 1.17, $CaCl_2$ 1.6, glucose 5.5 and EDTA 0.026. All reagents were purchased from Sigma (St. Louis, MO).

5.2.3 Statistical Analysis

Results are reported as mean±SEM. The statistical significance was evaluated using the unpaired Student's t test for simple comparison between two values. The concentration-response curves of the different groups were compared by ANOVA for repeated measurements followed by Bonferroni's correction. $P<0.05$ was considered to be significant. In all experiments, n equals the number of mice from which samples were obtained.

5.3 Results

5.3.1 Vascular Constriction and COX Activity

We found that PE-induced constriction was significantly suppressed in DE exposure group, compared with the control group (Fig.5.1). In the presence of indomechacin, PE-elicited constriction was reduced in both control and DE exposure groups (Fig.5.2A,B). In addition, the fractional changes of attenuated constriction was significantly reduced in DE group (31.7±4.6% vs 12.6± 4.2%, Filtered air vs. DE, $p<0.02$) (Fig.5.2C), suggesting a modification of COX activity after DE exposure, and an imbalance of COX-mediated metabolites towards to an increased production of relaxant.

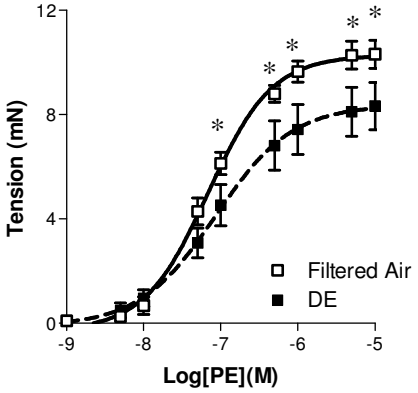

Figure 5.1 Reduced vasoconstriction in the thoracic aorta.
Exposure to DE attenuated PE-stimulated vasoconstriction, n=9, *P<0.05. Values are mean±SEM.

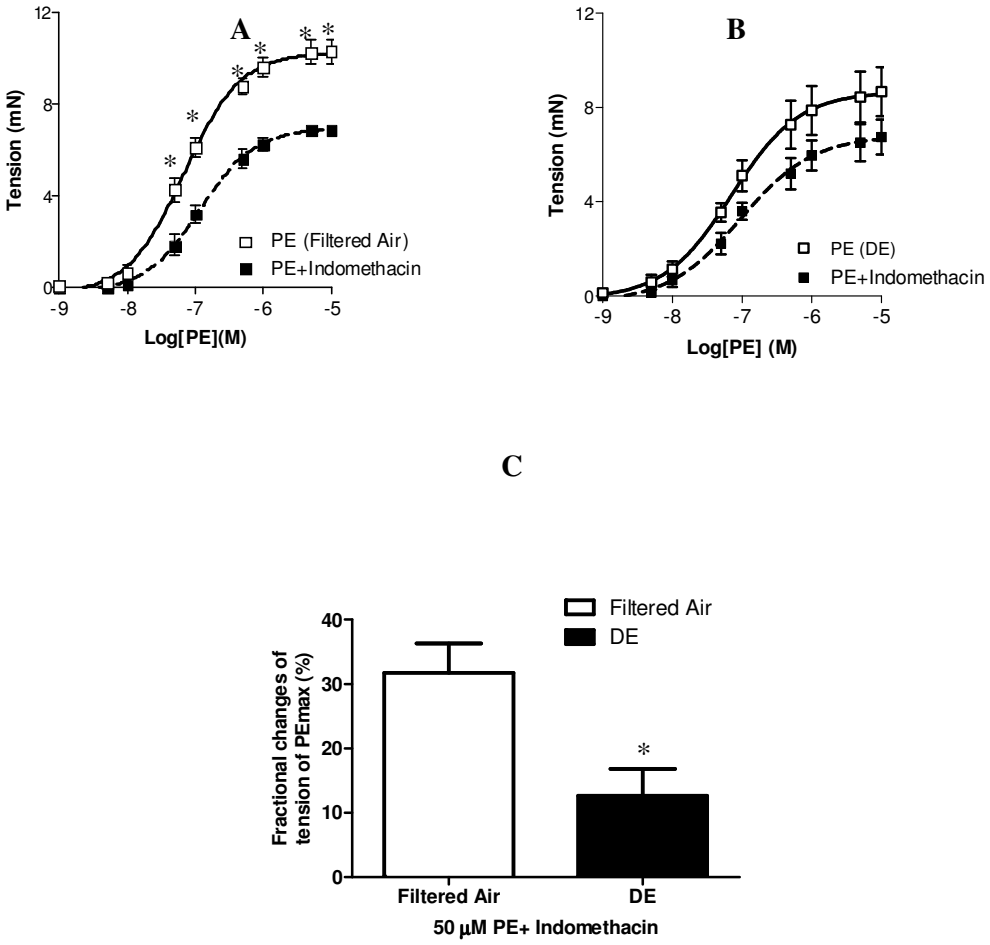

Figure 5.2 Reduced vasoconstriction in the presence of COX inhibitor (indomethacin) and reduced fractional constriction in the thoracic aorta. Concentration-response curves of PE-stimulated vasoconstriction shows that COX inhibitor caused significant reduction of constriction only in filtered air exposed mice (A) (n=9, *P<0.001), but not in DE group (B), n=9, p=0.17; C) The fractional changes of maximum vasoconstriction in the presence of indomethacin were significantly lower in DE exposure group than the control, n=9, *P<0.02. Values are mean±SEM.

5.3.2 Immunohistochemical Staining Analysis of COX1 and COX2 Expression in the Thoracic Aorta and Aortic Root

In the thoracic aorta, COX1 was expressed by endothelial cells, smooth muscle cells, and macrophages (Fig.5.3A,B,C,G)., COX2 was expressed by smooth muscle cells and macrophages (Fig.5.3D,E,F,G). In aortic root, COX1 and COX2 were expressed by macrophages (Fig.5.5B,C,D). The COX1 expression in the thoracic aorta and aortic root was similar between filtered air and DE exposure groups (Fig.5.4A,B,C & Fig.5.6A,B,C). We observed a significant enhancement of COX2 expression both in the thoracic aorta (1.1±0.1% vs 1.6 ± 0.1%, Filtered air vs. DE; $p<0.007$) (Fig.5.4D,E,F) and in aortic root (0.81±0.06% vs 0.99 ± 0.17%, Filtered air vs. DE; $p<0.02$) (Fig.5.6D,E,F).

A

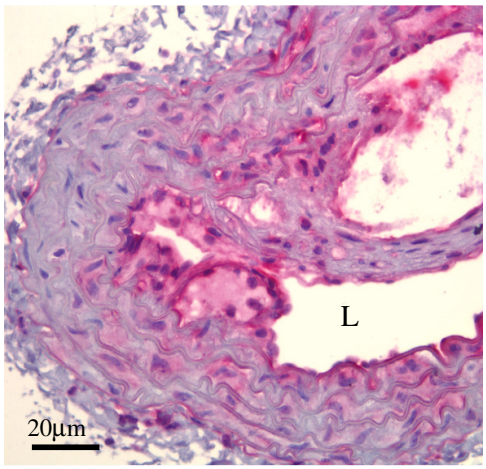

B

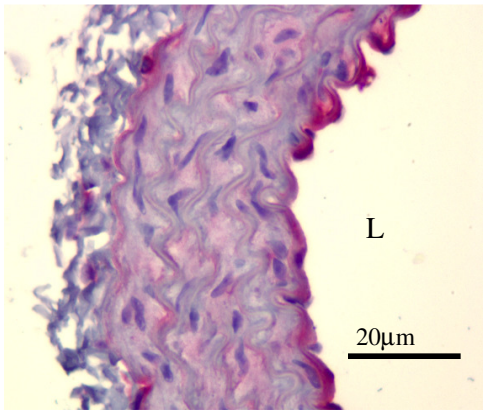

C

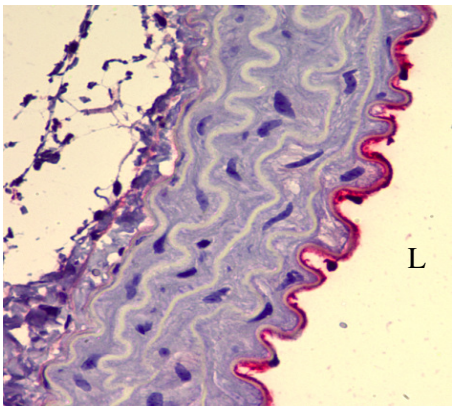

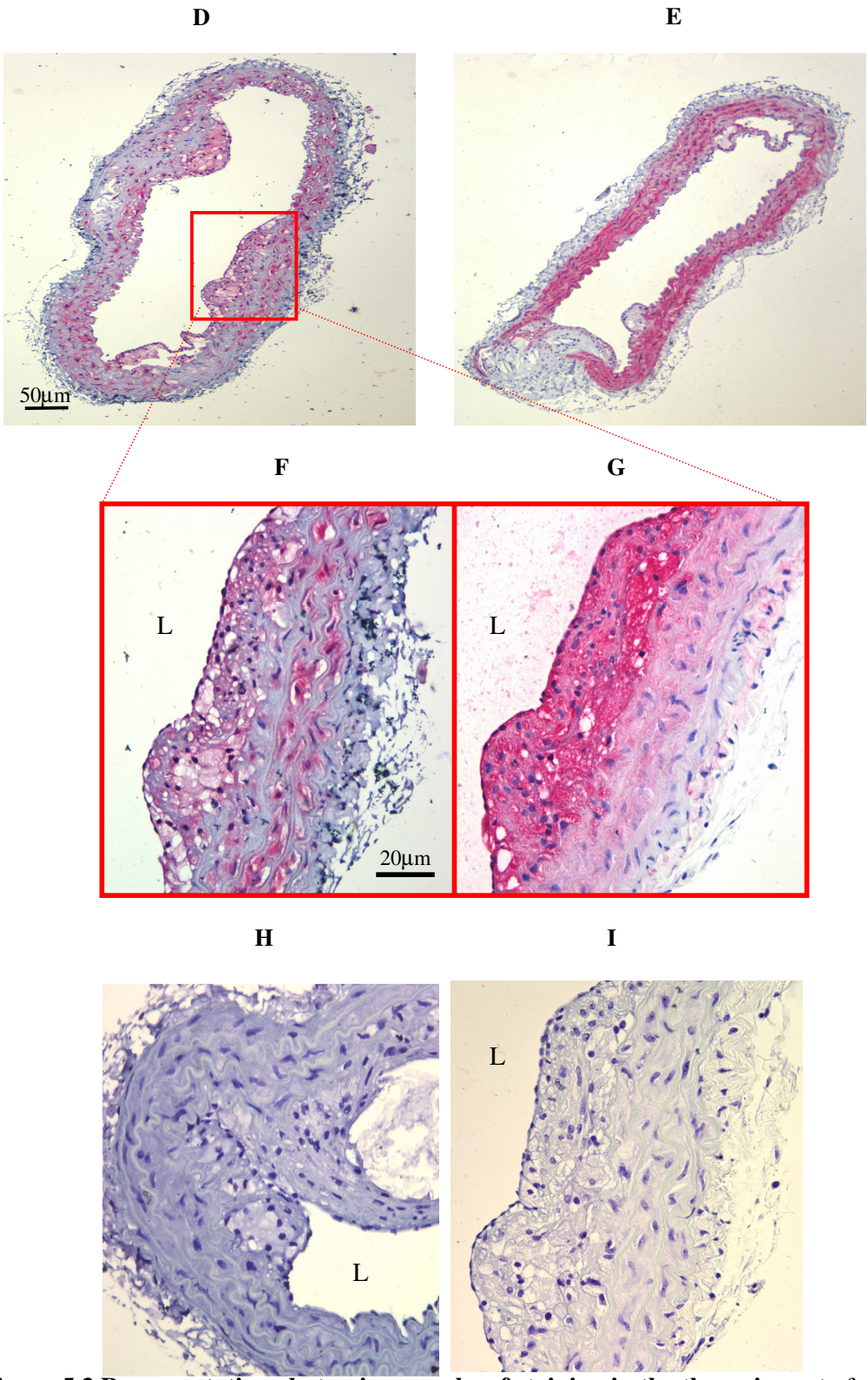

F4/

Figure 5.3 Representative photomicrographs of staining in the thoracic aorta for A) COX1 (400X); B) COX1 (600X); C) Endothelial cells (von Willerband factor; 600X); D) COX2 (100X); E) Smooth muscle cells (α-actin; 100X); F) COX2 (400X); and G) Macrophages (F4/80; 400X); H) Negative control for A (400X); I) Negative control for F and G (400X); L: lumen.

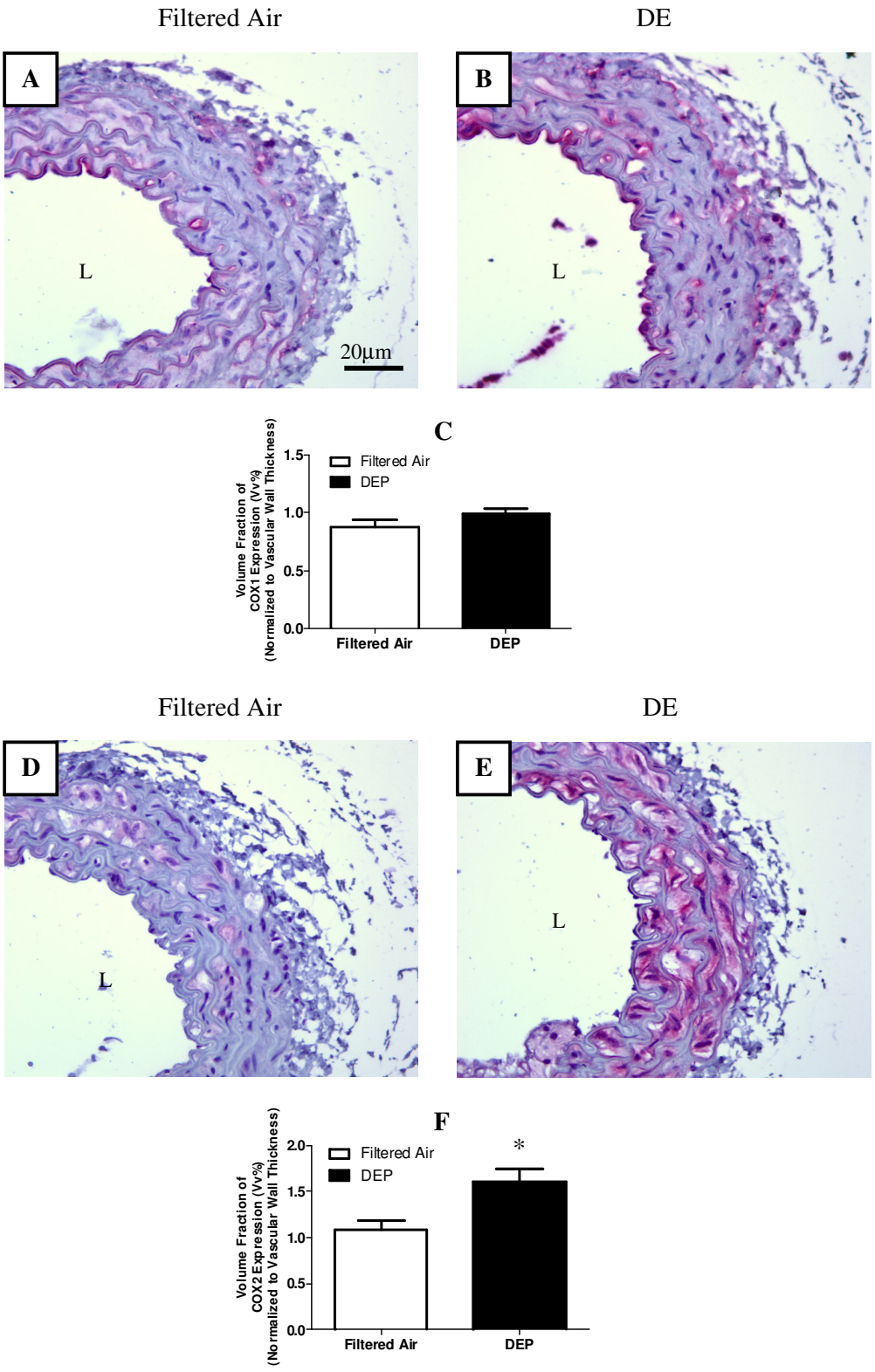

Figure 5.4 Immunohistochemical analysis of COX1 and COX2 expression in the thoracic aorta. Representative photomicrographs of staining for COX1 (A,B) and COX2 (D,E) in the thoracic aorta of mice exposed to filtered or DE; C) COX1 expression was not altered after DE exposure, n=8, p=.02; F) COX2 expression was increased in DE exposure group, compared with the control, n=8, *p<0.007. L: lumen. Magnification: orginal X400. Values are mean±SEM.

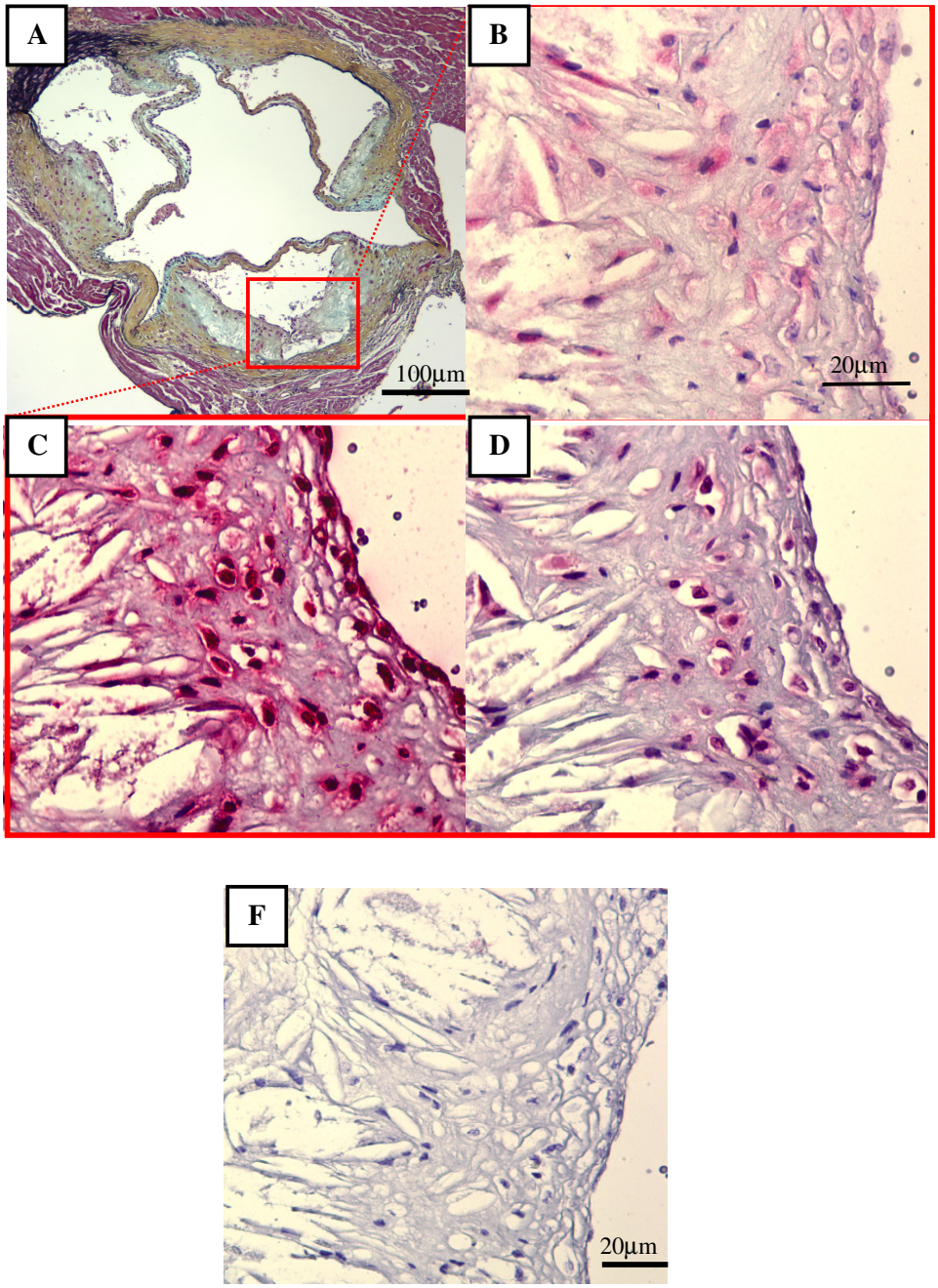

Figure 5.5 Representative photomicrographs of staining in aortic root for A) Movat staining (100X); B) Macrophages (F4/80; 600X); C) COX1 (600X); and D) COX2 (600X); F) Negative control (400X).

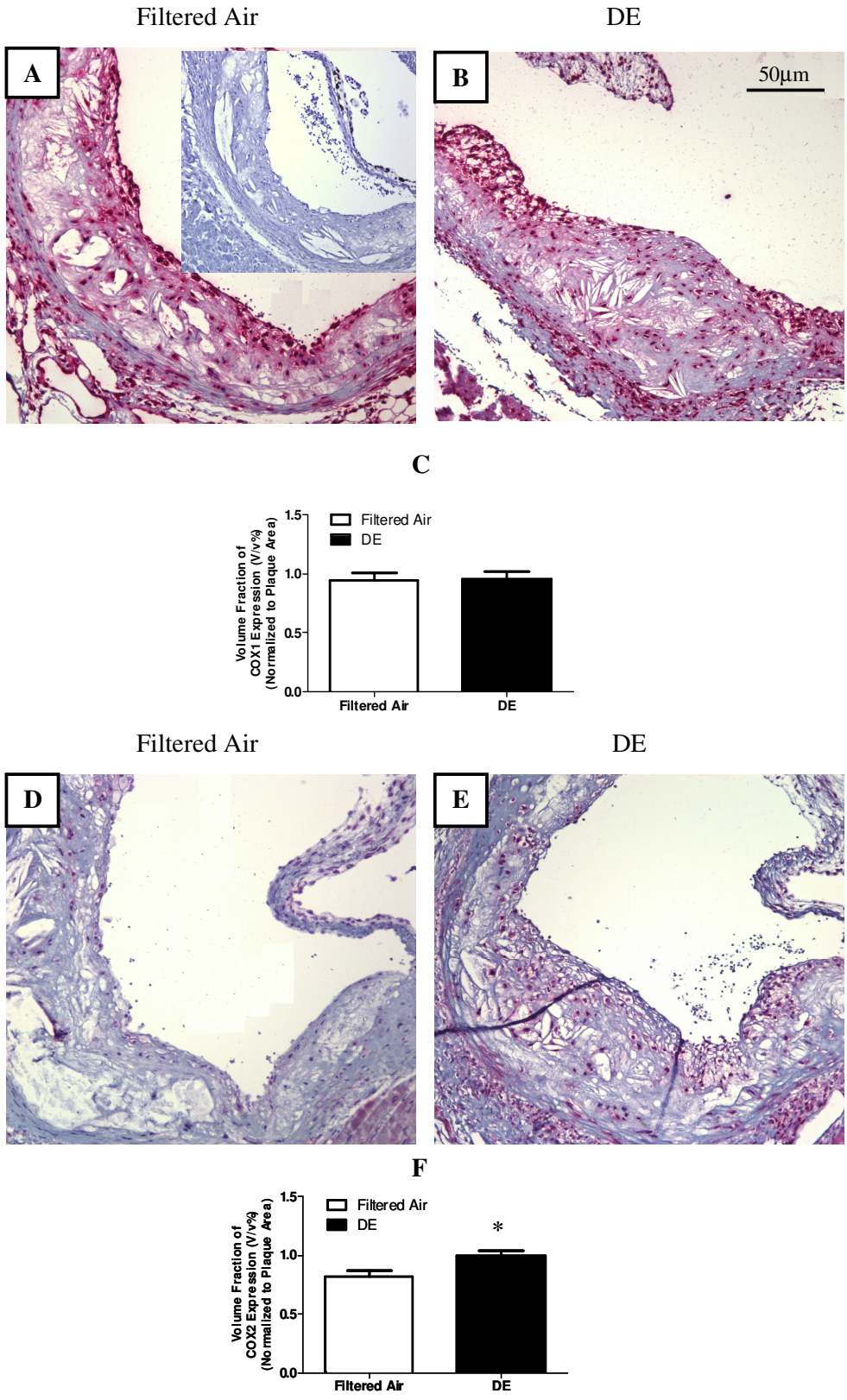

Figure 5.6 Immunohistochemical analysis of COX1 and COX2 expression in aortic root. Representative photomicrographs of staining for COX1(A,B) and COX2 (D,E) in artic root; C) COX1 expression was not altered after DE exposure, n=8, p=0.3; F) COX2 expression was increased in DE exposure group, n=8, *p<0.02. Magnification: orginal X200. Inset in A is the negative control. Values are mean±SEM.

5.3.3 Urine 2,3-dinor-6-keto $PGF_{1\alpha}$ Production

The urinary excretion of 2,3-dinor-6-keto $PGF_{1\alpha}$ is the major urinary metabolite of renal PGI_2. The 2,3-dinor-6-keto $PGF_{1\alpha}$ concentration was significantly increased by more than 15-fold after DE exposure, compared with the control (22.68±5.5 vs 344.6 ± 117.1pg/ml per Cr (mg/dl), Filtered air vs. DEP, $p<0.007$) (Fig.5.7).

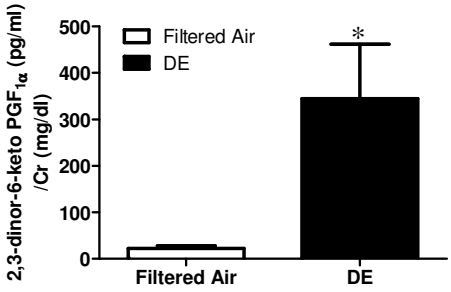

Figure 5.7 Urine 2,3-dinor-6-keto $PGF_{1\alpha}$ concentration. Urine 2,3-dinor-6-keto $PGF_{1\alpha}$ concentration was significantly higher after exposure to DE than the control, n=10, *P<0.007. Values are mean±SEM.

5.3.4 Real-Time RT- PCR of the mRNA expression of COX1, COX2 and PGI_2 in the Heart

To examine whether the mRNA expression of COX1, COX2 and PGI_2 was also altered, we extracted RNA from the heart tissue and performed quantitative real-time PCR using Taqman assay. We found no change in COX1 mRNA expression after exposure to DE, compared with the control (Fig.5.8A). However, the mRNA expression of COX2 was significantly increased after exposure to DE (38.0±1.8% vs 50.4 ± 3.6%, Filtered air vs. DE; $p<0.006$) (Fig.5.8B). The PGI_2 expression in the heart was also significantly augmented after DE exposure, compared with the control (71.4±1.1% vs 78.4± 2.5%, Filtered air vs. DE; $p<0.02$) (Fig.5.8C).

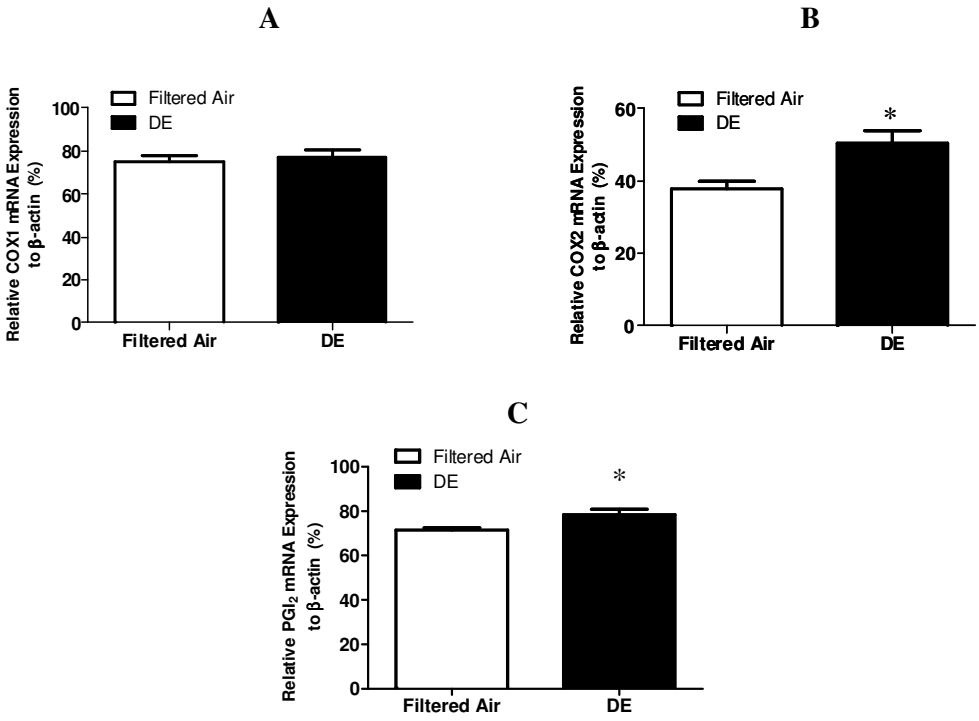

Figure 5.8 The mRNA expression of COX1, COX2 and PGI_2 in the heart. A) The mRNA expression of COX1 was not altered after exposure to DE, n=7 (filtered air), n=8 (DE), P>0.05; B) DE exposure significantly increased COX2 mRNA expression, n=7 (filtered air), n=8 (DE), *P< 0.006; C) The mRNA expression of PGI_2 significantly increased in DE exposure group (n=8), compared with filtered air exposure (n=7), *P< 0.02. Values are mean±SEM.

5.4 Discussion

COX1 or/and COX2 play an important role in the progression of atherosclerosis (248; 273). Inhibition of COX1/COX2 has been associated with the reduction of cardiovascular events. Here, we explored the contribution of both COX1 and COX2 to the vascular dysfunction induced by exposure to DE.

In this study, we demonstrate that DE exposure caused up-regulation of COX2 activity and expression in blood vessels. We also show that DE exposure caused an increase in PGI_2 production. We postulate that COX2 contributes to the excessive PGI_2 production. In addition, DE exposure caused significant attenuation of PE-stimulated vasoconstriction.

Prostanoid biosynthesis is significantly increased in response to inflammatory stimuli. Non-selective COX1/COX2 inhibitors, or non-steroidal anti-inflammatory drugs (NSAIDs), are widely used as anti-inflammatory agents, highlighting the pro-inflammatory role of the prostanoids. Traditionally, COX1 is recognized as a housekeeping enzyme that is constitutively expressed in endothelial cells, and vascular smooth muscle cells, and responsible for the production of physiological prostanoids to maintain cardiovascular homeostasis. Nevertheless, animal studies have shown that overexpression of COX1 is also implicated in a number of cardiovascular diseases, including hypertension (317) and atherosclerosis (273). The deleterious effects are mainly resulted from COX1-derived TXA2 production, a potent vasoconstrictor and platelet activator. TXA2 causes endothelial dysfunction and promotes vascular smooth muscle cell adhesion, migration, and proliferation (318). In this study, we examined COX1 protein and mRNA expression in the blood vessel, and aortic root. Consistent with previous reports, we found that COX1 was expressed by endothelial cells, smooth muscle cells, and macrophages (Fig.5.3). Our data show that DE exposure did not alter COX1 expression following DE exposure. In addition, we used selective TXA2 receptor antagonist (SQ29548), but failed to observe any modifications of vasoconstriction after DE exposure (Appendix D), suggesting that DE exposure did not have effects on TXA2 production that is predominantly regulated by COX1. Our results support the findings from other studies showing that the up-regulation of COX1 expression mainly occurs at the early, or acute stages of cardiovascular dysfunction (319).

COX2 is usually not detectable under normal physiological conditions, but can be up-regulated by inflammatory or other pathological stimuli. Both human and animal studies have demonstrated that COX2 is implicated in the progression of atheroslcerosis (320; 321). DE exposure can up-regulate COX2 protein and mRNA expression in human macrophages (322). Exposure to residual oil fly ash induced overexpression of COX2 in the lung, whereby leading to acute lung injury (274). In addition, exposure to motorcycle exhaust particles caused up-regulation of COX2 in rat vascular smooth muscle cells and promoted smooth muscle cell proliferation (323). We found that COX2 was predominantly expressed in smooth muscle cells and macrophages in the vascular wall and aortic root (Fig.5.3, Fig 5.5). We show that DE exposure up-regulated COX2 expression at both protein and mRNA levels (Fig.5.4F, Fig.5.6F, Fig.5.8B).

Vascular function study shows that PE-elicited constriction was attenuated (Fig.5.1), and we postulate that this was due to an imbalance between PGI_2 and TXA2 production. This idea is supported by an excessive production of the major metabolite of PGI_2 in the urine (Fig.5.7). In addition, PGI_2 mRNA expression in the heart was also enhanced after DE exposure (Fig. 5.8C). PGI_2 is mainly derived from COX2. Immunohistochemical and qPCR analysis show that COX2 expression in the heart was increased after DE exposure. The increased COX2 activity and expression likely play an essential role in mediating PGI_2 production.

To further confirm the specific contribution of COX1 and COX2 to the increased PGI_2 production, we administered a specific inhibitor of COX1 (SC560) or COX2 (NS398), respectively. Although we found a significant change in PE-stimulated vasoconstriction in the presence of non-specific COX inhibitor (indomethacin), we failed to observe any difference of vasoconstriction in the presence of the specific antagonists of COX1 (SC560) or COX2 (NS398) (Appendix E). We speculate that there was an interaction between COX1

and COX2 and the inhibition of both COX1 and COX2 activities was necessary to reveal the inhibitory effect. Other possible factors, that may be responsible for the negative results and we can not exclude, include the concentration of these antagonists and the time course of administration.

COX2 has been implicated in the progression of atheroslcerosis, and PGI_2 can also act as a pro-inflammatory prostanoid that enhances vascular permeability and promotes leukocyte infiltration. We postulate that COX2 up-regulation contributes to the DE-exposure induced cardiovascular dysfunction. COX2 could be a source for ROS (324); induce endothelial dysfunction by attenuating NO production (325); activate leukocyte chemotaxis; and promote smooth muscle cell migration (3), all factors that promote atherogenesis.

It is worth noting that COX2 is an intermediate enzyme, which is involved in the production of an array of PGs, thus COX2-mediated functions in cardiovascular system largely depend on the downstream enzymes present in a particular cell type. The evidence from clinic trials has shown that coxibs, a subclass of non-steroidal anti-inflammatory drugs designed to selectively inhibit COX2, are associated with increased cardiovascular events, including MI, and thrombotic stroke (327; 328). These side effects could result from reduced COX2-mediated PGI_2 production. PGI_2 is an anti-atherogenic molecular, and can protect the vasculature from inflammation and inhibit atherogenesis by reducing ROS production and inhibiting platelet activation (329). In addition, PGI_2 can also cause the up-regulation of eNOS expression and activity (330). To examine whether the increased PGI_2 has a beneficial effect or is just a compensatory effect, genetic modified animal models and/or PGI_2 analogs could help to understand the role of COX2 and PGI_2 in vascular diseases associated with exposure to DE.

In summary, we show that DE exposure caused up-regulation of COX2 (but not COX1) activity and expression in the blood vessels and the heart, which could contribute to DE exposure-induced cardiovascular disease.

Chapter 6

Exposure to Diesel Exhaust Enhances Soluble Guanylate Cyclase Expression in ApoE Knockout Mice

6.1 Introduction

The association between exposure to ambient particulate matter air pollution with diameter less than 10μm (or PM_{10}) and cardiovascular morbidity and mortality has been well established (22). However, the mechanisms underlying how PM_{10} impacts blood vessels are not fully understood. Abundant evidence indicates that endothelial dysfunction is an important component in the pathogenesis of PM_{10}-associated cardiovascular diseases (22; 287). The endothelium, a monolayer of cells separating blood from the vascular wall, serves as an important regulator to maintain vascular tone and vasculature integrity (276-278). It does so by producing a number of mediators, in particular, nitric oxide (NO) and endothelin (ET).

NO produced by endothelial cells can diffuse into the vascular smooth muscle cells and activates guanylyl cyclases (GC), which consequently catalyze the dephosphorylation of guanosine 5'-triphosphate (GTP) to 3',5'-cyclic guanosine monophosphate (cGMP), and relax blood vessels. There are 2 types of GC: soluble and particulate. Soluble GC (sGC) is expressed in cytosoplasm and particulate GC is expressed in cell membrane. In general, particulate GC does not respond to NO, and soluble GC is known as the NO receptor in smooth muscle cells (331). sGC is a heterodimer composed of an α subunit and a β subunit, each of which is further characterized into two isoforms: α_1, and α_2, β_1, and β_2. The

expression of subunits varies among different tissue types: α_1 and β_1 are expressed ubiquitously in blood vessels, but α_2 and β_2 are not expressed in vasculature. Studies have shown that α_1 subunit is essential for the basal NO and SNP-stimulated sGC activation, whereas β_1 subunit is critical for sGC specificity for GTP (331).

Endothelium-derived NO protects the blood vessels from developing atherosclerosis by suppressing vasoconstriction, attenuating monocyte chemotaxis, preventing the adherence of leukocytes to the endothelium, inhibiting platelet adherence and aggregation, and controlling the proliferation of vascular smooth muscle cell (279). A hallmark of endothelial dysfunction is an impairment of acetylcholine (ACh)-stimulated vasorelaxation. ACh can stimulate endothelial cell to produce NO. The loss of endothelium-derived NO bioactivity is critical to this abnormal response (165). NO is enzymatically synthesized by nitric oxide synthase (NOS) from L-arginine in the presence of co-factor terahydrobiopterin (BH4) (332). Three isoforms of NOS have been identified, including endothelial NOS (eNOS), neuronal NOS (nNOS), and inducible NOS (iNOS).

Exposure to PM_{10} can cause insufficient supply of eNOS substrate (L-arginine), inactivation/oxidation of cofactor BH4, attenuation of eNOS activity and expression, and degradation of NO bioactivity (22; 287), consequently resulting in the impairment of ACh-stimulated vasorelaxation, or endothelial dysfunciton. In addition, exposure to PM_{10} causes excessive ET-1 production (196), enhanced vascular sensitivity to ET-1 (284), and up-regulation of ET-1 mRNA expression (200), resulting in exaggerated vasoconstriction, which contribute to hypertension, MI, and stroke.Studies from our laboratory have shown that exposure to PM_{10} (e.g., ECH93), caused the acceleration of atherogenesis in rabbits (133; 143; 545). Sun and colleagues showed that exposure to concentrated ambient $PM_{2.5}$ caused progression of atherosclerosis in ApoE knockout mice (143). Thess findings have been supported by human studies showing that increased ambient PM is associated with the

development of atherosclerosis (144; 145; 300). Recently, we demonstrated that exposure to diesel exhaust (DE), a major component of urban $PM_{2.5}$, promotes the progression of atherosclerosis (280). In vitro and instillation studies have shown that DE exposure causes lung inflammation, and vascular endothelial dysfunction (180; 183). In the study, we examine whether DE exposure causes endothelial dysfunction, using a model of chronic inhalation exposure DE to ApoE knockout mice, and to investigate the signaling pathways that contribute to the DE exposure-induced endothelial dysfunction, and ultimately the progression of atherosclerosis.

6.2 Methods and Materials (Please refer to Chapter 2 for detailed information)

6.2.1 Methods

Male ApoE knockout mice (30-week old), fed with regular chow, were exposed for 7 weeks (5days/week, 6hrs/day) to DE controlled at the concentration of 200 $\mu g/m^3$ $PM_{2.5}$. Mice exposed to filtered air were the control. Animal procedures were approved by the Animal Care and Use Committee of the University of Washington.

After exposure, mice were euthanized. Plasma, and urine were collected and kept at –80°C. The thoracic aorta, abdominal aorta, and heart were carefully dissected from their connective tissues and kept in appropriate solution until assay.

To examine endothelial function, thoracic aortae were cut to 2mm rings and mounted on a wire myograph. The relaxant responses to acetylcholine (ACh), and sodium nitroprusside (SNP) were determined. To examine the effect of DE exposure on endogenous NO production, *N*G-nitro-L-arginine-methyl ester (L-NAME; 200μM) was used. In addition, a specific inhibitor for iNOS (1400W) was administered to examine the contribution of iNOS activity. The impact of DE exposure on ET-1 effect was examined using the ET

receptor antagonist (bosentan, 10 μM), selective inhibitor for ET_A (BQ123, 10μM) or ET_B (BQ788, 10μM), respectively.

Cryosections (5μm) were incubated with monoclonal anti- eNOS antibody (1:50, BD Transduction Laboratories) at room temperature for 1h. Paraffin-embedded sections (5μm) were incubated with rabbit polyclonal antibodies to $sGC\alpha_1$ (1:200), and $sGC\beta1$ (1:200) at 4°C overnight. The positive red staining was recognized, quantified by colour segmentation (Image Pro Plus), and normalized to the area of the atherosclerotic lesion.

Plasma NO level was assessed by measuring nitrite concentration using a NO-specific chemiluminescence analyzer (Sievers). Urine cGMP level was measured using a cGMP EIA kit (Cayman Chemical) and normalized to the urine creatinine (Cr.) concentration.

Total RNA was extracted from the abdominal aortae using RNeasy Fibrous Tissue Mini Kit (Qiagen). The mRNA expression of eNOS, $sGC\alpha_1$, β-actin, and hypoxanthine phosphoribosyltransferase-1 (HPRT1) was measured by qRT-PCR (TaqMan) using the ABI Prism 7900HT sequence detection system (Applied Biosystems). The values of gene expression were normalized to the values of β-actin, and HPRT1, and displayed as ratio relative to β-actin.

6.2.2 Solutions and Chemicals

The PSS consisted of the following (in mM): NaCl 119, KCl 4.7, KH_2PO_4 1.18, $NaHCO_3$ 24, $MgSO_47H_2O$ 1.17, $CaCl_2$ 1.6, glucose 5.5 and EDTA 0.026. All reagents were purchased from Sigma (St. Louis, MO).

6.2.3 Statistical Analysis

Results are reported as mean±SEM. The statistical significance was evaluated using the unpaired Student's t test for simple comparison between two values. The concentration-

response curves of the different groups were compared by ANOVA for repeated measurements followed by Bonferroni's correction. $P<0.05$ was considered to be significant. In all experiments, n equals the number of mice from which samples were obtained.

6.3 Results

6.3.1 Endothelial Function

ACh-stimulated relaxation was not impaired by DE exposure (Fig.6.1A); however, the concentration-response curve of SNP-induced endothelium-independent relaxation was significantly shifted to the left after DE exposure (pD_2 (-Log [EC50]): 7.9±0.1 vs 8.5±0.1; Filtered air vs. DE, $p<0.001$) (Fig.6.1B), suggesting an increase in smooth muscle cell sensitivity to NO. To examine whether the increased NO sensitivity was due to the reduction of endogenous NO production, we inhibited the NO production with a NOS antagonist (L-NAME). Indeed, the concentration-response curve of SNP shifted to the left in the presence of L-NAME (Fig.6.1C).

To examine the effect of DE exposure on the endogenous NO production, we used PE as an agonist. In the presence of L-NAME, the fractional change of PE-induced maximal constriction was not significantly different (29.1%±3.5 vs 38.7±2.9%; Filtered air vs. DE, $p=0.1$) (Fig.6.2C). However, exposure to DE significantly increased the fractional change of vasconstriction in the presence of specific inhibitor for iNOS (1400W) (7.2±2.1% vs 24.1±7.6%; Filtered air vs. DE, $p<0.04$) (Fig.6.2F), suggesting an increase in iNOS activity, which indirectly implys a reduction in eNOS activity.

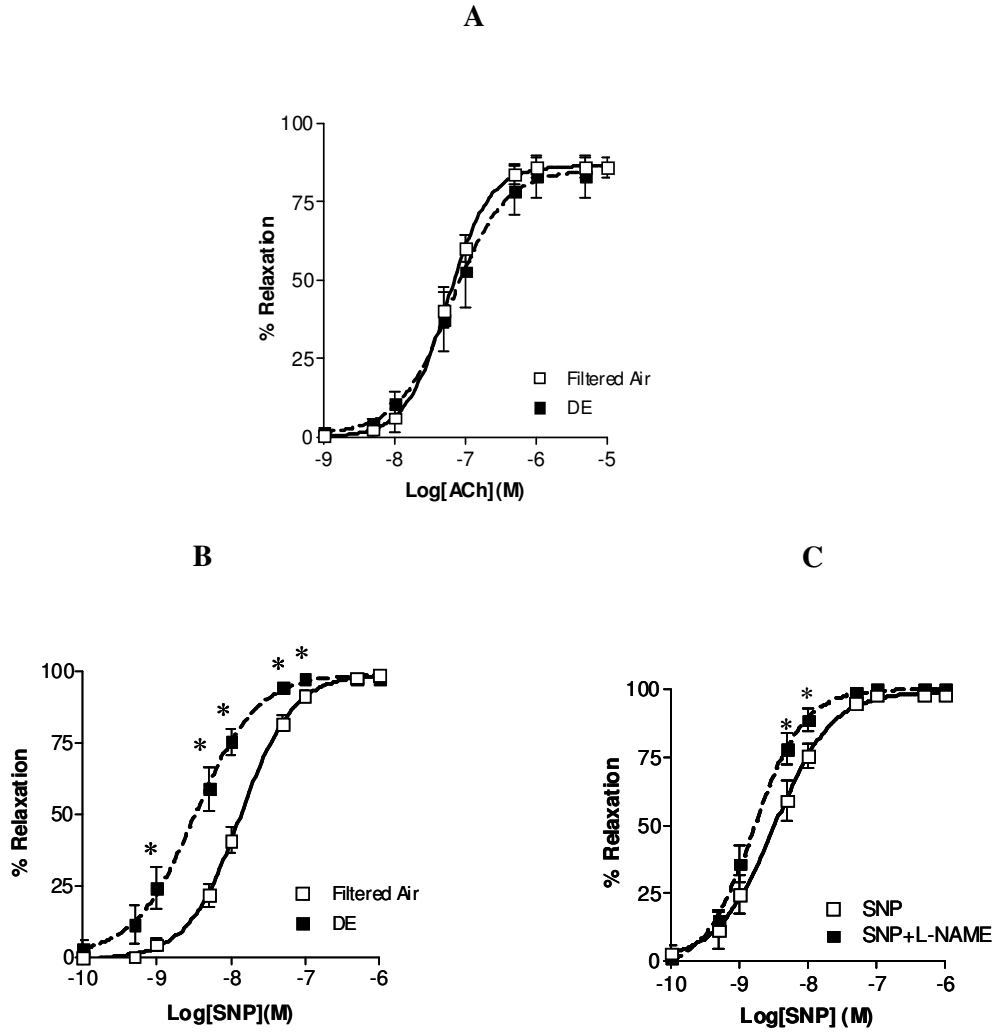

Figure 6.1 Concentration-response curves show that ACh-stimulated endothelium-dependent and SNP-elicited endothelium-independent relaxation. A) Concentration-response curves show that ACh-stimulated relaxation is not different between DE and filtered air exposure groups, n=6; B) The concentration-response curve of SNP-induced endothelium-independent relaxation shifted to the left after DE exposure, n=6, *P<0.05; C) Inhibition of NOS by L-NAME led to a left-shiftiness of the concentration-response curve of SNP relaxation, n=6, *P<0.05. Values are mean±SEM.

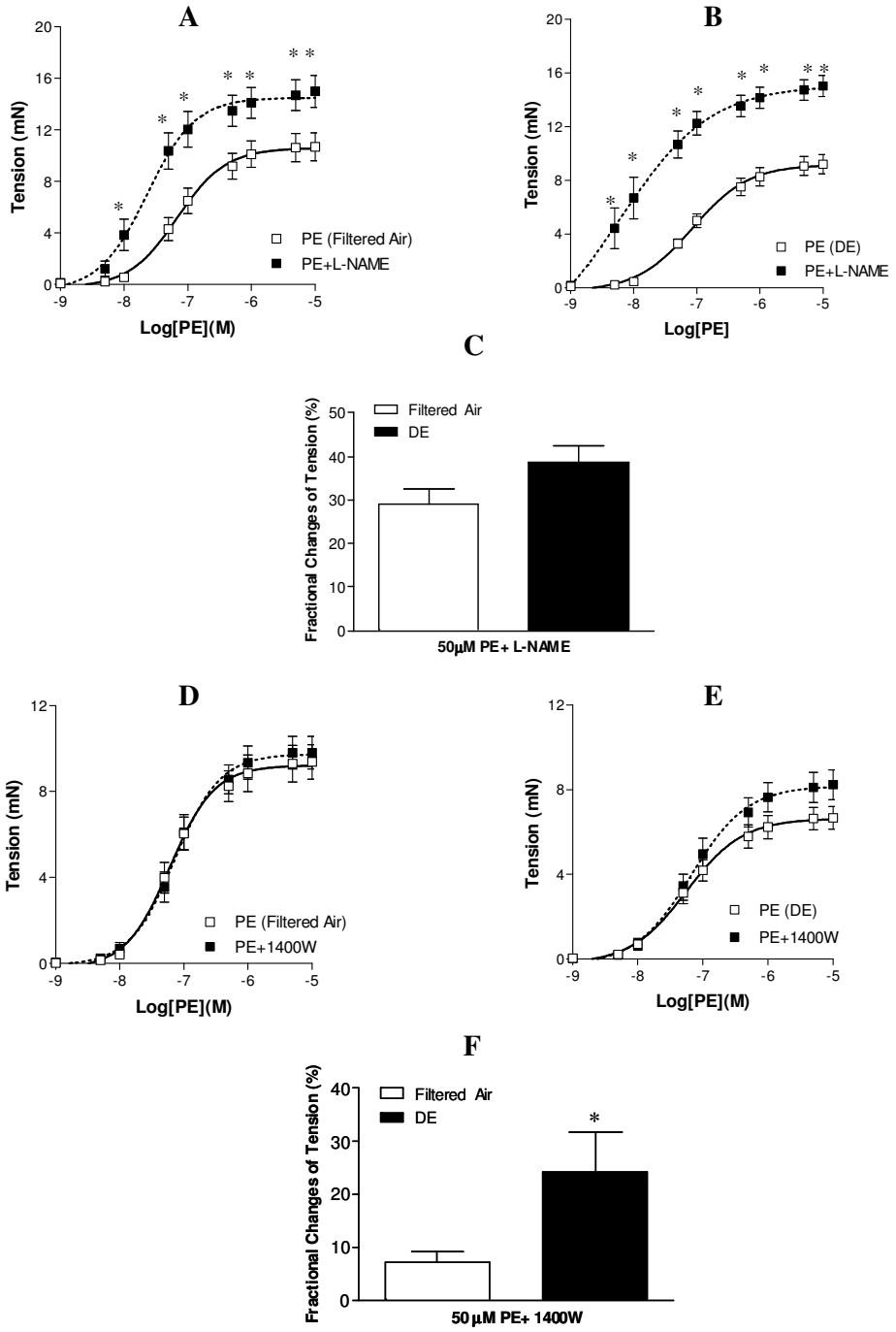

Figure 6.2 The effect of NOS inhibitors on PE-induced vasoconstriciton in the thoracic aorta. Concentration-response curves show that the inhibitor of NOS (L-NAME) significantly enhanced vasoconstriction in both control (A) and DE exposure groups (B) n=8, *P<0.01. However, the fractional change of maximum vasoconstriction in the presence of L-NAME was not significantly different between the control and DE exposure groups (C), n=8, p=0.10. Concentration-response curves show that the inhibitor of iNOS (1400W) did not significantly enhance vasoconstriction in both control (D) and DE group (E), n=9, p=0.11. However, 1400W caused a significant increase in fractional change of maximum vasoconstriction in DE exposure group, n=9, *P<0.04. Values are mean±SEM.

6.3.2 Immunohistochemical Staining of eNOS and sGC Expression in the Thoracic Aorta

eNOS expression in the thoracic aorta was markedly reduced after DE exposure (76.5±8.5% vs 45.2 ± 7.5%, Filtered air vs. DE; $p<0.02$) (Fig.6.3, A,B,C). sGCα1 expression was significantly increased following DE exposure (1.2±0.7% vs 8.9 ± 3.7%, Filtered air vs. DE; $p<0.02$) (Fig.6.3, D,E,F). The expression of sGCβ1 was similar, compared DE with filtered air group (Appendix F).

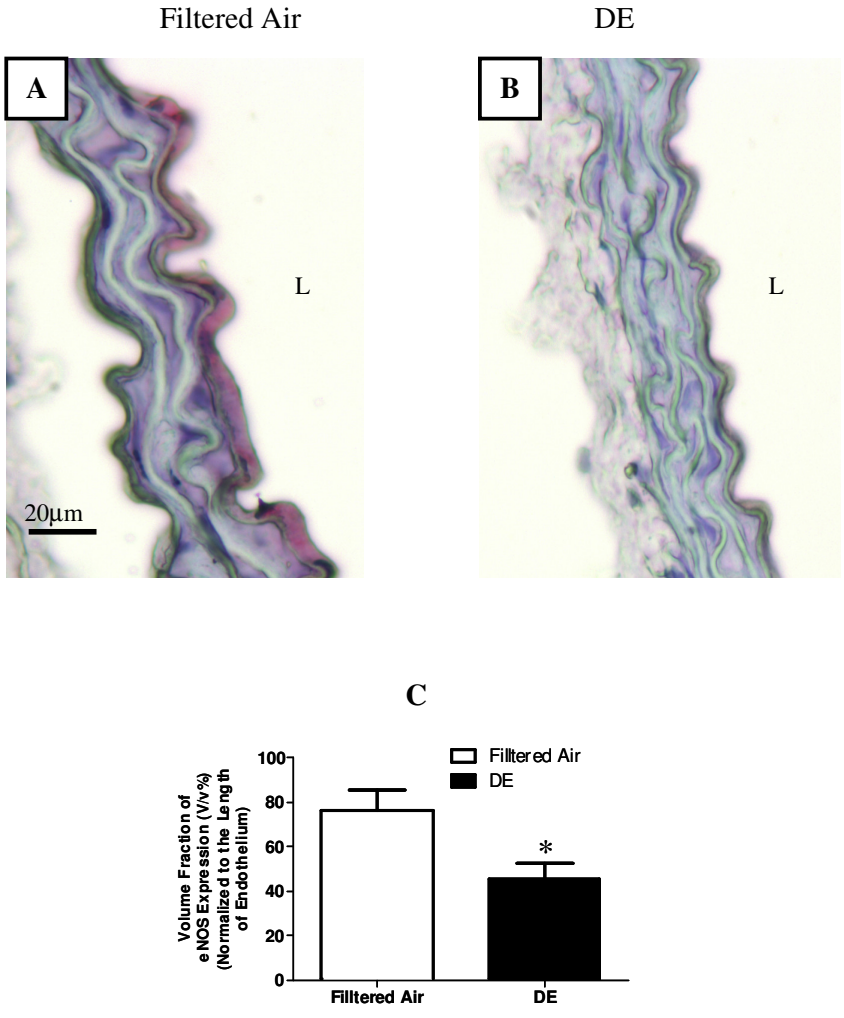

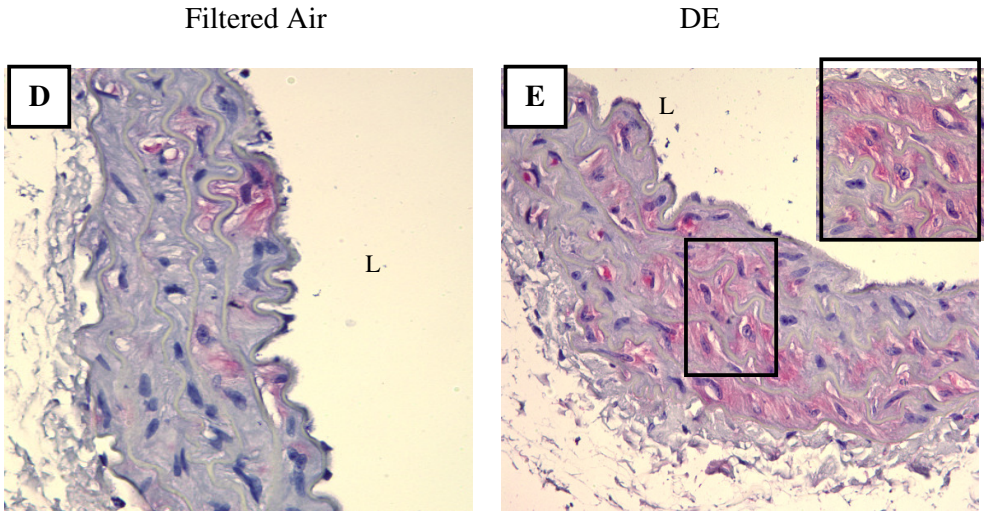

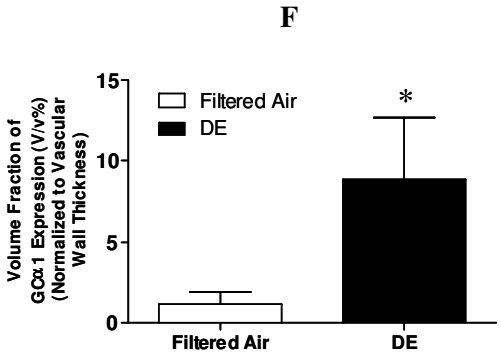

Figure 6.3 Immunohistochemical analysis of eNOS and sGCα_1 expression in the thoracic aorta. A,B) Representative photomicrographs of staining for eNOS in the thoracic aorta; C) Quantitative analysis shows that DE exposure significantly reduced eNOS expression in the thoracic aorta , n=9, *P<0.02; D,E) Representative photomicrographs of staining for sGCα_1 in the thoracic aorta; the inset in E) is a photomicrograph with higher magnification (600X); F) Quantitative analysis shows that exposure to DE enhanced sGCα1 expression in the thoracic aorta, n=9, *P<0.02. L: Lumen. Magnification: orginalX400. Values are mean±SEM.

6.3.3 Measurement of Plasma Nitrite and Urine cGMP Concentration

Plasma nitrite concentration was not different between filtered air and DE exposure groups (Fig.6.4A). Urine cGMP concentration was higher in DE group, but the difference was not statistically significant (Fig.6.4B).

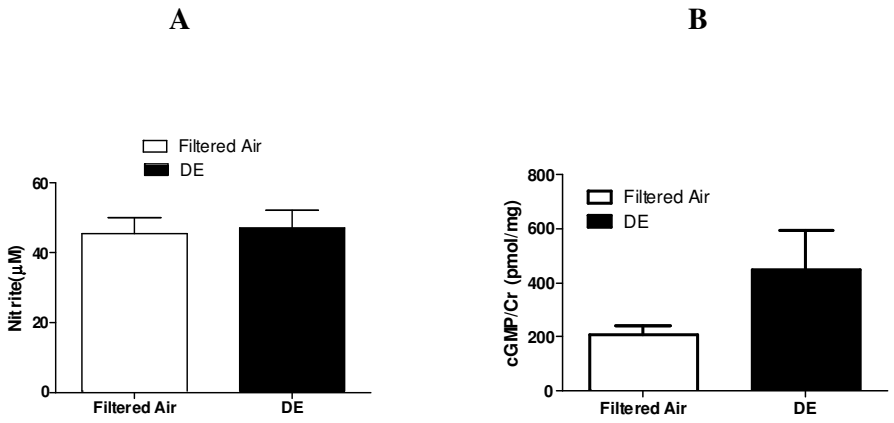

Figure 6.4 Measurement of plasma nitrite concentration and urine cGMP level. A) Plasma nitrite (NO metabolite) concentration was similar between filtered air and DE exposure group, n=12; p=0.7; B) Urine cGMP level was elevated after DE exposure (n=10), but the increase is not statistically significant from the control (n=9), p=0.4. Values are mean±SEM.

6.3.4 Real-Time RT- PCR of eNOS and sGCα1 mRNA Expression

RNA was extracted from the abdominal aorta to examine whether the mRNA expression of eNOS and $sGC\alpha_1$ was altered after DE exposure by real-time PCR using Taqman assay. Exposure to DE reduced eNOS mRNA expression (73.8±4.7% vs 67.8± 2.7%, Filtered air vs. DE; p=0.2) (Fig.6.5A), but the reduction did not reach statistical significance. Similar, the expression of $sGC\alpha_1$ was not significantly different, compared DE with filtered air group (Fig.6.5B).

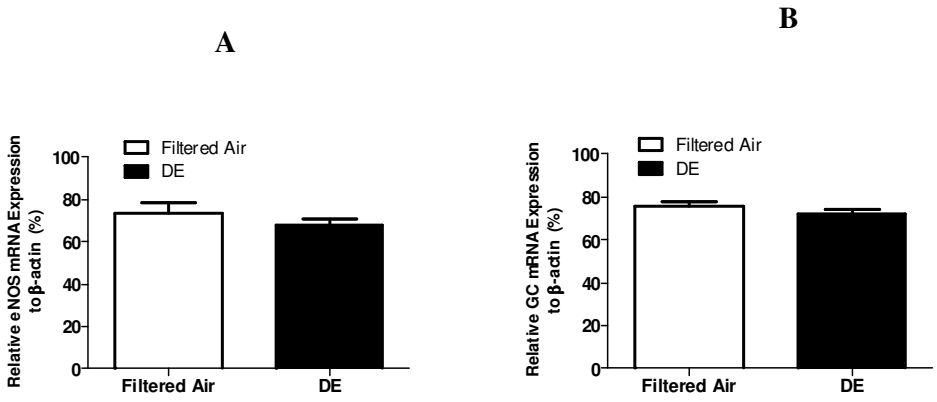

Figure 6.5 The mRNA expression of eNOS and sGCα1 in the abdominal aorta. A) The mRNA expression of was not significantly different, compared DE exposure (n=7) with the filtered air (n=10), p=0.2; B) The mRNA expression of $sGC\alpha_1$ was not significantly different after DE exposure (n=8), compared with filtered air exposure (n=10), p=0.2. Values are mean±SEM.

6.4 Discussion

In vitro and instillation studies have reported that exposure to PM_{10} (e.g., ECH93, residual oil fly ash, and DE), induced endothelial dysfunction (104; 177; 280); however, we did not observe a blunted ACh relaxation following a 7-week DE exposure to ApoE knockout mice (Fig.6.1A). Our finding is consistent with the results reported by Sun et al showing that exposing concentrated ambient particles to ApoE mice fed with regular chow did not impair ACh relaxation (143). In addition, a recently published inhalation study also showed that exposure of ApoE mice fed with regular chow to DE for 5 months did not attenuate ACh relaxation (297). The discrepancies could be due to the composition of different particles (ECH93 vs. DE), the size of the particles (PM_{10} vs. $PM_{2.5}$ vs. $PM_{0.1}$), and the route of exposure (in vitro vs. instillation vs. inhalation). In addition, the impairment of ACh relaxation was mostly observed after acute or subchronic exposure to PM_{10}, the diminished impairment of ACh relaxation following chronic exposure may result from a compensatory effect.

As no specific eNOS antagonists are commercially available, we used inhibitors for NOS and iNOS to examine eNOS activity indirectly. We found no significant difference of NOS activity using the non-specific NOS antagonist, L-NAME (Fig.6.2A); however, there was a significantly increased fractional change in PE-stimulated constriction in the presence of iNOS inhibitor (Fig.2B), suggesting an increase in iNOS activity, and indirectly indicating a reduction in eNOS activity, based on the observation that iNOS and eNOS are the most predominant NOS isoforms in mouse aorta (559). The result, implying suppressed eNOS activity, is supported by the immunohistochemistry analysis showing that DE exposure caused significant attenuation of eNOS expression in the thoracic aorta (Fig.6.3C). Taken together, the data, showing no impairment of ACh relaxation, but reduced endogenous eNOS-derived NO production and eNOS expression in the blood vessels, imply that a

"helper" mechanism(s) was turned on to compensate the reduction in endothelium-generated NO, whereby maintaining ACh-stimulated vascular relaxation after exposure to DE.

Clonidine can increase endothelial NO production and induce endothelial-dependent NO-mediated vasodilatation via the activation of endothelial α_2-adrenoceptors (560). To determine a potential contribution of endothelial α_2-adrenoceptors to the normality of ACh relaxation after exposure to DE, we examined vasorelaxation to clonidine. The clonidine-induced vasorelaxation was similar between DE and filtered air group (Appendix G), indicating that DE exposure did not have effect on the α_2-adrenoceptor-mediated response.

It was reported that plasma ET-1 concentration was elevated after exposure to ambient PM (561; 196). In addition, ET-1 expression in the blood vessels, and vascular sensitivity to ET-1 were also enhanced following DE exposure (284; 336). ET-1 causes vasoconstriction after binding to the ET_A receptor in smooth muscle cells. The increased ET-1 production is believed to contribute to hypertension, MI and stroke associated with exposure to ambient PM. Nevertheless, ET-1 can also cause endothelial-dependent NO-regulated relaxation by binding to the ET_B receptor in endothelial cells (113). Thus, we administered both non-selective ET receptor antagonist (bosentan), and selective antagonists for ET_A (BQ123) or ET_B receptors (BQ788), receptively, to examine the effects of DE exposure on different ET receptors. But we did not observe any difference of vascular constriction in the presence of different ET receptor antagonists (Appendix H), suggesting that exposure to DE had no effect on ET.

Interestingly, DE exposure increased SNP-induced NO-mediated endothelium-independent vasorelaxation. It was reported that blocking basal NO production by NOS inhibitor or removing the endothelium from a segment of blood vessel resulted in augmented SNP relaxation (338). This notion was supported by in vivo study showing that SNP relaxation was enhanced in eNOS knockout mice (339). Consistent with these results, we

also found that after inhibition of NOS activity with L-NAME, SNP relaxation was enhanced in the thoracic aorta of ApoE knockout mice (Fig.6.1C), suggesting that the reduced basal NO production contributed to the augmented SNP relaxation.

The mechanisms of the increased sensitivity to nitrovasodilators after removal of endothelium-derived NO have been investigated (340-342). Moncada and colleagues showed that the increased sensitivy was regulated at the sGC level, because the vasodilator actions of 8-bromo-cGMP was not affected (338). In this study, we showed that exposure to DE increased sGCα_1 expression in the blood vessels (Fig.6.3F). PM_{10} can up-regulate sGC activity by direct interaction with the blood vessels (343), or/and by direct interaction with DE constituents (33). We recently reported that exposure to DE induced peroxynitrite production, which can also enhance sGC activity (344). Nevertheless, how ambient DE interacts with sGC is not clear.

To examine whether the potentiated SNP response was derived from increased cGMP production, we measured levels of cGMP, and observed no elevation of urine cGMP in DE exposed mice, compared with the controls. This result suggests that the enhancement of SNP relaxation was predominately mediated at the NO receptor level, or via the up-regulation of sGC expression. We speculate that the suppressed basal endothelium-derived NO production, which occurred as a consequence of decreased eNOS expression, increased sGC activity and expression. The negative feedback-mediated sGC up-regulation could act as a compensatory effect maintaining a normal vascular function after exposure to DE. However, further investigation is needed to determine how this alteration of NO level regulates sGC activity in the blood vessels.

Moreover, the mRNA expression of eNOS and sGCα_1 was not affected by DE exposure (Fig.6.5), implying that DE exposure-induced reduction in eNOS expression and the up-regulation of sGC expression were regulated at post-translational levels.

In summary, we demonstrate that eNOS activity and expression were suppressed after DE exposure. However, ACh-stimulated endothelium-dependent relaxation was not impaired. We postulate that the up-regulation of sGC activity and expression in smooth muscle cells contribute to the unchanged ACh relaxation.

Chapter 7

Summary and Conclusions

Exposure to PM_{10} is an independent risk factor for cardiovascular events (22). The WHO estimates that air pollution is responsible for approximately three million premature deaths each year (World Health Organization (2002) World Health Report. [http:www.who.int/whr/2002/en]). Because of its ubiquitous and involuntary nature, exposure to PM_{10} may continuously enhance cardiovascular risk among millions of susceptible people worldwide in an often inconspicuous manner. Beyond serving as a simple trigger, PM_{10} also elicits numerous adverse biological responses (such as systemic inflammation) that may augment future cardiovascular risk after months or years of exposure. Among numerous constituents of PM_{10}, diesel exhaust particles (DEP) are the single biggest contributor, accounting for up to 90% of the PM_{10} in many cities around the world. Still, the effect of exposure to DE on cardiovascular dysfunction is not well understood. In this dissertation, the impact of exposure to DE on atherogenesis and the mechanisms underlying DE-induced progression of atherosclerosis were studied. Using a well-controlled inhalation model, this study has overcome some significant shortcomings of the population-based and instillation studies, especially in the inaccurate measurement of PM_{10} levels, and in the less established exposure approach that may not truly represent the exposure in the real-world exposure. This dissertation provides new insights into the mechanisms underlying the progression of atherosclerosis induced by exposure to DE. By understanfing the biological signaling pathways, and using appropriate medical prevention, more immediate and effective

strategies may be developed to alleviate DE-inudced cardiovascular mortality and morbidity. In addition, this work provides further evidence that can be used to influence policy, to ultimately reduce ambient particles levels, instead of focusing mainly on treating the symptoms and the cardiovascular diseases induced by exposure to PM.

7.1 Relationship between DE Inhalation and Atherogenesis

In this study, ApoE knockout mice, a well-established mouse model for atherosclerosis, were exposed to DE at environmentally relevant levels for 7 weeks (6h/day, 5day/week). Using a quantitative morphometric analysis, the data in Chapter 3 show that DE exposure results in compositional changes in atherosclerotic plaques (such as increased lipid content, foam cell formation, and smooth muscle cell content), which are associated with plaque vulnerability. This study provides new information that, in addition to PM_{10} and concentrated ambient particles, the exposure to DE for a relatively short period of time also promotes atherogenesis. Our results also show that DE is more active or potent in promoting ambient particle-associated atherogenesis, in comparision to the results from another inhalation study showing that ApoE mice needed a 6-month exposure to concentrated ambient particles to cause the progression of atherosclerosis.

Systemic inflammation is well established to play a key role in PM_{10}-associated cardiovascular dysfunction. We counted blood smear band cells, a marker of bone marrow stimulation, and found they were significantly increased after DE exposure (Fig.3.2A). In addition, the increased band cells were positively correlated with alveolar macrophages in the lung (Fig.3.2B), indicating an association between the magnitude of DE exposure and the systemic response. In addition, a strong association was seen between the magnitude of particle deposition in the lung and the compositional changes in atherosclerotic plaques, (Fig.3.6A), suggesting a connection between exposure to DE and the vascular consequences.

These findings are in accordance with the results found in Watanabe heritable hyperlipidemic rabbits, where accelerated atherosclerotic lesions were positively correlated with the number of alveolar macrophages that phagocytosed PM_{10} in the lung and the increase in circulating band cells (141). DE exposure increased the expression of a range of surrogate markers for ROS in aortic root, including iNOS, CD36, and NT (Fig.3.5). Moreover, systemic lipid and DNA oxidation were also increased after exposure to DE (Fig.3.7). The correlation between these ROS markers and compositional changes of atherosclerotic plaques (Fig.3.6 B,C) supports the idea that ROS is involved in the progression of atherosclerosis induced by DE exposure. Collectively, these results demonstrate that exposure of ApoE knockout mice fed with regular chow to DE change the composition of atherosclerotic plaques toward a more unstable phenotype. We also show that increased oxidative stress was involved in the DE-induced deleterious effect.

We did not examine the sources for DE-induced ROS produciton; however, a number of in vitro studies have shown that the NADPH oxidases, mitochondrial sources, and cytochrome P450 enzymes contribute to ambient PM-activated ROS-generating pathways (346-348). To untangle the ROS-generating pathways that are activated by exposure to DE, future ex vivo and/or in vitro experiments, incubating tissue cells (such as alveolar macrophages, epithelial cells, or isolated blood vessels) with DE collected from the filters may be worth investigating.

7.2 Mechanisms Underlying DE Exposure-induced Atherogenesis

7.2.1 Increased iNOS Expression

iNOS is capable of generating superoxide (299), which can cause modification of LDL leading to the acceleration of lipoprotein-uptake by macrophages and the formation of foam cells (310), a critical step in the development of atherosclerosis. The addition of oxygen free

radicals generated by iNOS can impair endothelial function by attenuation of eNOS activity and the expression and/ or through direct inactivation of NO (249), resulting in endothelial dysfunction and development of atherosclerosis. In addition, iNOS and/or its-mediated reactive oxygen species have been reported to modulate matrix degradation, to contribute to the degradation and reorganization of the extracellular matrix (ECM), thus increasing the instability of atherosclerotic plaque (350; 351). Studies have shown that exposure to PM up-regulates iNOS expression in the lung.

Here we measured iNOS activity and expression at both protein and mRNA levels using vascular function and molecular biology approaches. The study presented in Chapter 4 demonstrates that DE exposure attenuated vasoconstriction, which was partly due to the enhancement of iNOS activity (Fig. 4.1). In addition, we showed that exposure to DE up-regulated iNOS at both protein and mRNA levels in aorta and heart tissue (Fig.4.2 & Fig.4.5A). The positive correlation between increased iNOS expression in atherosclerotic plaque and increased band cells (Appendix I), indicates a systemic inflammatory response-regulated reaction. The correlation between increased iNOS expression and alveolar macrophages, and the association between increased iNOS expression and foam cell formation in atherosclerotic plaques (Fig.7.4B) also suggests that DE-induced up-regulation of iNOS plays an important role in the progression of atherosclerosis. The expression of iNOS that co-localized with CD36 and NT (Fig.4.4) implies a ROS-mediated up-regulation of iNOS expression and activity, mediated by NF-κB activation (Fig.4.6). Collectively, we show that exposure to DE up-regulates iNOS activity and expression, which could be critically important in the progression of atherosclerosis induced by DE exposure.

To validate the notion that up-regulation of iNOS by DE exposure contributes to atherogenesis, we may investigate the exposure of iNOS/ApoE double knockout mice to DE. In addition, exposure iNOS/ApoE double knockout mice to DE with administering the

specific iNOS antagonist (1400W) may provide supportive information to understand the pivotal roles of iNOS in DE exposure-induced atherogenesis.

7.2.2 Increased COX2 Expression

Inflammation is characteristic of all the phases of atherosclerosis progression, from the initial formation of the early lesions to the rupture of advanced plaques, at both systemic and local levels. Cyclooxygenase (COX), a key enzyme in the conversion of arachidonic acid to prostanoids, has some potential molecular mechanisms that may contribute to atherogenesis and atherosclerotic plaque instability (273; 352). Additional evidence led us to examine the COX pathway with the iNOS blocker, 1400W, which did not completely restore the suppressed PE-elicited vasoconstriction, though, in the presence of both COX and iNOS blockers, the attenuated PE-stimulated vasoconstriction after exposure to DE was completely restored (Appendix J). This indicates that the exposure to DE enhanced both COX and iNOS activities.

The study presented in Chapter 5 shows that exposure to DE increased COX activity (Fig. 5.2), predominantly due to the up-regulated expression of COX2, but not of COX1, in the vascular wall (Fig.5.4). In addition, we showed that the expression of COX2, but not COX1, was enhanced in atherosclerotic lesions in aortic root (Fig.5.6). Moreover, the mRNA expression of COX2 was increased (Fig.5.8A,B). We also correlated COX2 expression with both the magnitude of DE exposure (indicated by total alveolar macrophages in the lung and the alveolar macrophages positive for particles) and systemic response (indicated by band cells) to determine the relationship between COX2, the lung effect and the systemic response, but no significant association was found. This suggests that COX expression in atherosclerosis plaque following DE exposure was mediated locally in vascular walls. iNOS has been reported to cause up-regulation of COX, especially under pathological

conditions (353; 354). We observed that the expression of COX2 and iNOS by macrophages and smooth muscle cells are co-localized in blood vessels (Appendix J). We speculate that iNOS contributes to the up-regulation of COX2 locally. The pathway(s) leading to COX activation by NO/iNOS are unclear, but may involve an interaction at the iron-heme center of COX molecule where NO interacts with iron- containing enzymes leading to either a stimulation (such as via soluble guanylate cyclase) or inhibition (such as via aconitase) of the enzymatic activity (355; 356). This interaction between NO and COX activation may be a critical determinant in the optimal functioning of COX. For example, in pathological conditions such as inflammation, where both COX and iNOS pathways are augmented, regulation of COX activity by NO/iNOS may represent an important mechanism by which the initial inflammatory response can be amplified.

Collectively, we show that exposure to DE enhances COX2 (but not COX1) expression, possibly by interacting with inflammatory mediators, such as iNOS. Nevertheless, the interaction between COX2 and iNOS activation and the way in which how COX2 up-regulation is related to DE-induced vascular abnormality, warrants further investigation.

7.2.3 Vascular Endothelial Function

The endothelium consists of a monolayer of endothelial cells, and is located at the interface between the blood and the vessel wall. In addition to physiologically protecting the interaction between blood cell and the vessel wall, the endothelium also secretes a number of vasoactive substances (such as NO and ET-1) to regulate vascular smooth muscle tone, and prevents atherogenesis by reducing coagulation, leukocyte adhesion, and vascular smooth muscle cell proliferation and migration. A number of in vitro experiments have shown that exposure to PM_{10} induces endothelial dysfunction (104; 143; 177; 280; 358).

The study presented in Chapter 6 delineates the effect of DE exposure on endothelial function. We found that exposure to DE did not blunt ACh relaxation of the thoracic aorta (Fig.6.1A). Nevertheless, indirect evidence from the vascular function study, using NOS and iNOS blockers, respectively, implied that endogenous NO production was suppressed after exposure to DE (Fig.6.2). An immunohistochemical analysis showed that the expression of eNOS in the thoracic aorta was attenuated (Fig.6.3C). Interestingly, the concentration-response curve of SNP-induced endothelial-independent relaxation was shifted to the left (Fig.6.1B), suggesting an increase in smooth muscle sensitivity to NO, which could be explained by enhanced sGC expression or/and increased cGMP production in vascular smooth musclce cells. Indeed, we observed that DE exposure enhanced the sGCα1 expression (Fig.6.3F), though the elevation of cGMP production was not statistically significant (Fig.6.4B). We have also found that iNOS was up-regulated after DE exposure, but found that ACh relaxation was not affected in the presence of the iNOS blocker (1400W) (Appendix K), indicating that iNOS did not contribute to this unchanged ACh relaxation response. De and colleagues showed an interaction between NO and PGI_2, and that the release of these two endothelial relaxants are coupled (359). COX2 is recognized as the predominant mediator of PGI_2 production. We speculate that the COX2-mediated increase of PGI_2 may contribute to the intact ACh relation as a compensatory effect. Our finding of an increased PGI_2 expression in blood vessels and an elevation of PGI_2 metabolite in mouse urine, suggests the involvement of PGI_2 in ACh-relaxation after DE inhalation. Collectively, exposure to DE attenuated the eNOS expression in blood vessels, but the ACh-induced relaxation was not affected. This phenomenon could be due to compensatory effects from the up-regulated expression of sGC and PGI_2. The interactions among these endothelium mediators need to be further delineated.

In summary, our study significantly extends previous data showing that PM_{10} potentiates atherosclerotic lesion development in animals (141; 143). I have demonstrated that exposure to DE at an environmentally relevant concentration causes progression of atherosclerosis in ApoE knockout mice fed with regular chow. Our results support the notion that the generation of systemic oxidative stress and up-regulation of iNOS are responsible for the observed vascular effects. Our data also indicate an interaction between iNOS and COX2 induced by exposure to DE. In addition, compensatory reactions may also be engaged after exposure to DE, in maintaining vascular homeostasis.

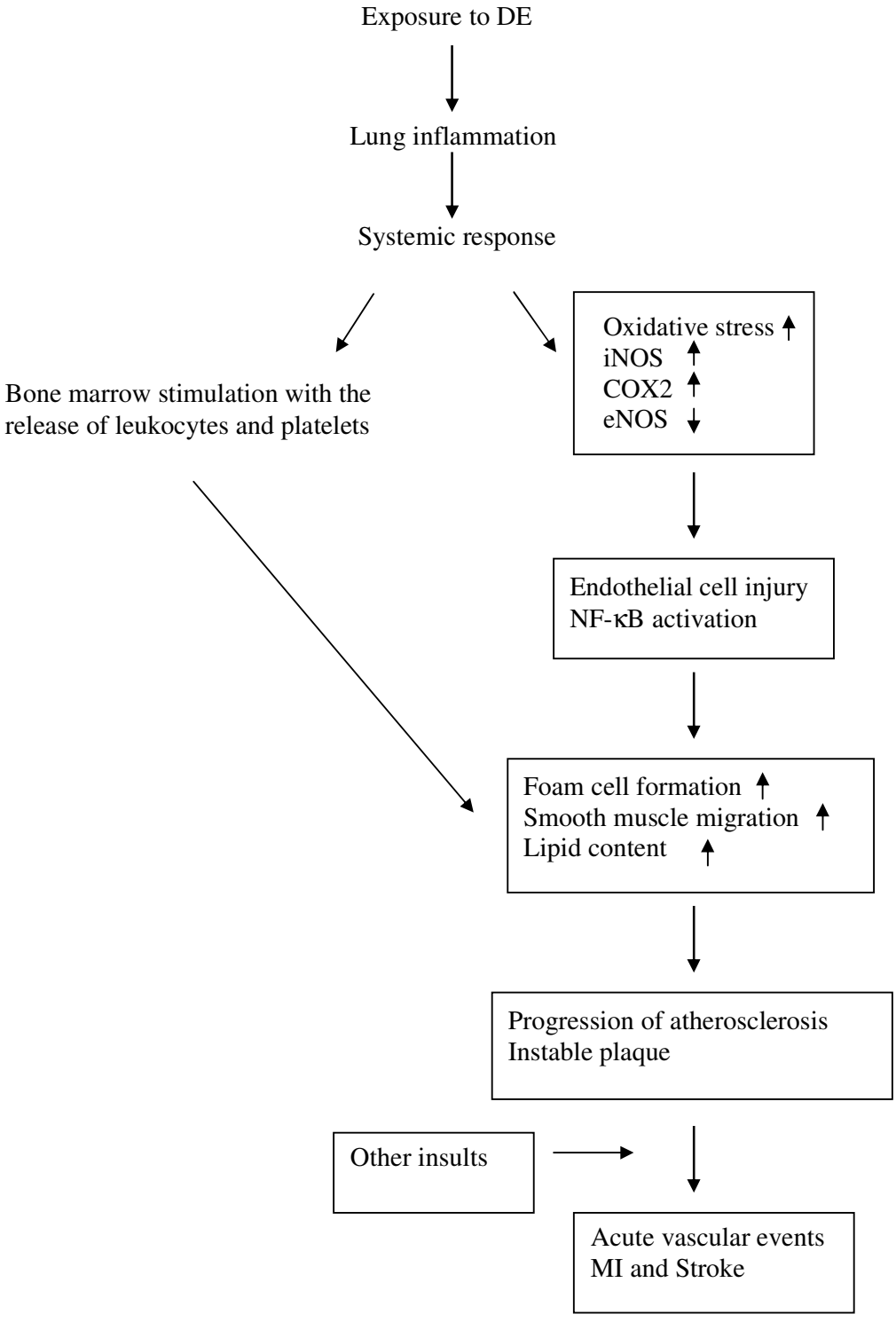

Figure 7.1 Summary of the signalling pathways contributing to DE inhalation-induced atherogenesis

7.3 Limitations:

1. DE has an odor, and it might not be well controlled in the filtered air (control) exposure because the intermission of exposure to DE and filtered air exposures was less than 2 weeks, and the odor in exposure facility might not be cleared by HEPA, and potential effects of the odor was not addressed.
2. Although ApoE knockout mice is an established model for atheroclerosis, plaque rapture, which is considered to be pathogenesis of MI, is rarely observed in this mouse model, and this fact may restrict the possibilities of examining and approving the hypothesis: DE causes plaque rapture, hence lead to MI, and stroke.
3. To confirm the causal effect of exposure to DE and up-regulation of iNOS and COX2, transgenic mice would be needed.
4. The exposure protocol used in this study was well controlled and freshly generated. The lab exposure may not fully represent real-life diesel exhaust exposure. For example, people may be exposed to diesel exhaust that was not freshly (less than 10min) generated, but produced by these cars miles away and travelled in the air for a while. The aged diesel exhaust may have different composition comparing with freshly generated diesel exhaust, hence the impact of aged and freshly generated diesel exhaust on the blood vessels could be different.

7.4 Future Directions

In this dissertation, in addition to demonstrating DE inhalation-induced compositional modification of atherosclerotic plaque, I examined three signaling pathways that may be responsible for the progression of atherosclerosis in response to DE inhalation. Our results have also led to a number of questions; in particular how the three closely related signaling cascades (iNOS, COX, and eNOS) interact with each other. Transgenic animal models

(deficient in iNOS, COX, or eNOS genes) may be useful for clarifying the interactions of these enzymes. Clearly, a better understanding of the mechanisms would be valuable for future interventions to decrease the impact of exposure to particulate matter air pollution, considering the dramatic effect on cardiovascular morbidity and mortality. Because endothelial dysfunction can occur before the symptoms of cardiovascular diseases appear, it is particularly imperative to know how the processes involved in NO synthesis and availability are affected and how these changes can be prevented or therapeutically treated. Also, it is important to learn how changes in NOS and COX activities are related to other outcomes of PM exposure, such as changes in heart rate variability, autonomic disturbances, and arrhythmias. Our findings also support the observations from a number of epidemiological studies, that pre-existing pathological conditions accelerate the progression of atherosclerosis. More work is required to establish how susceptibility-enhancing states (high cholesterol, smoking, and hypertension) can promote PM_{10} toxicity or cardiovascular exacerbations. The result of such studies may also suggest mechanisms that determine cardiovascular disease vulnerability and risk that could be used in designing urgently needed epidemiological studies to determine which specific sub-populations may be more sensitive to the effects of PM_{10}. Moreover, studies are required to interpret some important questions derived from epidemiological observations, such as lag effects, dose-response effects, and the possibility of a threshold level for igniting a cardiovascular effect. Furthermore, an acute exposure model may be necessary to reveal the mechanisms underlie DE-induced acute cardiovascular events.

Bibliography

1. **Nemery B, Hoet PH, Nemmar A**. The Meuse Valley fog of 1930: an air pollution disaster. Lancet 2001;357:704-708

2. **LOGAN WP**. Mortality in the London fog incident, 1952. Lancet 1953;1:336-338

3. **Dockery DW, Pope CA, III, Xu X, et al**. An association between air pollution and mortality in six U.S. cities. N.Engl.J.Med. 1993;329:1753-1759

4. **Hoek G, Brunekreef B, Fischer P, van Wijnen J**. The association between air pollution and heart failure, arrhythmia, embolism, thrombosis, and other cardiovascular causes of death in a time series study. Epidemiology 2001;12:355-357

5. **Katsouyanni K, Touloumi G, Samoli E, et al**. Confounding and effect modification in the short-term effects of ambient particles on total mortality: results from 29 European cities within the APHEA2 project. Epidemiology 2001;12:521-531

6. **Pope CA, III, Schwartz J, Ransom MR**. Daily mortality and PM10 pollution in Utah Valley. Arch.Environ.Health 1992;47:211-217

7. **Pope CA, III, Thun MJ, Namboodiri MM, et al**. Particulate air pollution as a predictor of mortality in a prospective study of U.S. adults. Am.J.Respir.Crit Care Med. 1995;151:669-674

8. **Pope CA, III, Hansen ML, Long RW, et al**. Ambient particulate air pollution, heart rate variability, and blood markers of inflammation in a panel of elderly subjects. Environ.Health Perspect. 2004;112:339-345

9. **Schwartz J**. Air pollution and hospital admissions for heart disease in eight U.S. counties. Epidemiology 1999;10:17-22

10. **Zanobetti A, Schwartz J, Dockery DW**. Airborne particles are a risk factor for hospital admissions for heart and lung disease. Environ.Health Perspect. 2000;108:1071-1077

11. **Ware JH**. Particulate air pollution and mortality--clearing the air. N.Engl.J.Med. 2000;343:1798-1799

12. **Morrow PE, Haseman JK, Hobbs CH, Driscoll KE, Vu V, Oberdorster G**. The maximum tolerated dose for inhalation bioassays: toxicity vs overload. Fundam.Appl.Toxicol. 1996;29:155-167

13. **Donaldson K, Stone V, Clouter A, Renwick L, MacNee W**. Ultrafine particles. Occup.Environ.Med. 2001;58:211-6, 199

14. **Salvi SS, Frew A, Holgate S**. Is diesel exhaust a cause for increasing allergies? Clin.Exp.Allergy 1999;29:4-8

15. **Maheswaran R, Haining RP, Brindley P, et al**. Outdoor air pollution, mortality, and hospital admissions from coronary heart disease in Sheffield, UK: a small-area level ecological study. Eur.Heart J. 2005;26:2543-2549

16. **Schuetzle D, Lee FS, Prater TJ**. The identification of polynuclear aromatic hydrocarbon (PAH) derivatives in mutagenic fractions of diesel particulate extracts. Int.J.Environ.Anal.Chem. 1981;9:93-144

17. **Weisenberger B**. Health effect of diesel emissions: a current status report. J.Soc.Occup.Med. 1981;31:4-8

18. **Nemmar A, Delaunois A, Nemery B, et al**. Inflammatory effect of intratracheal instillation of ultrafine particles in the rabbit: role of C-fiber and mast cells. Toxicol.Appl.Pharmacol. 1999;160:250-261

19. **Oberdorster G, Finkelstein J, Ferin J, et al**. Ultrafine particles as a potential environmental health hazard. Studies with model particles. Chest 1996;109:68S-69S

20. **Burnett RT, Smith-Doiron M, Stieb D, Cakmak S, Brook JR**. Effects of particulate and gaseous air pollution on cardiorespiratory hospitalizations. Arch.Environ.Health 1999;54:130-139

21. **Zanobetti A, Schwartz J**. The effect of particulate air pollution on emergency admissions for myocardial infarction: a multicity case-crossover analysis. Environ.Health Perspect. 2005;113:978-982

22. **Brook RD, Rajagopalan S, Pope CA, III, et al**. Particulate matter air pollution and cardiovascular disease: An update to the scientific statement from the American Heart Association. Circulation 2010;121:2331-2378

23. **Anderson HR, Atkinson RW, Peacock JL, Sweeting MJ, Marston L**. Ambient particulate matter and health effects: publication bias in studies of short-term associations. Epidemiology 2005;16:155-163

24. Committee on the Medical Effects of Air Pollutants. Cardiovascular Disease and Air Pollution: A Report by the Committee on the Medical Effects of Air Pollutant's Cardiovascular Sub-Group. London, UK: Department of Health, National Health Service; 2006

25. **Dominici F, Daniels M, McDermott A, Zeger SL, Samet J.** Shape of the exposure-response relation and mortality displacement in the NMMAPS database. In: Revised Analyses of Time-Series of Air Pollution and Health. Special Report. Boston, Mass: Health Effects Institute; 2003

26. **Analitis A, Katsouyanni K, Dimakopoulou K, et al**. Short-term effects of ambient particles on cardiovascular and respiratory mortality. Epidemiology 2006;17:230-233

27. **Klemm RJ, Mason R.** Replication of reanalysis of Harvard six-city mortality study. In: Revised Analyses of Time-Series of Air Pollution and Health. Boston, Mass: Health Effects Institute; 2003

28. **Franklin M, Zeka A, Schwartz J**. Association between PM2.5 and all-cause and specific-cause mortality in 27 US communities. J.Expo.Sci.Environ.Epidemiol. 2007;17:279-287

29. **Ostro B, Broadwin R, Green S, Feng WY, Lipsett M**. Fine particulate air pollution and mortality in nine California counties: results from CALFINE. Environ.Health Perspect. 2006;114:29-33

30. **Le TA, Medina S, Samoli E, et al**. Short-term effects of particulate air pollution on cardiovascular diseases in eight European cities. J.Epidemiol.Community Health 2002;56:773-779

31. **Omori T, Fujimoto G, Yoshimura I, Nitta H, Ono M**. Effects of particulate matter on daily mortality in 13 Japanese cities. J.Epidemiol. 2003;13:314-322

32. **Wong CM, Vichit-Vadakan N, Kan H, Qian Z**. Public Health and Air Pollution in Asia (PAPA): a multicity study of short-term effects of air pollution on mortality. Environ.Health Perspect. 2008;116:1195-1202

33. **Zanobetti A, Schwartz J**. The effect of fine and coarse particulate air pollution on mortality: a national analysis. Environ.Health Perspect. 2009;117:898-903

34. **Dockery DW, Pope CA, III, Xu X, et al**. An association between air pollution and mortality in six U.S. cities. N.Engl.J.Med. 1993;329:1753-1759

35. **Pope CA, III, Burnett RT, Thun MJ, et al**. Lung cancer, cardiopulmonary mortality, and long-term exposure to fine particulate air pollution. JAMA 2002;287:1132-1141

36. **Pope CA, III, Ezzati M, Dockery DW**. Fine-particulate air pollution and life expectancy in the United States. N.Engl.J.Med. 2009;360:376-386

37. **Clancy L, Goodman P, Sinclair H, Dockery DW**. Effect of air-pollution control on death rates in Dublin, Ireland: an intervention study. Lancet 2002;360:1210-1214

38. **Laden F, Schwartz J, Speizer FE, Dockery DW**. Reduction in fine particulate air pollution and mortality: Extended follow-up of the Harvard Six Cities study. Am.J.Respir.Crit Care Med. 2006;173:667-672

39. **Eftim SE, Samet JM, Janes H, McDermott A, Dominici F**. Fine particulate matter and mortality: a comparison of the six cities and American Cancer Society cohorts with a medicare cohort. Epidemiology 2008;19:209-216

40. **Pope CA, III, Burnett RT, Thurston GD, et al**. Cardiovascular mortality and long-term exposure to particulate air pollution: epidemiological evidence of general pathophysiological pathways of disease. Circulation 2004;109:71-77

41. **Zeger SL, Dominici F, McDermott A, Samet JM**. Mortality in the Medicare population and chronic exposure to fine particulate air pollution in urban centers (2000-2005). Environ.Health Perspect. 2008;116:1614-1619

42. **Miller KA, Siscovick DS, Sheppard L, et al**. Long-term exposure to air pollution and incidence of cardiovascular events in women. N.Engl.J.Med. 2007;356:447-458

43. **Filleul L, Rondeau V, Vandentorren S, et al**. Twenty five year mortality and air pollution: results from the French PAARC survey. Occup.Environ.Med. 2005;62:453-460

44. **Gehring U, Heinrich J, Kramer U, et al**. Long-term exposure to ambient air pollution and cardiopulmonary mortality in women. Epidemiology 2006;17:545-551

45. **Naess O, Nafstad P, Aamodt G, Claussen B, Rosland P**. Relation between concentration of air pollution and cause-specific mortality: four-year exposures to nitrogen dioxide and particulate matter pollutants in 470 neighborhoods in Oslo, Norway. Am.J.Epidemiol. 2007;165:435-443

46. **Beelen R, Hoek G, van den Brandt PA, et al**. Long-term effects of traffic-related air pollution on mortality in a Dutch cohort (NLCS-AIR study). Environ.Health Perspect. 2008;116:196-202

47. **Elliott P, Shaddick G, Wakefield JC, de HC, Briggs DJ**. Long-term associations of outdoor air pollution with mortality in Great Britain. Thorax 2007;62:1088-1094

48. **Bagate K, Meiring JJ, Cassee FR, Borm PJ**. The effect of particulate matter on resistance and conductance vessels in the rat. Inhal.Toxicol. 2004;16:431-436

49. **Le Tertre A, Medina S, Samoli E, et al**. Short-term effects of particulate air pollution on cardiovascular diseases in eight European cities. J.Epidemiol.Community Health 2002;56:773-779

50. **Lee JT, Kim H, Hong YC, Kwon HJ, Schwartz J, Christiani DC**. Air pollution and daily mortality in seven major cities of Korea, 1991-1997. Environ.Res. 2000;84:247-254

51. **Linn WS, Szlachcic Y, Gong H, Jr., Kinney PL, Berhane KT**. Air pollution and daily hospital admissions in metropolitan Los Angeles. Environ.Health Perspect. 2000;108:427-434

52. **Maheswaran R, Haining RP, Brindley P, et al**. Outdoor air pollution and stroke in Sheffield, United Kingdom: a small-area level geographical study. Stroke 2005;36:239-243

53. **Morris RD, Naumova EN**. Carbon monoxide and hospital admissions for congestive heart failure: evidence of an increased effect at low temperatures. Environ.Health Perspect. 1998;106:649-653

54. **Peters A, Liu E, Verrier RL, et al**. Air pollution and incidence of cardiac arrhythmia. Epidemiology 2000;11:11-17

55. **Ponka A, Savela M, Virtanen M**. Mortality and air pollution in Helsinki. Arch.Environ.Health 1998;53:281-286

56. **Samet JM, Dominici F, Curriero FC, Coursac I, Zeger SL**. Fine particulate air pollution and mortality in 20 U.S. cities, 1987-1994. N.Engl.J.Med. 2000;343:1742-1749

57. **Kaiser J**. Air pollution. Evidence mounts that tiny particles can kill. Science 2000;289:22-23

58. **McDonnell WF, Abbey DE, Nishino N, Lebowitz MD**. Long-term ambient ozone concentration and the incidence of asthma in nonsmoking adults: the AHSMOG Study. Environ.Res. 1999;80:110-121

59. **Abbey DE, Nishino N, McDonnell WF, et al**. Long-term inhalable particles and other air pollutants related to mortality in nonsmokers. Am.J.Respir.Crit Care Med. 1999;159:373-382

60. **Goldberg MS, Burnett RT, Bailar JC, III, et al**. Identification of persons with cardiorespiratory conditions who are at risk of dying from the acute effects of ambient air particles. Environ.Health Perspect. 2001;109 Suppl 4:487-494

61. **Zanobetti A, Schwartz J**. Are diabetics more susceptible to the health effects of airborne particles? Am.J.Respir.Crit Care Med. 2001;164:831-833

62. **Seaton A, MacNee W, Donaldson K, Godden D**. Particulate air pollution and acute health effects. Lancet 1995;345:176-178

63. **Peters A, Doring A, Wichmann HE, Koenig W**. Increased plasma viscosity during an air pollution episode: a link to mortality? Lancet 1997;349:1582-1587

64. **Gilmour PS, Morrison ER, Vickers MA, et al**. The procoagulant potential of environmental particles (PM10). Occup.Environ.Med. 2005;62:164-171

65. **Ulrich MM, Alink GM, Kumarathasan P, Vincent R, Boere AJ, Cassee FR**. Health effects and time course of particulate matter on the cardiopulmonary system in rats with lung inflammation. J.Toxicol.Environ.Health A 2002;65:1571-1595

66. **Nemmar A, Hoylaerts MF, Hoet PH, Vermylen J, Nemery B**. Size effect of intratracheally instilled particles on pulmonary inflammation and vascular thrombosis. Toxicol.Appl.Pharmacol. 2003;186:38-45

67. **Gilmour PS, Morrison ER, Vickers MA, et al**. The procoagulant potential of environmental particles (PM10). Occup.Environ.Med. 2005;62:164-171

68. **Tan WC, Qiu D, Liam BL, et al**. The human bone marrow response to acute air pollution caused by forest fires. Am.J.Respir.Crit Care Med. 2000;161:1213-1217

69. **Goto Y, Ishii H, Hogg JC, et al**. Particulate matter air pollution stimulates monocyte release from the bone marrow. Am.J.Respir.Crit Care Med. 2004;170:891-897

70. **Terashima T, Wiggs B, English D, Hogg JC, van Eeden SF**. Phagocytosis of small carbon particles (PM10) by alveolar macrophages stimulates the release of polymorphonuclear leukocytes from bone marrow. Am.J.Respir.Crit Care Med. 1997;155:1441-1447

71. **Godleski JJ, Verrier RL, Koutrakis P, et al**. Mechanisms of morbidity and mortality from exposure to ambient air particles. Res.Rep.Health Eff.Inst. 2000;5-88

72. **Nemmar A, Vanbilloen H, Hoylaerts MF, Hoet PH, Verbruggen A, Nemery B**. Passage of intratracheally instilled ultrafine particles from the lung into the systemic circulation in hamster. Am.J.Respir.Crit Care Med. 2001;164:1665-1668

73. **Nemmar A, Hoet PH, Vanquickenborne B, et al**. Passage of inhaled particles into the blood circulation in humans. Circulation 2002;105:411-414

74. **Terashima T, Wiggs B, English D, Hogg JC, van Eeden SF**. Phagocytosis of small carbon particles (PM10) by alveolar macrophages stimulates the release of polymorphonuclear leukocytes from bone marrow. Am.J.Respir.Crit Care Med. 1997;155:1441-1447

75. **Cheng TJ, Hwang JS, Wang PY, et al**. Effects of concentrated ambient particles on heart rate and blood pressure in pulmonary hypertensive rats. Environ.Health Perspect. 2003;111:147-150

76. **Peters A, Liu E, Verrier RL, et al**. Air pollution and incidence of cardiac arrhythmia. Epidemiology 2000;11:11-17

77. **Brook RD**. Cardiovascular effects of air pollution. Clin.Sci.(Lond) 2008;115:175-187

78. **Vincent R, Bjarnason SG, Adamson IY, et al**. Acute pulmonary toxicity of urban particulate matter and ozone. Am.J.Pathol. 1997;151:1563-1570

79. **van Eeden SF, Tan WC, Suwa T, et al**. Cytokines involved in the systemic inflammatory response induced by exposure to particulate matter air pollutants (PM(10)). Am.J.Respir.Crit Care Med. 2001;164:826-830

80. **Happo MS, Salonen RO, Halinen AI, et al**. Dose and time dependency of inflammatory responses in the mouse lung to urban air coarse, fine, and ultrafine particles from six European cities. Inhal.Toxicol. 2007;19:227-246

81. **Ishii H, Fujii T, Hogg JC, et al**. Contribution of IL-1 beta and TNF-alpha to the initiation of the peripheral lung response to atmospheric particulates (PM10). Am.J.Physiol Lung Cell Mol.Physiol 2004;287:L176-L183

82. **Quay JL, Reed W, Samet J, Devlin RB**. Air pollution particles induce IL-6 gene expression in human airway epithelial cells via NF-kappaB activation. Am.J.Respir.Cell Mol.Biol. 1998;19:98-106

83. **Mitani H, Katayama N, Araki H, et al**. Activity of interleukin 6 in the differentiation of monocytes to macrophages and dendritic cells. Br.J.Haematol. 2000;109:288-295

84. **Nijsten MW, de Groot ER, ten Duis HJ, Klasen HJ, Hack CE, Aarden LA**. Serum levels of interleukin-6 and acute phase responses. Lancet 1987;2:921

85. **Suwa T, Hogg JC, English D, Van Eeden SF**. Interleukin-6 induces demargination of intravascular neutrophils and shortens their transit in marrow. Am.J.Physiol Heart Circ.Physiol 2000;279:H2954-H2960

86. **Kishimoto T, Akira S, Narazaki M, Taga T**. Interleukin-6 family of cytokines and gp130. Blood 1995;86:1243-1254

87. **Topham MK, Carveth HJ, McIntyre TM, Prescott SM, Zimmerman GA**. Human endothelial cells regulate polymorphonuclear leukocyte degranulation. FASEB J. 1998;12:733-746

88. **Mundandhara SD, Becker S, Madden MC**. Effects of diesel exhaust particles on human alveolar macrophage ability to secrete inflammatory mediators in response to lipopolysaccharide. Toxicol.In Vitro 2006;20:614-624

89. **Amakawa K, Terashima T, Matsuzaki T, Matsumaru A, Sagai M, Yamaguchi K**. Suppressive effects of diesel exhaust particles on cytokine release from human and murine alveolar macrophages. Exp.Lung Res. 2003;29:149-164

90. **Yang HM, Barger MW, Castranova V, Ma JK, Yang JJ, Ma JY**. Effects of diesel exhaust particles (DEP), carbon black, and silica on macrophage responses to lipopolysaccharide: evidence of DEP suppression of macrophage activity. J.Toxicol.Environ.Health A 1999;58:261-278

91. **Fujii T, Hayashi S, Hogg JC, Vincent R, van Eeden SF**. Particulate matter induces cytokine expression in human bronchial epithelial cells. Am.J.Respir.Cell Mol.Biol. 2001;25:265-271

92. **Fujii T, Hayashi S, Hogg JC, et al**. Interaction of alveolar macrophages and airway epithelial cells following exposure to particulate matter produces mediators that stimulate the bone marrow. Am.J.Respir.Cell Mol.Biol. 2002;27:34-41

93. **Carter JD, Ghio AJ, Samet JM, Devlin RB**. Cytokine production by human airway epithelial cells after exposure to an air pollution particle is metal-dependent. Toxicol.Appl.Pharmacol. 1997;146:180-188

94. **Gilmour PS, Rahman I, Hayashi S, Hogg JC, Donaldson K, MacNee W**. Adenoviral E1A primes alveolar epithelial cells to PM(10)-induced transcription of interleukin-8. Am.J.Physiol Lung Cell Mol.Physiol 2001;281:L598-L606

95. **Fujii T, Hayashi S, Hogg JC, Vincent R, van Eeden SF**. Particulate matter induces cytokine expression in human bronchial epithelial cells. Am.J.Respir.Cell Mol.Biol. 2001;25:265-271

96. **Molinelli AR, Madden MC, McGee JK, Stonehuerner JG, Ghio AJ**. Effect of metal removal on the toxicity of airborne particulate matter from the Utah Valley. Inhal.Toxicol. 2002;14:1069-1086

97. **Ishii H, Hayashi S, Hogg JC, et al**. Alveolar macrophage-epithelial cell interaction following exposure to atmospheric particles induces the release of mediators involved in monocyte mobilization and recruitment. Respir.Res. 2005;6:87

98. **Bleck B, Tse DB, Jaspers I, Curotto de Lafaille MA, Reibman J**. Diesel exhaust particle-exposed human bronchial epithelial cells induce dendritic cell maturation. J.Immunol. 2006;176:7431-7437

99. **Yokota S, Seki T, Furuya M, Ohara N**. Acute functional enhancement of circulatory neutrophils after intratracheal instillation with diesel exhaust particles in rats. Inhal.Toxicol. 2005;17:671-679

100. **Yokota S, Furuya M, Seki T, Marumo H, Ohara N, Kato A**. Delayed exacerbation of acute myocardial ischemia/reperfusion-induced arrhythmia by tracheal instillation of diesel exhaust particles. Inhal.Toxicol. 2004;16:319-331

101. **Seagrave J, Knall C, McDonald JD, Mauderly JL**. Diesel particulate material binds and concentrates a proinflammatory cytokine that causes neutrophil migration. Inhal.Toxicol. 2004;16 Suppl 1:93-98

102. **Samet JM, Reed W, Ghio AJ, et al**. Induction of prostaglandin H synthase 2 in human airway epithelial cells exposed to residual oil fly ash. Toxicol.Appl.Pharmacol. 1996;141:159-168

103. **Mukae H, Vincent R, Quinlan K, et al**. The effect of repeated exposure to particulate air pollution (PM10) on the bone marrow. Am.J.Respir.Crit Care Med. 2001;163:201-209

104. **Tamagawa E, Bai N, Morimoto K, et al**. Particulate matter exposure induces persistent lung inflammation and endothelial dysfunction. Am.J.Physiol Lung Cell Mol.Physiol 2008;295:L79-L85

105. **Shukla A, Timblin C, BeruBe K, et al**. Inhaled particulate matter causes expression of nuclear factor (NF)-kappaB-related genes and oxidant-dependent NF-kappaB activation in vitro. Am.J.Respir.Cell Mol.Biol. 2000;23:182-187

106. **Kennedy T, Ghio AJ, Reed W, et al**. Copper-dependent inflammation and nuclear factor-kappaB activation by particulate air pollution. Am.J.Respir.Cell Mol.Biol. 1998;19:366-378

107. **Kido T, Tamagawa E, Bai N, et al**. Particulate Matter Induces IL-6 Translocation from the Lung to the Systemic Circulation. Am.J.Respir.Cell Mol.Biol. 2010;

108. **Peters A, Frohlich M, Doring A, et al**. Particulate air pollution is associated with an acute phase response in men; results from the MONICA-Augsburg Study. Eur.Heart J. 2001;22:1198-1204

109. **Ruckerl R, Ibald-Mulli A, Koenig W, et al**. Air pollution and markers of inflammation and coagulation in patients with coronary heart disease. Am.J.Respir.Crit Care Med. 2006;173:432-441

110. **Stiller-Winkler R, Idel H, Leng G, Spix C, Dolgner R**. Influence of air pollution on humoral immune response. J.Clin.Epidemiol. 1996;49:527-534

111. **Hadnagy W, Stiller-Winkler R, Idel H**. Immunological alterations in sera of persons living in areas with different air pollution. Toxicol.Lett. 1996;88:147-153

112. **Friedman GD, Klatsky AL, Siegelaub AB**. The leukocyte count as a predictor of myocardial infarction. N.Engl.J.Med. 1974;290:1275-1278

113. **Goto Y, Hogg JC, Shih CH, Ishii H, Vincent R, van Eeden SF**. Exposure to ambient particles accelerates monocyte release from bone marrow in atherosclerotic rabbits. Am.J.Physiol Lung Cell Mol.Physiol 2004;287:L79-L85

114. **Terashima T, Wiggs B, English D, Hogg JC, van Eeden SF**. Phagocytosis of small carbon particles (PM10) by alveolar macrophages stimulates the release of polymorphonuclear leukocytes from bone marrow. Am.J.Respir.Crit Care Med. 1997;155:1441-1447

115. **Mukae H, Hogg JC, English D, Vincent R, van Eeden SF**. Phagocytosis of particulate air pollutants by human alveolar macrophages stimulates the bone marrow. Am.J.Physiol Lung Cell Mol.Physiol 2000;279:L924-L931

116. **Terashima T, English D, Hogg JC, van Eeden SF**. Release of polymorphonuclear leukocytes from the bone marrow by interleukin-8. Blood 1998;92:1062-1069

117. **van Eeden SF, Kitagawa Y, Sato Y, Hogg JC**. Polymorphonuclear leukocytes released from the bone marrow and acute lung injury. Chest 1999;116:43S-46S

118. **Goto Y, Hogg JC, Suwa T, Quinlan KB, van Eeden SF**. A novel method to quantify the turnover and release of monocytes from the bone marrow using the thymidine analog 5'-bromo-2'-deoxyuridine. Am.J.Physiol Cell Physiol 2003;285:C253-C259

119. **Lawrence E, Van ES, English D, Hogg JC**. Polymorphonuclear leukocyte (PMN) migration in streptococcal pneumonia: comparison of older PMN with those recently released from the marrow. Am.J.Respir.Cell Mol.Biol. 1996;14:217-224

120. **Biswas P, Delfanti F, Bernasconi S, et al**. Interleukin-6 induces monocyte chemotactic protein-1 in peripheral blood mononuclear cells and in the U937 cell line. Blood 1998;91:258-265

121. **Schieffer B, Schieffer E, Hilfiker-Kleiner D, et al**. Expression of angiotensin II and interleukin 6 in human coronary atherosclerotic plaques: potential implications for inflammation and plaque instability. Circulation 2000;101:1372-1378

122. **Empana JP, Jouven X, Canoui-Poitrine F, et al**. C-reactive protein, interleukin 6, fibrinogen and risk of sudden death in European middle-aged men: the PRIME study. Arterioscler.Thromb.Vasc.Biol. 2010;30:2047-2052

123. **Van LF**. Markers of inflammation as predictors in cardiovascular disease. Clin.Chim.Acta 2000;293:31-52

24. **Cermak J, Key NS, Bach RR, Balla J, Jacob HS, Vercellotti GM**. C-reactive protein induces human peripheral blood monocytes to synthesize tissue factor. Blood 1993;82:513-520

125. **Nakagomi A, Freedman SB, Geczy CL**. Interferon-gamma and lipopolysaccharide potentiate monocyte tissue factor induction by C-reactive protein: relationship with age, sex, and hormone replacement treatment. Circulation 2000;101:1785-1791

126. **Pasceri V, Willerson JT, Yeh ET**. Direct proinflammatory effect of C-reactive protein on human endothelial cells. Circulation 2000;102:2165-2168

127. **Willerson JT**. Systemic and local inflammation in patients with unstable atherosclerotic plaques. Prog.Cardiovasc.Dis. 2002;44:469-478

128. **Yeh ET, Anderson HV, Pasceri V, Willerson JT**. C-reactive protein: linking inflammation to cardiovascular complications. Circulation 2001;104:974-975

129. **Li H, Cybulsky MI, Gimbrone MA, Jr., Libby P**. An atherogenic diet rapidly induces VCAM-1, a cytokine-regulatable mononuclear leukocyte adhesion molecule, in rabbit aortic endothelium. Arterioscler.Thromb. 1993;13:197-204

130. **Barna BP, Thomassen MJ, Zhou P, Pettay J, Singh-Burgess S, Deodhar SD**. Activation of alveolar macrophage TNF and MCP-1 expression in vivo by a synthetic peptide of C-reactive protein. J.Leukoc.Biol. 1996;59:397-402

131. **Verma S, Li SH, Badiwala MV, et al**. Endothelin antagonism and interleukin-6 inhibition attenuate the proatherogenic effects of C-reactive protein. Circulation 2002;105:1890-1896

132. **Rollins BJ, Yoshimura T, Leonard EJ, Pober JS**. Cytokine-activated human endothelial cells synthesize and secrete a monocyte chemoattractant, MCP-1/JE. Am.J.Pathol. 1990;136:1229-1233

133. **Yatera K, Hsieh J, Hogg JC, et al**. Particulate matter air pollution exposure promotes recruitment of monocytes into atherosclerotic plaques. Am.J.Physiol Heart Circ.Physiol 2008;294:H944-H953

134. **Khandoga A, Stampfl A, Takenaka S, et al**. Ultrafine particles exert prothrombotic but not inflammatory effects on the hepatic microcirculation in healthy mice in vivo. Circulation 2004;109:1320-1325

135. **Hermans C, Bernard A**. Lung epithelium-specific proteins: characteristics and potential applications as markers. Am.J.Respir.Crit Care Med. 1999;159:646-678

136. **Stone V**. Environmental air pollution. Am.J.Respir.Crit Care Med. 2000;162:S44-S47

137. **Gumbleton M**. Caveolae as potential macromolecule trafficking compartments within alveolar epithelium. Adv.Drug Deliv.Rev. 2001;49:281-300

138. **Ghio AJ, Hall A, Bassett MA, Cascio WE, Devlin RB**. Exposure to concentrated ambient air particles alters hematologic indices in humans. Inhal.Toxicol. 2003;15:1465-1478

139. **Mills NL, Amin N, Robinson SD, et al**. Do inhaled carbon nanoparticles translocate directly into the circulation in humans? Am.J.Respir.Crit Care Med. 2006;173:426-431

140. **Ross R**. Atherosclerosis--an inflammatory disease. N.Engl.J.Med. 1999;340:115-126

141. **Suwa T, Hogg JC, Quinlan KB, Ohgami A, Vincent R, van Eeden SF**. Particulate air pollution induces progression of atherosclerosis. J.Am.Coll.Cardiol. 2002;39:935-942

142. **Lund AK, Knuckles TL, Obot AC, et al**. Gasoline exhaust emissions induce vascular remodeling pathways involved in atherosclerosis. Toxicol.Sci. 2007;95:485-494

143. **Sun Q, Wang A, Jin X, et al**. Long-term air pollution exposure and acceleration of atherosclerosis and vascular inflammation in an animal model. JAMA 2005;294:3003-3010

144. **Kunzli N, Jerrett M, Mack WJ, et al**. Ambient air pollution and atherosclerosis in Los Angeles. Environ.Health Perspect. 2005;113:201-206

145. **Hoffmann B, Moebus S, Mohlenkamp S, et al**. Residential exposure to traffic is associated with coronary atherosclerosis. Circulation 2007;116:489-496

146. **Aikawa M, Libby P**. The vulnerable atherosclerotic plaque: pathogenesis and therapeutic approach. Cardiovasc.Pathol. 2004;13:125-138

147. **Stary HC, Chandler AB, Glagov S, et al**. A definition of initial, fatty streak, and intermediate lesions of atherosclerosis. A report from the Committee on Vascular Lesions of the Council on Arteriosclerosis, American Heart Association. Arterioscler.Thromb. 1994;14:840-856

148. **Moreno PR, Falk E, Palacios IF, Newell JB, Fuster V, Fallon JT**. Macrophage infiltration in acute coronary syndromes. Implications for plaque rupture. Circulation 1994;90:775-778

149. **Spagnoli LG, Mauriello A, Sangiorgi G, et al**. Extracranial thrombotically active carotid plaque as a risk factor for ischemic stroke. JAMA 2004;292:1845-1852

150. **Spagnoli LG, Bonanno E, Mauriello A, et al**. Multicentric inflammation in epicardial coronary arteries of patients dying of acute myocardial infarction. J.Am.Coll.Cardiol. 2002;40:1579-1588

151. **Libby P**. Inflammation in atherosclerosis. Nature 2002;420:868-874

152. **Mahley RW**. Apolipoprotein E: cholesterol transport protein with expanding role in cell biology. Science 1988;240:622-630

153. **Smith JD, Plump AS, Hayek T, Walsh A, Breslow JL**. Accumulation of human apolipoprotein E in the plasma of transgenic mice. J.Biol.Chem. 1990;265:14709-14712

154. **Miyata M, Smith JD**. Apolipoprotein E allele-specific antioxidant activity and effects on cytotoxicity by oxidative insults and beta-amyloid peptides. Nat.Genet. 1996;14:55-61

155. **Riddell DR, Graham A, Owen JS**. Apolipoprotein E inhibits platelet aggregation through the L-arginine:nitric oxide pathway. Implications for vascular disease. J.Biol.Chem. 1997;272:89-95

156. **Ishigami M, Swertfeger DK, Granholm NA, Hui DY**. Apolipoprotein E inhibits platelet-derived growth factor-induced vascular smooth muscle cell migration and proliferation by suppressing signal transduction and preventing cell entry to G1 phase. J.Biol.Chem. 1998;273:20156-20161

157. **Farrer LA, Cupples LA, Haines JL, et al**. Effects of age, sex, and ethnicity on the association between apolipoprotein E genotype and Alzheimer disease. A meta-analysis. APOE and Alzheimer Disease Meta Analysis Consortium. JAMA 1997;278:1349-1356

158. **Zhang SH, Reddick RL, Piedrahita JA, Maeda N**. Spontaneous hypercholesterolemia and arterial lesions in mice lacking apolipoprotein E. Science 1992;258:468-471

159. **Nakashima Y, Plump AS, Raines EW, Breslow JL, Ross R**. ApoE-deficient mice develop lesions of all phases of atherosclerosis throughout the arterial tree. Arterioscler.Thromb. 1994;14:133-140

160. **Reddick RL, Zhang SH, Maeda N**. Atherosclerosis in mice lacking apo E. Evaluation of lesional development and progression. Arterioscler.Thromb. 1994;14:141-147

161. **Breslow JL**. Mouse models of atherosclerosis. Science 1996;272:685-688

162. **Rosenfeld ME, Tsukada T, Gown AM, Ross R**. Fatty streak initiation in Watanabe Heritable Hyperlipemic and comparably hypercholesterolemic fat-fed rabbits. Arteriosclerosis 1987;7:9-23

163. **Davies MJ, Woolf N, Rowles PM, Pepper J**. Morphology of the endothelium over atherosclerotic plaques in human coronary arteries. Br.Heart J. 1988;60:459-464

164. **Matsumoto A, Naito M, Itakura H, et al**. Human macrophage scavenger receptors: primary structure, expression, and localization in atherosclerotic lesions. Proc.Natl.Acad.Sci.U.S.A 1990;87:9133-9137

165. **Stary HC, Chandler AB, Dinsmore RE, et al**. A definition of advanced types of atherosclerotic lesions and a histological classification of atherosclerosis. A report from the Committee on Vascular Lesions of the Council on Arteriosclerosis, American Heart Association. Circulation 1995;92:1355-1374

166. **Furchgott RF, Zawadzki JV**. The obligatory role of endothelial cells in the relaxation of arterial smooth muscle by acetylcholine. Nature 1980;288:373-376

167. **Hansson GK**. Inflammation, atherosclerosis, and coronary artery disease. N.Engl.J.Med. 2005;352:1685-1695

168. **Arnold WP, Mittal CK, Katsuki S, Murad F**. Nitric oxide activates guanylate cyclase and increases guanosine 3':5'-cyclic monophosphate levels in various tissue preparations. Proc.Natl.Acad.Sci.U.S.A 1977;74:3203-3207

169. **Harteneck C, Koesling D, Soling A, Schultz G, Bohme E**. Expression of soluble guanylyl cyclase. Catalytic activity requires two enzyme subunits. FEBS Lett. 1990;272:221-223

170. **Foerster J, Harteneck C, Malkewitz J, Schultz G, Koesling D**. A functional heme-binding site of soluble guanylyl cyclase requires intact N-termini of alpha 1 and beta 1 subunits. Eur.J.Biochem. 1996;240:380-386

171. **Alp NJ, McAteer MA, Khoo J, Choudhury RP, Channon KM**. Increased endothelial tetrahydrobiopterin synthesis by targeted transgenic GTP-cyclohydrolase I overexpression reduces endothelial dysfunction and atherosclerosis in ApoE-knockout mice. Arterioscler.Thromb.Vasc.Biol. 2004;24:445-450

172. **Alp NJ, Mussa S, Khoo J, et al**. Tetrahydrobiopterin-dependent preservation of nitric oxide-mediated endothelial function in diabetes by targeted transgenic GTP-cyclohydrolase I overexpression. J.Clin.Invest 2003;112:725-735

173. **Hansson GK, Libby P**. The immune response in atherosclerosis: a double-edged sword. Nat.Rev.Immunol. 2006;6:508-519

174 **Marczin N, Antonov A, Papapetropoulos A, et al**. Monocyte-induced downregulation of nitric oxide synthase in cultured aortic endothelial cells. Arterioscler.Thromb.Vasc.Biol. 1996;16:1095-1103

175. **Knowles JW, Reddick RL, Jennette JC, Shesely EG, Smithies O, Maeda N**. Enhanced atherosclerosis and kidney dysfunction in eNOS(-/-)Apoe(-/-) mice are ameliorated by enalapril treatment. J.Clin.Invest 2000;105:451-458

176. **Cheng YW, Kang JJ**. Inhibition of agonist-induced vasocontraction and impairment of endothelium-dependent vasorelaxation by extract of motorcycle exhaust particles in vitro. J.Toxicol.Environ.Health A 1999;57:75-87

177. **Ikeda M, Suzuki M, Watarai K, Sagai M, Tomita T**. Impairment of endothelium-dependent relaxation by diesel exhaust particles in rat thoracic aorta. Jpn.J.Pharmacol. 1995;68:183-189

178. **Ludmer PL, Selwyn AP, Shook TL, et al**. Paradoxical vasoconstriction induced by acetylcholine in atherosclerotic coronary arteries. N.Engl.J.Med. 1986;315:1046-1051

179. **Muto E, Hayashi T, Yamada K, Esaki T, Sagai M, Iguchi A**. Endothelial-constitutive nitric oxide synthase exists in airways and diesel exhaust particles inhibit the effect of nitric oxide. Life Sci. 1996;59:1563-1570

180. **Bai Y, Suzuki AK, Sagai M**. The cytotoxic effects of diesel exhaust particles on human pulmonary artery endothelial cells in vitro: role of active oxygen species. Free Radic.Biol.Med. 2001;30:555-562

181. **Verma S, Wang CH, Li SH, et al**. A self-fulfilling prophecy: C-reactive protein attenuates nitric oxide production and inhibits angiogenesis. Circulation 2002;106:913-919

182. **Ikeda M, Shitashige M, Yamasaki H, Sagai M, Tomita T**. Oxidative modification of low density lipoprotein by diesel exhaust particles. Biol.Pharm.Bull. 1995;18:866-871

183. **Sagai M, Saito H, Ichinose T, Kodama M, Mori Y**. Biological effects of diesel exhaust particles. I. In vitro production of superoxide and in vivo toxicity in mouse. Free Radic.Biol.Med. 1993;14:37-47

184. **Liao JK, Shin WS, Lee WY, Clark SL**. Oxidized low-density lipoprotein decreases the expression of endothelial nitric oxide synthase. J.Biol.Chem. 1995;270:319-324

185. **Cuzzocrea S, Mazzon E, Dugo L, Di PR, Caputi AP, Salvemini D**. Superoxide: a key player in hypertension. FASEB J. 2004;18:94-101

186. **Ito T, Ikeda M, Yamasaki H, Sagai M, Tomita T**. Peroxynitrite formation by diesel exhaust particles in alveolar cells: Links to pulmonary inflammation. Environmental.Toxicology and Pharmacology 2000;9:1-8

187. **Lim HB, Ichinose T, Miyabara Y, et al**. Involvement of superoxide and nitric oxide on airway inflammation and hyperresponsiveness induced by diesel exhaust particles in mice. Free Radic.Biol.Med. 1998;25:635-644

188. **Liu Y, Bubolz AB, Shi Y, Newman PJ, Newman DK, Gutterman DD**. Peroxynitrite reduces the endothelium derived hyperpolarizing factor component of coronary flow-mediated dilation in PECAM-1-knock out mice. Am.J.Physiol Regul.Integr.Comp Physiol 2005;

189. **White CR, Brock TA, Chang LY, et al**. Superoxide and peroxynitrite in atherosclerosis. Proc.Natl.Acad.Sci.U.S.A 1994;91:1044-1048

190. **Beckman JS, Beckman TW, Chen J, Marshall PA, Freeman BA**. Apparent hydroxyl radical production by peroxynitrite: implications for endothelial injury from nitric oxide and superoxide. Proc.Natl.Acad.Sci.U.S.A 1990;87:1620-1624

191. **Yanagisawa M, Kurihara H, Kimura S, et al**. A novel potent vasoconstrictor peptide produced by vascular endothelial cells. Nature 1988;332:411-415

192. **Mathew V, Hasdai D, Lerman A**. The role of endothelin in coronary atherosclerosis. Mayo Clin.Proc. 1996;71:769-777

193. **Teplyakov AI**. Endothelin-1 involved in systemic cytokine network inflammatory response at atherosclerosis. J.Cardiovasc.Pharmacol. 2004;44 Suppl 1:S274-S275

194. **Lerman A, Edwards BS, Hallett JW, Heublein DM, Sandberg SM, Burnett JC, Jr.** Circulating and tissue endothelin immunoreactivity in advanced atherosclerosis. N.Engl.J.Med. 1991;325:997-1001

195. **Lerman A, Holmes DR, Jr., Bell MR, Garratt KN, Nishimura RA, Burnett JC, Jr.** Endothelin in coronary endothelial dysfunction and early atherosclerosis in humans. Circulation 1995;92:2426-2431

196. **Bouthillier L, Vincent R, Goegan P, et al**. Acute effects of inhaled urban particles and ozone: lung morphology, macrophage activity, and plasma endothelin-1. Am.J.Pathol. 1998;153:1873-1884

197. **Peters A, Dockery DW, Muller JE, Mittleman MA**. Increased particulate air pollution and the triggering of myocardial infarction. Circulation 2001;103:2810-2815

198. **Batalha JR, Saldiva PH, Clarke RW, et al**. Concentrated ambient air particles induce vasoconstriction of small pulmonary arteries in rats. Environ.Health Perspect. 2002;110:1191-1197

199. **Brook RD, Brook JR, Urch B, Vincent R, Rajagopalan S, Silverman F**. Inhalation of fine particulate air pollution and ozone causes acute arterial vasoconstriction in healthy adults. Circulation 2002;105:1534-1536

200. **Thomson E, Goegan P, Kumarathasan P, Vincent R**. Air pollutants increase gene expression of the vasoconstrictor endothelin-1 in the lungs. Biochim.Biophys.Acta 2004;1689:75-82

201. **Papapetropoulos A, Antonov A, Virmani R, et al**. Monocyte- and cytokine-induced downregulation of angiotensin-converting enzyme in cultured human and porcine endothelial cells. Circ.Res. 1996;79:512-523

202. **Ulrich MM, Alink GM, Kumarathasan P, Vincent R, Boere AJ, Cassee FR**. Health effects and time course of particulate matter on the cardiopulmonary system in rats with lung inflammation. J.Toxicol.Environ.Health A 2002;65:1571-1595

203. **Bonetti PO, Lerman LO, Lerman A**. Endothelial dysfunction: a marker of atherosclerotic risk. Arterioscler.Thromb.Vasc.Biol. 2003;23:168-175

204. **Creager MA, Cooke JP, Mendelsohn ME, et al**. Impaired vasodilation of forearm resistance vessels in hypercholesterolemic humans. J.Clin.Invest 1990;86:228-234

205. **Celermajer DS, Sorensen KE, Georgakopoulos D, et al**. Cigarette smoking is associated with dose-related and potentially reversible impairment of endothelium-dependent dilation in healthy young adults. Circulation 1993;88:2149-2155

206. **Forstermann U, Closs EI, Pollock JS, et al**. Nitric oxide synthase isozymes. Characterization, purification, molecular cloning, and functions. Hypertension 1994;23:1121-1131

207. **Heba G, Krzeminski T, Porc M, Grzyb J, mbinska-Kiec A**. Relation between expression of TNF alpha, iNOS, VEGF mRNA and development of heart failure after experimental myocardial infarction in rats. J.Physiol Pharmacol. 2001;52:39-52

208. **Bu DX, Erl W, de MR, Hansson GK, Yan ZQ**. IKKbeta-dependent NF-kappaB pathway controls vascular inflammation and intimal hyperplasia. FASEB J. 2005;19:1293-1295

209. **Ling L, Cao Z, Goeddel DV**. NF-kappaB-inducing kinase activates IKK-alpha by phosphorylation of Ser-176. Proc.Natl.Acad.Sci.U.S.A 1998;95:3792-3797

210. **Sun Z, Andersson R**. NF-kappaB activation and inhibition: a review. Shock 2002;18:99-106

211. **Hoffmann A, Levchenko A, Scott ML, Baltimore D**. The IkappaB-NF-kappaB signaling module: temporal control and selective gene activation. Science 2002;298:1241-1245

212. **Janssen-Heininger YM, Poynter ME, Baeuerle PA**. Recent advances towards understanding redox mechanisms in the activation of nuclear factor kappaB. Free Radic.Biol.Med. 2000;28:1317-1327

213. **Xie Q, Nathan C**. The high-output nitric oxide pathway: role and regulation. J.Leukoc.Biol. 1994;56:576-582

214. **Wilcox JN, Subramanian RR, Sundell CL, et al**. Expression of multiple isoforms of nitric oxide synthase in normal and atherosclerotic vessels. Arterioscler.Thromb.Vasc.Biol. 1997;17:2479-2488

215. **Luoma JS, Yla-Herttuala S**. Expression of inducible nitric oxide synthase in macrophages and smooth muscle cells in various types of human atherosclerotic lesions. Virchows Arch. 1999;434:561-568

216. **Ischiropoulos H, al-Mehdi AB**. Peroxynitrite-mediated oxidative protein modifications. FEBS Lett. 1995;364:279-282

217. **Cromheeke KM, Kockx MM, De Meyer GR, et al**. Inducible nitric oxide synthase colocalizes with signs of lipid oxidation/peroxidation in human atherosclerotic plaques. Cardiovasc.Res. 1999;43:744-754

218. **Detmers PA, Hernandez M, Mudgett J, et al**. Deficiency in inducible nitric oxide synthase results in reduced atherosclerosis in apolipoprotein E-deficient mice. J.Immunol. 2000;165:3430-3435

219. **Endemann G, Stanton LW, Madden KS, Bryant CM, White RT, Protter AA**. CD36 is a receptor for oxidized low density lipoprotein. J.Biol.Chem. 1993;268:11811-11816

220. **Silverstein RL, Febbraio M**. CD36 and atherosclerosis. Curr.Opin.Lipidol. 2000;11:483-491

221. **Han J, Hajjar DP, Febbraio M, Nicholson AC**. Native and modified low density lipoproteins increase the functional expression of the macrophage class B scavenger receptor, CD36. J.Biol.Chem. 1997;272:21654-21659

222. **Febbraio M, Podrez EA, Smith JD, et al**. Targeted disruption of the class B scavenger receptor CD36 protects against atherosclerotic lesion development in mice. J.Clin.Invest 2000;105:1049-1056

223. **Huh HY, Pearce SF, Yesner LM, Schindler JL, Silverstein RL**. Regulated expression of CD36 during monocyte-to-macrophage differentiation: potential role of CD36 in foam cell formation. Blood 1996;87:2020-2028

224. **Nakata A, Nakagawa Y, Nishida M, et al**. CD36, a novel receptor for oxidized low-density lipoproteins, is highly expressed on lipid-laden macrophages in human atherosclerotic aorta. Arterioscler.Thromb.Vasc.Biol. 1999;19:1333-1339

225. **Han J, Nicholson AC**. Lipoproteins modulate expression of the macrophage scavenger receptor. Am.J.Pathol. 1998;152:1647-1654

226. **Nozaki S, Kashiwagi H, Yamashita S, et al**. Reduced uptake of oxidized low density lipoproteins in monocyte-derived macrophages from CD36-deficient subjects. J.Clin.Invest 1995;96:1859-1865

227 **Cuzzocrea S, Mazzon E, Dugo L, Di PR, Caputi AP, Salvemini D**. Superoxide: a key player in hypertension. FASEB J. 2004;18:94-101

228. **Pacher P, Beckman JS, Liaudet L**. Nitric oxide and peroxynitrite in health and disease. Physiol Rev. 2007;87:315-424

229. **Gilmour PS, Brown DM, Lindsay TG, Beswick PH, MacNee W, Donaldson K**. Adverse health effects of PM10 particles: involvement of iron in generation of hydroxyl radical. Occup.Environ.Med. 1996;53:817-822

230. **Jimenez LA, Thompson J, Brown DA, et al**. Activation of NF-kappaB by PM(10) occurs via an iron-mediated mechanism in the absence of IkappaB degradation. Toxicol.Appl.Pharmacol. 2000;166:101-110

231. **Kadiiska MB, Mason RP, Dreher KL, Costa DL, Ghio AJ**. In vivo evidence of free radical formation in the rat lung after exposure to an emission source air pollution particle. Chem.Res.Toxicol. 1997;10:1104-1108

232. **Donaldson K, Stone V, Seaton A, MacNee W**. Ambient particle inhalation and the cardiovascular system: potential mechanisms. Environ.Health Perspect. 2001;109 Suppl 4:523-527

233. **Stone V, Tuinman M, Vamvakopoulos JE, et al**. Increased calcium influx in a monocytic cell line on exposure to ultrafine carbon black. Eur.Respir.J. 2000;15:297-303

234. **Brown DM, Stone V, Findlay P, MacNee W, Donaldson K**. Increased inflammation and intracellular calcium caused by ultrafine carbon black is independent of transition metals or other soluble components. Occup.Environ.Med. 2000;57:685-691

235. **Li XY, Brown D, Smith S, MacNee W, Donaldson K**. Short-term inflammatory responses following intratracheal instillation of fine and ultrafine carbon black in rats. Inhal.Toxicol. 1999;11:709-731

236. **Brown DM, Donaldson K, Borm PJ, et al**. Calcium and ROS-mediated activation of transcription factors and TNF-alpha cytokine gene expression in macrophages exposed to ultrafine particles. Am.J.Physiol Lung Cell Mol.Physiol 2004;286:L344-L353

237. **Dolmetsch RE, Xu K, Lewis RS**. Calcium oscillations increase the efficiency and specificity of gene expression. Nature 1998;392:933-936

238. **Stringer B, Kobzik L**. Environmental particulate-mediated cytokine production in lung epithelial cells (A549): role of preexisting inflammation and oxidant stress. J.Toxicol.Environ.Health A 1998;55:31-44

239. **Cushing SD, Berliner JA, Valente AJ, et al**. Minimally modified low density lipoprotein induces monocyte chemotactic protein 1 in human endothelial cells and smooth muscle cells. Proc.Natl.Acad.Sci.U.S.A 1990;87:5134-5138

240. **Miyazawa K, Kiyono S, Inoue K**. Modulation of stimulus-dependent human platelet activation by C-reactive protein modified with active oxygen species. J.Immunol. 1988;141:570-574

241. **Rahman I, MacNee W**. Role of transcription factors in inflammatory lung diseases. Thorax 1998;53:601-612

242. **Li XY, Donaldson K, Rahman I, MacNee W**. An investigation of the role of glutathione in increased epithelial permeability induced by cigarette smoke in vivo and in vitro. Am.J.Respir.Crit Care Med. 1994;149:1518-1525

243. **Vane JR**. Inhibition of prostaglandin synthesis as a mechanism of action for aspirin-like drugs. Nat.New Biol. 1971;231:232-235

244. **Crofford LJ**. COX-1 and COX-2 tissue expression: implications and predictions. J.Rheumatol.Suppl 1997;49:15-19

245. **Dubois RN, Abramson SB, Crofford L, et al**. Cyclooxygenase in biology and disease. FASEB J. 1998;12:1063-1073

246. **Schafer AI**. Effects of nonsteroidal antiinflammatory drugs on platelet function and systemic hemostasis. J.Clin.Pharmacol. 1995;35:209-219

247. **Hinz B, Brune K**. Cyclooxygenase-2--10 years later. J.Pharmacol.Exp.Ther. 2002;300:367-375

248. **Schonbeck U, Sukhova GK, Graber P, Coulter S, Libby P**. Augmented expression of cyclooxygenase-2 in human atherosclerotic lesions. Am.J.Pathol. 1999;155:1281-1291

249. **Cipollone F, Prontera C, Pini B, et al**. Overexpression of functionally coupled cyclooxygenase-2 and prostaglandin E synthase in symptomatic atherosclerotic plaques as a basis of prostaglandin E(2)-dependent plaque instability. Circulation 2001;104:921-927

251. **Chenevard R, Hurlimann D, Bechir M, et al**. Selective COX-2 inhibition improves endothelial function in coronary artery disease. Circulation 2003;107:405-409

252. **Pope CA, III, Dockery DW**. Health effects of fine particulate air pollution: lines that connect. J.Air Waste Manag.Assoc. 2006;56:709-742

253. **Ebelt ST, Wilson WE, Brauer M**. Exposure to ambient and nonambient components of particulate matter: a comparison of health effects. Epidemiology 2005;16:396-405

254. **Hedley AJ, Wong CM, Thach TQ, Ma S, Lam TH, Anderson HR**. Cardiorespiratory and all-cause mortality after restrictions on sulphur content of fuel in Hong Kong: an intervention study. Lancet 2002;360:1646-1652

255. **Dominici F, Peng RD, Zeger SL, White RH, Samet JM**. Particulate air pollution and mortality in the United States: did the risks change from 1987 to 2000? Am.J.Epidemiol. 2007;166:880-888

256. **Tonne C, Melly S, Mittleman M, Coull B, Goldberg R, Schwartz J**. A case-control analysis of exposure to traffic and acute myocardial infarction. Environ.Health Perspect. 2007;115:53-57

257. **Peters A, von KS, Heier M, et al**. Exposure to traffic and the onset of myocardial infarction. N.Engl.J.Med. 2004;351:1721-1730

258. **Maynard D, Coull BA, Gryparis A, Schwartz J**. Mortality risk associated with short-term exposure to traffic particles and sulfates. Environ.Health Perspect. 2007;115:751-755

259. **Abbey DE, Nishino N, McDonnell WF, et al**. Long-term inhalable particles and other air pollutants related to mortality in nonsmokers. Am.J.Respir.Crit Care Med. 1999;159:373-382

260. **Finkelstein MM, Jerrett M, Sears MR**. Traffic air pollution and mortality rate advancement periods. Am.J.Epidemiol. 2004;160:173-177

261. **Beelen R, Hoek G, van den Brandt PA, et al**. Long-term effects of traffic-related air pollution on mortality in a Dutch cohort (NLCS-AIR study). Environ.Health Perspect. 2008;116:196-202

262. **Rosenlund M, Bellander T, Nordquist T, Alfredsson L**. Traffic-generated air pollution and myocardial infarction. Epidemiology 2009;20:265-271

263. **Beelen R, Hoek G, Houthuijs D, et al**. The joint association of air pollution and noise from road traffic with cardiovascular mortality in a cohort study. Occup.Environ.Med. 2009;66:243-250

264. **Peretz A, Peck EC, Bammler TK, et al**. Diesel exhaust inhalation and assessment of peripheral blood mononuclear cell gene transcription effects: an exploratory study of healthy human volunteers. Inhal.Toxicol. 2007;19:1107-1119

265. **Brauner EV, Forchhammer L, Moller P, et al**. Exposure to ultrafine particles from ambient air and oxidative stress-induced DNA damage. Environ.Health Perspect. 2007;115:1177-1182

266. **Vinzents PS, Moller P, Sorensen M, et al**. Personal exposure to ultrafine particles and oxidative DNA damage. Environ.Health Perspect. 2005;113:1485-1490

267. **Sorensen M, Daneshvar B, Hansen M, et al**. Personal PM2.5 exposure and markers of oxidative stress in blood. Environ.Health Perspect. 2003;111:161-166

268. **Stuehr DJ, Marletta MA**. Induction of nitrite/nitrate synthesis in murine macrophages by BCG infection, lymphokines, or interferon-gamma. J.Immunol. 1987;139:518-525

269. **Kuhlencordt PJ, Chen J, Han F, Astern J, Huang PL**. Genetic deficiency of inducible nitric oxide synthase reduces atherosclerosis and lowers plasma lipid peroxides in apolipoprotein E-knockout mice. Circulation 2001;103:3099-3104

270. **Takano H, Lim HB, Miyabara Y, Ichinose T, Yoshikawa T, Sagai M**. Manipulation of the L-arginine-nitric oxide pathway in airway inflammation induced by diesel exhaust particles in mice. Toxicology 1999;139:19-26

271. **Becher R, Bucht A, Ovrevik J, et al**. Involvement of NADPH oxidase and iNOS in rodent pulmonary cytokine responses to urban air and mineral particles. Inhal.Toxicol. 2007;19:645-655

272. **Kawabe J, Ushikubi F, Hasebe N**. Prostacyclin in vascular diseases. - Recent insights and future perspectives -. Circ.J. 2010;74:836-843

273. **Pratico D, Tillmann C, Zhang ZB, Li H, FitzGerald GA**. Acceleration of atherogenesis by COX-1-dependent prostanoid formation in low density lipoprotein receptor knockout mice. Proc.Natl.Acad.Sci.U.S.A 2001;98:3358-3363

274. **Samet JM, Ghio AJ, Costa DL, Madden MC**. Increased expression of cyclooxygenase 2 mediates oil fly ash-induced lung injury. Exp.Lung Res. 2000;26:57-69

275. **Vogel CF, Sciullo E, Wong P, Kuzmicky P, Kado N, Matsumura F**. Induction of proinflammatory cytokines and C-reactive protein in human macrophage cell line U937 exposed to air pollution particulates. Environ.Health Perspect. 2005;113:1536-1541

276. **Gibbons GH**. Endothelial function as a determinant of vascular function and structure: a new therapeutic target. Am.J.Cardiol. 1997;79:3-8

277. **Sullivan GW, Sarembock IJ, Linden J**. The role of inflammation in vascular diseases. J.Leukoc.Biol. 2000;67:591-602

278. **Gimbrone MA, Jr.** Endothelial dysfunction, hemodynamic forces, and atherosclerosis. Thromb.Haemost. 1999;82:722-726

279. **Vanhoutte PM**. Endothelial dysfunction: the first step toward coronary arteriosclerosis. Circ.J. 2009;73:595-601

280. **Nurkiewicz TR, Porter DW, Barger M, et al**. Systemic microvascular dysfunction and inflammation after pulmonary particulate matter exposure. Environ.Health Perspect. 2006;114:412-419

281. **Kumagai Y, Taira J, Sagai M**. Apparent inhibition of superoxide dismutase activity in vitro by diesel exhaust particles. Free Radic.Biol.Med. 1995;18:365-371

282. **Kumagai Y, Arimoto T, Shinyashiki M, et al**. Generation of reactive oxygen species during interaction of diesel exhaust particle components with NADPH-cytochrome P450 reductase and involvement of the bioactivation in the DNA damage. Free Radic.Biol.Med. 1997;22:479-487

283. **Teplyakov AI**. Endothelin-1 involved in systemic cytokine network inflammatory response at atherosclerosis. J.Cardiovasc.Pharmacol. 2004;44 Suppl 1:S274-S275

284. **Langrish JP, Lundback M, Mills NL, et al**. Contribution of endothelin 1 to the vascular effects of diesel exhaust inhalation in humans. Hypertension 2009;54:910-915

285. **Brook RD, Franklin B, Cascio W, et al**. Air pollution and cardiovascular disease: a statement for healthcare professionals from the Expert Panel on Population and Prevention Science of the American Heart Association. Circulation 2004;109:2655-2671

286. **Taber DF, Morrow JD, Roberts LJ**. A nomenclature system for the isoprostanes. Prostaglandins 1997;53:63-67

287. **Bai N, Khazaei M, van Eeden SF, Laher I**. The pharmacology of particulate matter air pollution-induced cardiovascular dysfunction. Pharmacol.Ther. 2007;113:16-29

288. **Podrez EA, Febbraio M, Sheibani N, et al**. Macrophage scavenger receptor CD36 is the major receptor for LDL modified by monocyte-generated reactive nitrogen species. J.Clin.Invest 2000;105:1095-1108

404. **Ni M, Chen WQ, Zhang Y**. Animal models and potential mechanisms of plaque destabilisation and disruption. Heart 2009;95:1393-1398

290. **Burke AP, Farb A, Malcom GT, Liang YH, Smialek J, Virmani R**. Coronary risk factors and plaque morphology in men with coronary disease who died suddenly. N.Engl.J.Med. 1997;336:1276-1282

291. **Guo X, Liu ES, Ko JK, et al**. Protective role of cyclooxygenase inhibitors in the adverse action of passive cigarette smoking on the initiation of experimental colitis in rats. Eur.J.Pharmacol. 2001;411:193-203

292. **Weisenberger B**. Health effect of diesel emissions: a current status report. J.Soc.Occup.Med. 1981;31:4-8

293. **Hoek G, Brunekreef B, Goldbohm S, Fischer P, van den Brandt PA**. Association between mortality and indicators of traffic-related air pollution in the Netherlands: a cohort study. Lancet 2002;360:1203-1209

294. **Ni M, Chen WQ, Zhang Y**. Animal models and potential mechanisms of plaque destabilisation and disruption. Heart 2009;95:1393-1398

295. **Schwartz SM, Galis ZS, Rosenfeld ME, Falk E**. Plaque rupture in humans and mice. Arterioscler.Thromb.Vasc.Biol. 2007;27:705-713

296. **Hirano S, Furuyama A, Koike E, Kobayashi T**. Oxidative-stress potency of organic extracts of diesel exhaust and urban fine particles in rat heart microvessel endothelial cells. Toxicology 2003;187:161-170

297. **Quan C, Sun Q, Lippmann M, Chen LC**. Comparative effects of inhaled diesel exhaust and ambient fine particles on inflammation, atherosclerosis, and vascular dysfunction. Inhal.Toxicol. 2010;22:738-753

298. **Sprague AH, Khalil RA**. Inflammatory cytokines in vascular dysfunction and vascular disease. Biochem.Pharmacol. 2009;78:539-552

299. **Xia Y, Zweier JL**. Superoxide and peroxynitrite generation from inducible nitric oxide synthase in macrophages. Proc.Natl.Acad.Sci.U.S.A 1997;94:6954-6958

300. **Kunzli N, Jerrett M, Garcia-Esteban R, et al**. Ambient air pollution and the progression of atherosclerosis in adults. PLoS.One. 2010;5:e9096

301. **Nathan C, Xie QW**. Regulation of biosynthesis of nitric oxide. J.Biol.Chem. 1994;269:13725-13728

302. **Taylor BS, de Vera ME, Ganster RW, et al**. Multiple NF-kappaB enhancer elements regulate cytokine induction of the human inducible nitric oxide synthase gene. J.Biol.Chem. 1998;273:15148-15156

303. **Xie QW, Whisnant R, Nathan C**. Promoter of the mouse gene encoding calcium-independent nitric oxide synthase confers inducibility by interferon gamma and bacterial lipopolysaccharide. J.Exp.Med. 1993;177:1779-1784

304. **Okayama Y, Kuwahara M, Suzuki AK, Tsubone H**. Role of reactive oxygen species on diesel exhaust particle-induced cytotoxicity in rat cardiac myocytes. J.Toxicol.Environ.Health A 2006;69:1699-1710

305. **Brown DM, Stone V, Findlay P, Macnee W, Donaldson K**. Increased inflammation and intracellular calcium caused by ultrafine carbon black is independent of transition metals or other soluble components. Occup.Environ.Med. 2000;57:685-691

306. **Donaldson K, MacNee W**. Potential mechanisms of adverse pulmonary and cardiovascular effects of particulate air pollution (PM10). Int.J.Hyg.Environ.Health 2001;203:411-415

307. **Li N, Wang M, Oberley TD, Sempf JM, Nel AE**. Comparison of the pro-oxidative and proinflammatory effects of organic diesel exhaust particle chemicals in bronchial epithelial cells and macrophages. J.Immunol. 2002;169:4531-4541

308. **Baulig A, Garlatti M, Bonvallot V, et al**. Involvement of reactive oxygen species in the metabolic pathways triggered by diesel exhaust particles in human airway epithelial cells. Am.J.Physiol Lung Cell Mol.Physiol 2003;285:L671-L679

309. **Rudell B, Blomberg A, Helleday R, et al**. Bronchoalveolar inflammation after exposure to diesel exhaust: comparison between unfiltered and particle trap filtered exhaust. Occup.Environ.Med. 1999;56:527-534

310. **Krieger M, Acton S, Ashkenas J, Pearson A, Penman M, Resnick D**. Molecular flypaper, host defense, and atherosclerosis. Structure, binding properties, and functions of macrophage scavenger receptors. J.Biol.Chem. 1993;268:4569-4572

311. **Endemann G, Stanton LW, Madden KS, Bryant CM, White RT, Protter AA**. CD36 is a receptor for oxidized low density lipoprotein. J.Biol.Chem. 1993;268:11811-11816

312. **Graham A, Hogg N, Kalyanaraman B, O'Leary V, rley-Usmar V, Moncada S**. Peroxynitrite modification of low-density lipoprotein leads to recognition by the macrophage scavenger receptor. FEBS Lett. 1993;330:181-185

313. **Cipollone F, Rocca B, Patrono C**. Cyclooxygenase-2 expression and inhibition in atherothrombosis. Arterioscler.Thromb.Vasc.Biol. 2004;24:246-255

314. **Kawabe J, Yuhki K, Okada M, et al**. Prostaglandin I2 promotes recruitment of endothelial progenitor cells and limits vascular remodeling. Arterioscler.Thromb.Vasc.Biol. 2010;30:464-470

315. **Egan KM, Lawson JA, Fries S, et al**. COX-2-derived prostacyclin confers atheroprotection on female mice. Science 2004;306:1954-1957

316. **Warner TD, Mitchell JA**. Cyclooxygenases: new forms, new inhibitors, and lessons from the clinic. FASEB J. 2004;18:790-804

317. **Virdis A, Colucci R, Fornai M, et al**. Cyclooxygenase-1 is involved in endothelial dysfunction of mesenteric small arteries from angiotensin II-infused mice. Hypertension 2007;49:679-686

318. **McClelland S, Gawaz M, Kennerknecht E, et al**. Contribution of cyclooxygenase-1 to thromboxane formation, platelet-vessel wall interactions and atherosclerosis in the ApoE null mouse. Atherosclerosis 2009;202:84-91

319. **Belton OA, Duffy A, Toomey S, Fitzgerald DJ**. Cyclooxygenase isoforms and platelet vessel wall interactions in the apolipoprotein E knockout mouse model of atherosclerosis. Circulation 2003;108:3017-3023

320. **Rott D, Zhu J, Burnett MS, et al**. Effects of MF-tricyclic, a selective cyclooxygenase-2 inhibitor, on atherosclerosis progression and susceptibility to cytomegalovirus replication in apolipoprotein-E knockout mice. J.Am.Coll.Cardiol. 2003;41:1812-1819

321. **Burleigh ME, Babaev VR, Oates JA, et al**. Cyclooxygenase-2 promotes early atherosclerotic lesion formation in LDL receptor-deficient mice. Circulation 2002;105:1816-1823

322. **Hofer TP, Bitterle E, Beck-Speier I, et al**. Diesel exhaust particles increase LPS-stimulated COX-2 expression and PGE2 production in human monocytes. J.Leukoc.Biol. 2004;75:856-864

323. **Tzeng HP, Yang RS, Ueng TH, Liu SH**. Upregulation of cyclooxygenase-2 by motorcycle exhaust particulate-induced reactive oxygen species enhances rat vascular smooth muscle cell proliferation. Chem.Res.Toxicol. 2007;20:1170-1176

324. **Racz A, Veresh Z, Lotz G, Bagi Z, Koller A**. Cyclooxygenase-2 derived thromboxane A(2) and reactive oxygen species mediate flow-induced constrictions of venules in hyperhomocysteinemia. Atherosclerosis 2010;208:43-49

325. **Hermann M, Camici G, Fratton A, et al**. Differential effects of selective cyclooxygenase-2 inhibitors on endothelial function in salt-induced hypertension. Circulation 2003;108:2308-2311

326. **Li SL, Reddy MA, Cai Q, et al**. Enhanced proatherogenic responses in macrophages and vascular smooth muscle cells derived from diabetic db/db mice. Diabetes 2006;55:2611-2619

327. **Bresalier RS, Sandler RS, Quan H, et al**. Cardiovascular events associated with rofecoxib in a colorectal adenoma chemoprevention trial. N.Engl.J.Med. 2005;352:1092-1102

328. **Nussmeier NA, Whelton AA, Brown MT, et al**. Complications of the COX-2 inhibitors parecoxib and valdecoxib after cardiac surgery. N.Engl.J.Med. 2005;352:1081-1091

329. **Egan KM, Lawson JA, Fries S, et al**. COX-2-derived prostacyclin confers atheroprotection on female mice. Science 2004;306:1954-1957

330. **Niwano K, Arai M, Tomaru K, Uchiyama T, Ohyama Y, Kurabayashi M**. Transcriptional stimulation of the eNOS gene by the stable prostacyclin analogue beraprost is mediated through cAMP-responsive element in vascular endothelial cells: close link between PGI2 signal and NO pathways. Circ.Res. 2003;93:523-530

331. **Hanafy KA, Krumenacker JS, Murad F**. NO, nitrotyrosine, and cyclic GMP in signal transduction. Med.Sci.Monit. 2001;7:801-819

332. **Palmer RM, Ashton DS, Moncada S**. Vascular endothelial cells synthesize nitric oxide from L-arginine. Nature 1988;333:664-666

333. **Mungrue IN, Bredt DS, Stewart DJ, Husain M**. From molecules to mammals: what's NOS got to do with it? Acta Physiol Scand. 2003;179:123-135

334. **Figueroa XF, Poblete MI, Boric MP, Mendizabal VE, dler-Graschinsky E, Huidobro-Toro JP**. Clonidine-induced nitric oxide-dependent vasorelaxation mediated by endothelial alpha(2)-adrenoceptor activation. Br.J.Pharmacol. 2001;134:957-968

335. **Kang YJ, Li Y, Zhou Z, et al**. Elevation of serum endothelins and cardiotoxicity induced by particulate matter (PM2.5) in rats with acute myocardial infarction. Cardiovasc.Toxicol. 2002;2:253-261

336 **Lund AK, Lucero J, Lucas S, et al**. Vehicular emissions induce vascular MMP-9 expression and activity associated with endothelin-1-mediated pathways. Arterioscler.Thromb.Vasc.Biol. 2009;29:511-517

337. **Tirapelli CR, Casolari DA, Yogi A, et al**. Functional characterization and expression of endothelin receptors in rat carotid artery: involvement of nitric oxide, a vasodilator prostanoid and the opening of K+ channels in ETB-induced relaxation. Br.J.Pharmacol. 2005;146:903-912

338. **Moncada S, Rees DD, Schulz R, Palmer RM**. Development and mechanism of a specific supersensitivity to nitrovasodilators after inhibition of vascular nitric oxide synthesis in vivo. Proc.Natl.Acad.Sci.U.S.A 1991;88:2166-2170

339. **Madhani M, Okorie M, Hobbs AJ, MacAllister RJ**. Reciprocal regulation of human soluble and particulate guanylate cyclases in vivo. Br.J.Pharmacol. 2006;149:797-801

340. **Shirasaki Y, Su C**. Endothelium removal augments vasodilation by sodium nitroprusside and sodium nitrite. Eur.J.Pharmacol. 1985;114:93-96

341. **Luscher TF, Richard V, Yang ZH**. Interaction between endothelium-derived nitric oxide and SIN-1 in human and porcine blood vessels. J.Cardiovasc.Pharmacol. 1989;14 Suppl 11:S76-S80

342. **Busse R, Pohl U, Mulsch A, Bassenge E**. Modulation of the vasodilator action of SIN-1 by the endothelium. J.Cardiovasc.Pharmacol. 1989;14 Suppl 11:S81-S85

343. **Bagate K, Meiring JJ, Gerlofs-Nijland ME, Cassee FR, Borm PJ**. Signal transduction pathways involved in particulate matter induced relaxation in rat aorta--spontaneous hypertensive versus Wistar Kyoto rats. Toxicol.In Vitro 2006;20:52-62

344. **Li J, Li W, Altura BT, Altura BM**. Peroxynitrite-induced relaxation in isolated canine cerebral arteries and mechanisms of action. Toxicol.Appl.Pharmacol. 2004;196:176-182

345. **Tofler GH, Muller JE**. Triggering of acute cardiovascular disease and potential preventive strategies. Circulation 2006;114:1863-1872

346. **Li Z, Hyseni X, Carter JD, Soukup JM, Dailey LA, Huang YC**. Pollutant particles enhanced H2O2 production from NAD(P)H oxidase and mitochondria in human pulmonary artery endothelial cells. Am.J.Physiol Cell Physiol 2006;291:C357-C365

347. **Han JY, Takeshita K, Utsumi H**. Noninvasive detection of hydroxyl radical generation in lung by diesel exhaust particles. Free Radic.Biol.Med. 2001;30:516-525

348. **Okayama Y, Kuwahara M, Suzuki AK, Tsubone H**. Role of reactive oxygen species on diesel exhaust particle-induced cytotoxicity in rat cardiac myocytes. J.Toxicol.Environ.Health A 2006;69:1699-1710

349. **Bonetti PO, Lerman LO, Lerman A**. Endothelial dysfunction: a marker of atherosclerotic risk. Arterioscler.Thromb.Vasc.Biol. 2003;23:168-175

350. **Rajagopalan S, Meng XP, Ramasamy S, Harrison DG, Galis ZS**. Reactive oxygen species produced by macrophage-derived foam cells regulate the activity of vascular matrix metalloproteinases in vitro. Implications for atherosclerotic plaque stability. J.Clin.Invest 1996;98:2572-2579

351. **Steed MM, Tyagi N, Sen U, Schuschke DA, Joshua IG, Tyagi SC**. Functional consequences of the collagen/elastin switch in vascular remodeling in hyperhomocysteinemic wild-type, eNOS-/-, and iNOS-/- mice. Am.J.Physiol Lung Cell Mol.Physiol 2010;299:L301-L311

352. **Burleigh ME, Babaev VR, Oates JA, et al**. Cyclooxygenase-2 promotes early atherosclerotic lesion formation in LDL receptor-deficient mice. Circulation 2002;105:1816-1823

353. **Ye Y, Martinez JD, Perez-Polo RJ, Lin Y, Uretsky BF, Birnbaum Y**. The role of eNOS, iNOS, and NF-kappaB in upregulation and activation of cyclooxygenase-2 and infarct size reduction by atorvastatin. Am.J.Physiol Heart Circ.Physiol 2008;295:H343-H351

354. **Kim SF, Huri DA, Snyder SH**. Inducible nitric oxide synthase binds, S-nitrosylates, and activates cyclooxygenase-2. Science 2005;310:1966-1970

355. **Kalyanaraman B, Mason RP, Tainer B, Eling TE**. The free radical formed during the hydroperoxide-mediated deactivation of ram seminal vesicles is hemoprotein-derived. J.Biol.Chem. 1982;257:4764-4768

356. **Karthein R, Nastainczyk W, Ruf HH**. EPR study of ferric native prostaglandin H synthase and its ferrous NO derivative. Eur.J.Biochem. 1987;166:173-180

357. **Hansen CS, Sheykhzade M, Moller P, et al**. Diesel exhaust particles induce endothelial dysfunction in apoE-/- mice. Toxicol.Appl.Pharmacol. 2007;219:24-32

358. **Mills NL, Tornqvist H, Robinson SD, et al**. Diesel exhaust inhalation causes vascular dysfunction and impaired endogenous fibrinolysis. Circulation 2005;112:3930-3936

359. **de NG, Gryglewski RJ, Warner TD, Vane JR**. Receptor-mediated release of endothelium-derived relaxing factor and prostacyclin from bovine aortic endothelial cells is coupled. Proc.Natl.Acad.Sci.U.S.A 1988;85:2334-2338

APPENDIX A

Expression of Proteoglycan in Aortic Root Lesion

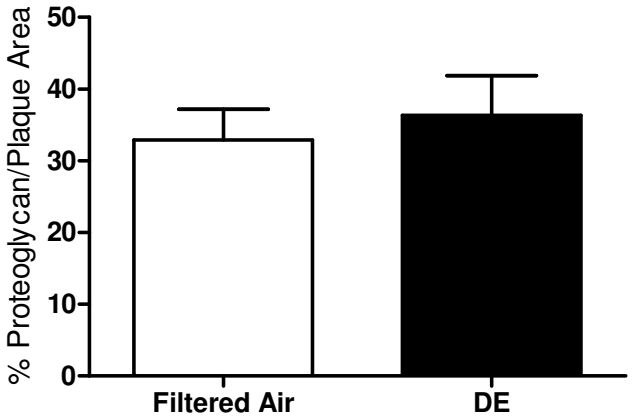

The expression of proteoglycan in aortic root lesion was not affected by exposure to DE.

APPENDIX B

Effect on the Thickness of Smooth Muscle in Thoracic Aorta

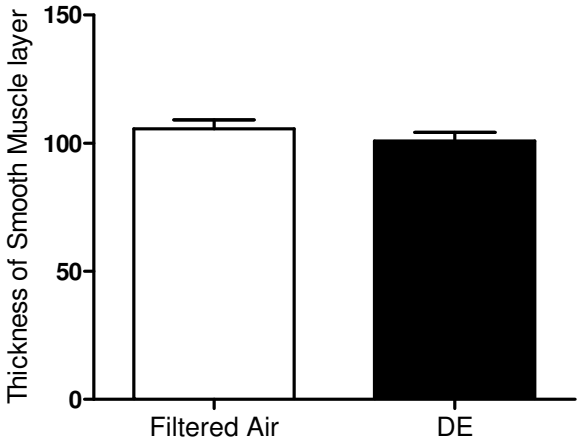

Exposure to DE had no effect on the thickness of smooth muscle of thoracic aorta.

APPENDIX C

Association between iNOS Expression and the Cellular Features of Atherosclerotic Plaque in Aortic Root

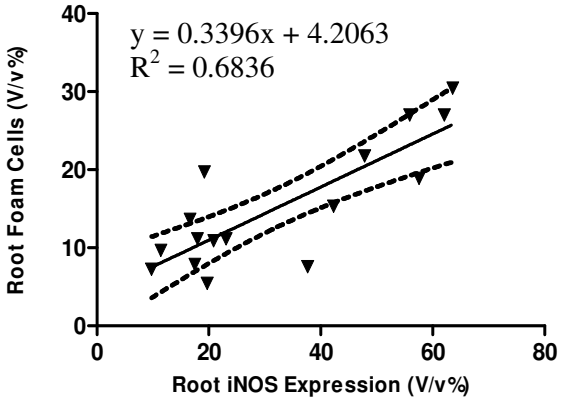

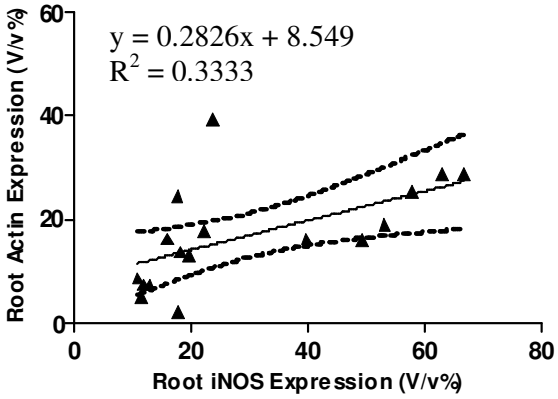

There is a positive correlation between iNOS expression with both foam cell formation ($p<0.001$) and the number of smooth muscle cells ($p<0.02$) in atherosclerotic plaques in aortic root.

APPENDIX D

No Changes of Vasoconstriction in the Presence of TXA2 Inhibitor

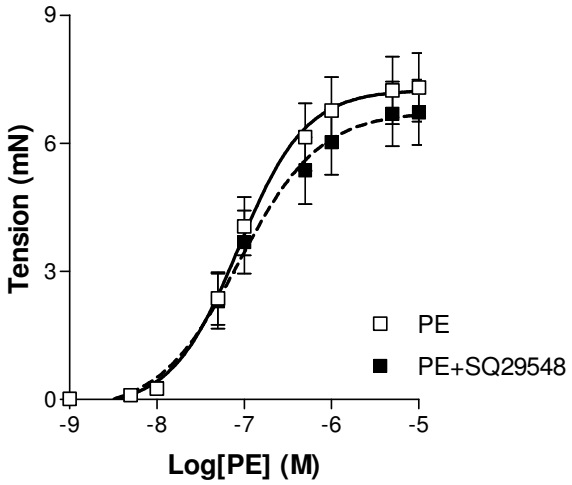

PE-concentration response curve shows that vasoconstriction of the thoracic aorta in DE exposure group was not different in the presence of TXA2 inhibitor (SQ29548).

APPENDIX E

Vascular Function Analysis of COX1 and COX2 Activity

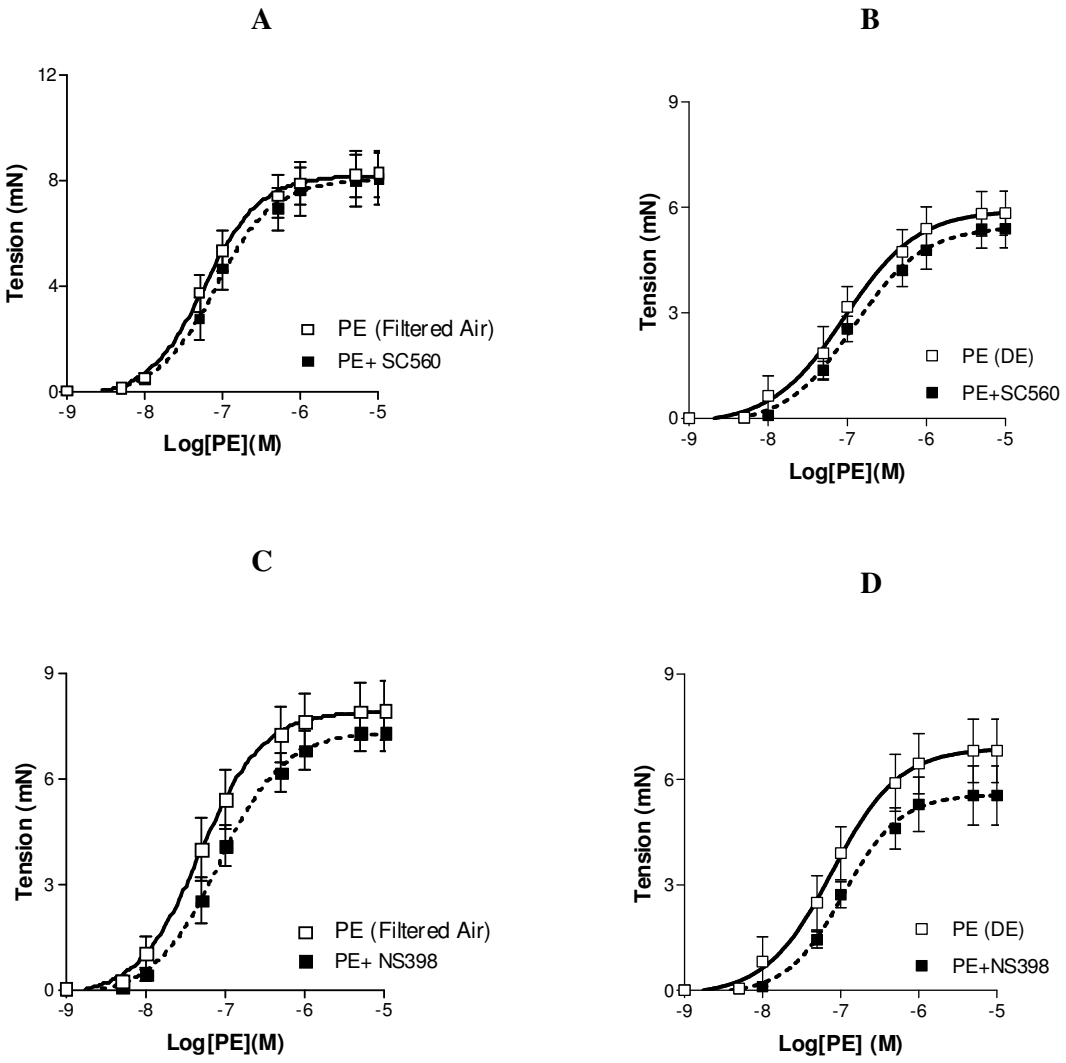

To examine the effect of DE exposure on COX1 and COX2 activity, the specific antagonists for COX1 (SC560) and COX2 (NS398) were administered, respectively. Concentration-response curves show that PE-elicited vasoconstriction was not different in the presence of these antagonists, comparing DE exposure and the control. n=6. Values are mean±SEM.

APPENDIX F

No Modification of DE Exposure on the Expression of sGCβ1 in the Thoracic Aorta

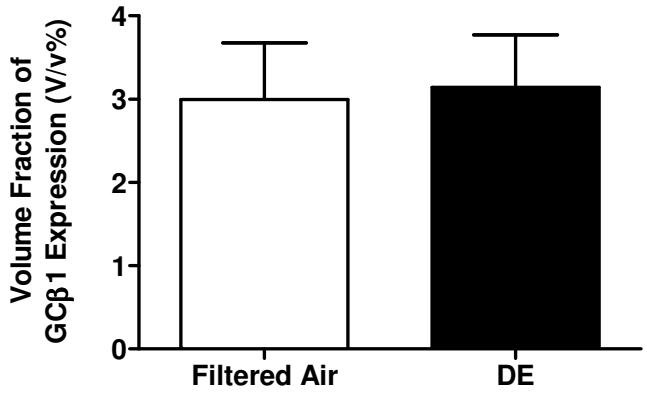

The expression of sGCβ1 in the thoracic aorta was not different after exposure to DE compared with the control.

APPENDIX G

Concentration-Response Curve of Clonidine-Induced Vasorelaxation

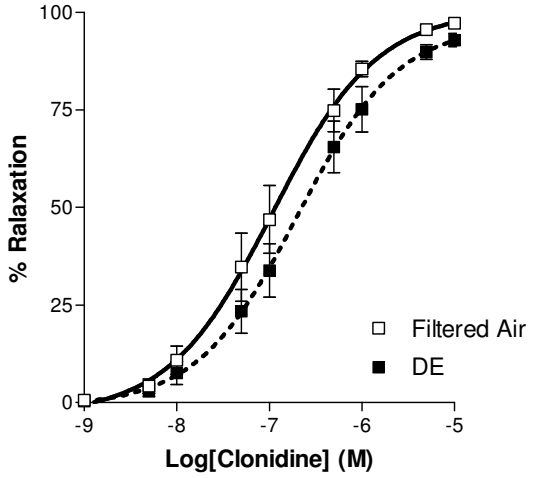

Concentration-response curves show that clonidine-induced vasorelaxation was not different, compared DE exposure with the control. n=6. Values are mean±SEM.

APPENDIX H

Vascular Function Analysis of Endothelin-1 Activity

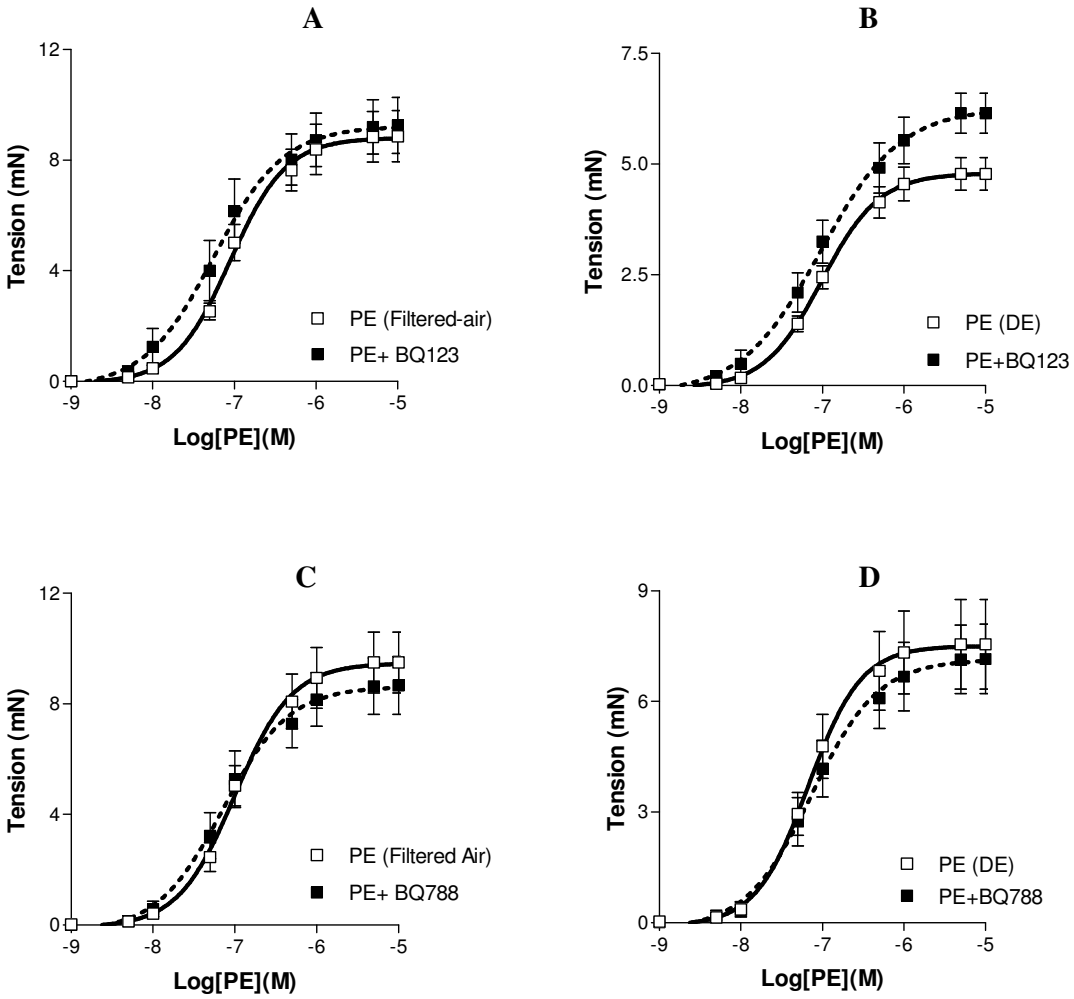

To examine the effect of DE exposure on endothelin-1 (ET-1) activity, the specific antagonists for ET_A (BQ123) and ET_B receptors (BQ788), were administered, respectively. Concentration-response curves show that PE-elicited vasoconstriction was not different in the presence of these antagonists, compared DE exposure with the control. n=6. Values are mean±SEM.

APPENDIX I

Correlation between iNOS Expression and Band Cells

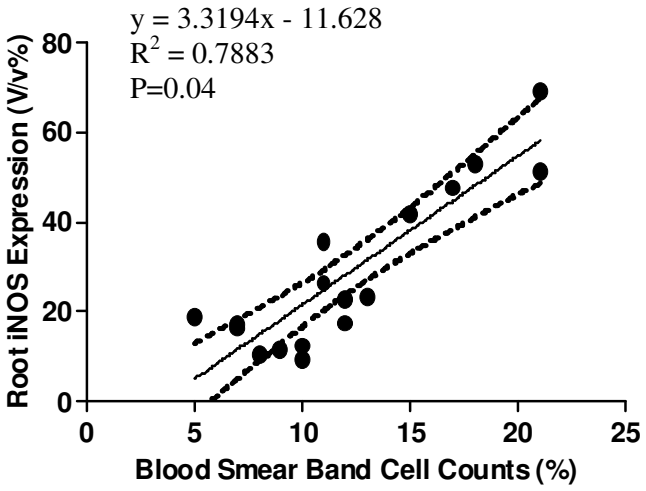

There is a positive correlation between increased iNOS expression in atherosclerotic plaque of aortic root and increased circulating band cells.

APPENDIX J

Vascular Function Analysis and Immunohistochemistry Analysis of COX and iNOS Activity and Expression

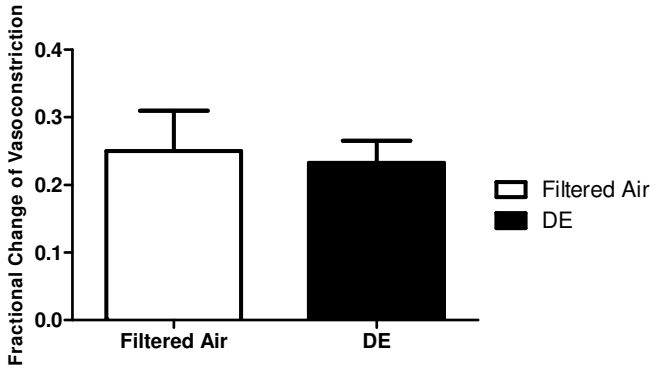

The attenuated PE-stimulated vasoconstriction after exposure to DE was completely restored in the present of both COX and iNOS blockers. n=6. Values are mean±SEM.

A **B**

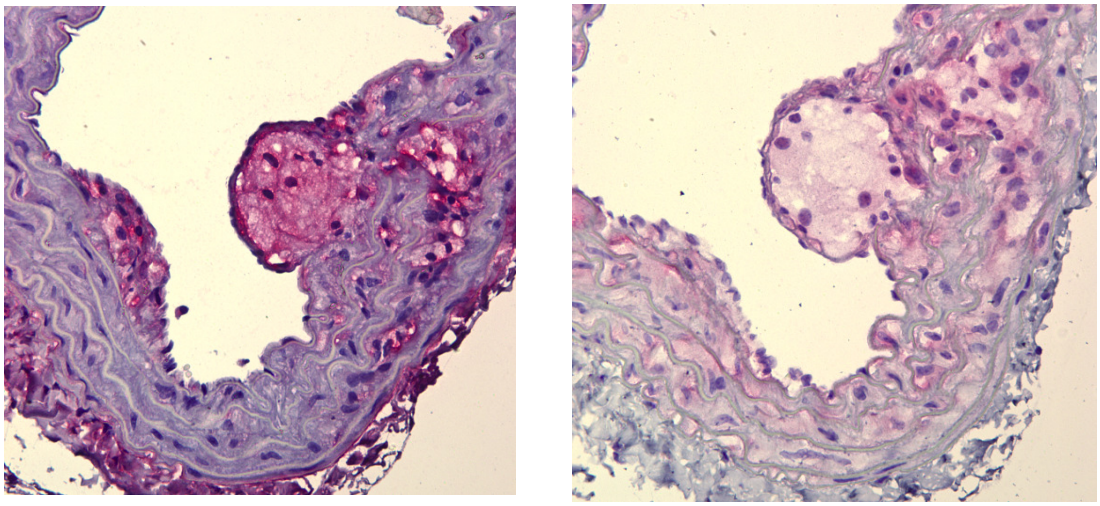

Representative photomicrographs of staining for iNOS (A) and COX2 (B) (400X) that were co-locally expressed by macrophages and smooth muscle cells in the thoracic aorta..

APPENDIX K

Vascular Function Analysis of the Effect of iNOS on ACh Relaxation

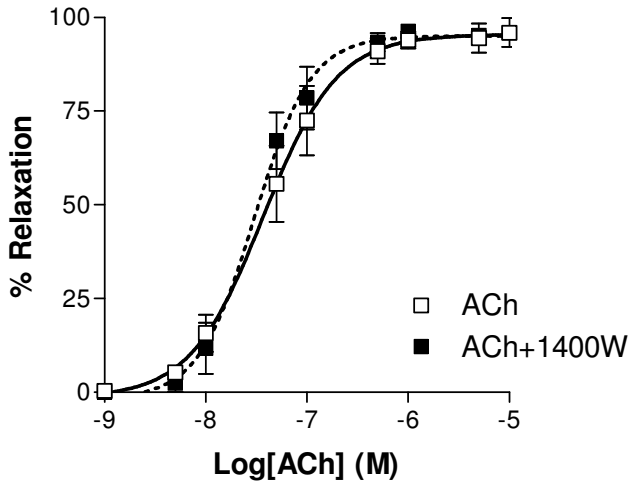

Concentration-response curves show that ACh-induced endothelium-dependent vasorelaxation was not altered by the iNOS blocker (1400W), compared DE with filtered air exposure. These experiments were done using the thoracic aorta of ApoE mice exposed to DE. n= 6. Values are mean±SEM.